Starch-based Nano-biocomposites

Fengwei Xie [a], Eric Pollet [b], Peter J. Halley [a], Luc Avérous [b],[*]

[a] Australian Institute for Bioengineering and Nanotechnology, The University of Queensland, Brisbane, Qld 4072, Australia

Fax: +61 7 3346 3973; Email: f.xie@uq.edu.au, fwhsieh@gmail.com (F. Xie)

[b] LIPHT-ECPM, EAc(CNRS) 4379, Université de Strasbourg, 25 rue Becquerel, 67087 Strasbourg Cedex 2, France

Fax: +33 368852716; Email: luc.averous@unistra.fr (L. Avérous)

[*] Corresponding author. Tel.: +33 368852784; fax: +33 368852716.

Email address: luc.averous@unistra.fr (L. Avérous)

ABSTRACT

The last decade has seen the development of green materials, which intends to reduce the human impact on the environment. Green polymers are obviously tendency subset of this stream and numerous bio-sourced plastics (bioplastics) have been developed. Starch as an agro-sourced polymer has received much attention recently due to its strong advantages such as low cost, wide availability, and total compostability without toxic residues. However, despite considerable commercial products being available, the fundamental properties (mechanical properties, moisture sensitivity, etc.) of plasticised starch-based materials have to be enhanced to enable such materials to be truly competitive with traditional petroleum-based plastics over a wider range of applications. Regarding this, one of the most promising technical advances has been the development of nano-biocomposites, namely dispersion of nano-sized filler into a starch biopolymer matrix. This paper reviews the state-of-the-art in the field of starch-based nano-biocomposites. Various types of nanofillers that have been used with plasticised starch are discussed such as phyllosilicates (montmorillonite, hectorite, sepiolite, etc.), polysaccharide nanofillers (nanowhiskers/nanoparticles from cellulose, starch, chitin, and chitosan), carbonaceous nanofillers (carbon nanotubes, graphite oxide, and carbon black), and many more. The main preparation strategies for starch-based nano-biocomposites with these types of nanofillers and the corresponding dispersion state and related properties are also discussed. The critical issues in this area are also addressed.

2

Contents

Nomenclature

Nomenclature

[AMIM]Cl	1-allyl-3-methylimidazolium chloride
BCNW	bacterial cellulose nanowhisker
CA	citric acid
CB	carbon black
CEC	cationic exchange capacity
CMC	carboxymethyl cellulose sodium
CNT	carbon nanotube
CNW	cellulose nanowhisker
CS	cationic starch
d_{001}	interlayer spacing, or d-spacing
DMSO	dimethyl sulphoxide
DP	degree of polymerisation
E	Young's modulus
E'	storage modulus (by dynamic mechanical analysis)
GO	graphite oxide
HA	hydroxyapatite
L/D	length-to-diameter ratio, i.e. aspect ratio
LDH	layered double hydroxide
MMT	montmorillonite
MMT–Na$^+$	sodium montmorillonite
MWCNT	multi-wall carbon nanotube
OMMT	organomodified montmorillonite
OMMT–CS	cationic starch–organomodified montmorillonite
PBAT	poly(butylene adipate-co-terephthalate)

PBSA	poly(butylene succinate-*co*-adipate)
PCL	polycaprolactone
PLA	poly(lactic acid) / polylactide
PVA	poly(vinyl alcohol)
SEM	scanning electron microscopy
SNP	starch nanoparticles
SWCNT	single-wall carbon nanotube
T_d	thermal decomposition temperature
T_m	melting temperature
TEM	transmission electron microscopy
T_g	glass transition temperature
UV	ultraviolet
XRD	X-ray diffraction
ΔH_m	melting enthalpy
ε_b	elongation at break
σ	tensile strength

1. Introduction

Due to the environmental concerns and the shortage of fossil resources (as demonstrated by the approaching of peak oil for example), the use of starch resources in non-food applications has experienced considerable development in the past decades. Starch has advantages such as low cost, wide availability, and total compostability without toxic residues. By using conventional polymer processing techniques, starch, like many other polymers, can be produced into different end-use forms such as extruded, moulded, thermoformed or blown articles [1].

However, starch-based materials are known to have limitations such as poor processability and properties (e.g. weak mechanical properties, poor long-term stability, and high water sensitivity). Formulation development and understanding of starch thermal [1-5] and rheological [6-11] properties could be the keys to solve these critical problems. Further, various starch-based blends and biocomposites have been developed, showing improved performance [12-15]. Recently, along with the exponential momentum of the development in polymer nanocomposites [16-21], much attention has been focused on the use of nano-sized fillers (at least one dimension in the nanometer range, i.e. 1–100 nm) in improving the performance of and adding new functionalities to starch-based materials.

Various nanofillers have been examined with plasticised starch, including phyllosilicates, polysaccharide nanofillers, carbonaceous nanofillers, and many more (cf. Table 1). They have different geometry (size and shape) and surface chemistry. Regarding their shapes, three distinct types of nanofillers can be observed, i.e. *nanoparticles*, *nanotubes*, and *nanolayers* [22]. Nevertheless, the term "nanoparticles" is also frequently used in broad sense to describe a nanofiller regardless of its shape.

[Insert Table 1 here]

Unlike most conventional synthetic polymers, starch has unique chemical structure and processing behaviour. Therefore, the preparation and properties of starch-based nano-biocomposites are inherently dissimilar to those of other polymer nanocomposite systems. Furthermore, the incorporation of appropriately tuned nanoparticles into starch as a biopolymer with complex structures and special properties will provide a rich new class of polymer nanocomposites able to be designed for a wide range of both conventional and emerging applications. For these reasons, this paper will provide a comprehensive review on starch-based nano-biocomposites, which can be interesting to both fundamental research and industrial applications.

2. From native starch to plasticised starch-based materials

This section describes the fundamentals of starch as a biopolymer and the most essential aspects of it to be used as a material.

2.1. Granular and molecular structures of native starch

Starch granules are mainly found in seeds, roots, and tubers of different origins such as maize (corn), wheat, potato, and rice. The granule is well known to possess multi-level structures from macro to molecular scales, i.e. starch granules (<1~100 μm), alternating amorphous and semicrystalline shells (growth rings) (100~400 nm), crystalline and amorphous lamellae (periodicity) (9~10 nm), and macromolecular chains (~nm) [23-26]. It presents a concentric three-dimensional architecture from the hilum with a total crystallinity varying from 15% to 45% depending on the botanical

9

source [27]. Starch is a polysaccharide consisting of D-glucose units, referred to as homoglucan or glucopyranose, and has two major biomacromolecules, i.e. amylose and amylopectin (cf. Figure 1). Amylose is a sparsely branched carbohydrate mainly based on α(1–4) bonds with a molecular weight of 10^5–10^6 and can have a degree of polymerisation (DP) as high as 600 [23]. On the other hand, amylopectin is a highly multiple-branched polymer with a high molecular weight of 10^7–10^9. It is one of the largest natural polymers on earth [23]. Amylopectin is based on α(1–4) (around 95%) and α(1–6) (around 5%) links, with constituting branching points localised every 22–70 glucose units and with pending chains of DP ≈ 15, which are mainly responsible for the materials' crystallininity. This specific structure has a profound effect on the physical and biological properties [23,25]. Besides, in starch granules are also found very small amounts of proteins, lipids and phosphorus depending on the botanical resource [24,25]. These components can interact with the carbohydrate chains during processing (e.g. Maillard reaction) and then modify the behaviour of the starchy materials.

[Insert Figure 1 here]

Depending on the source, amylose content of starch can be varied from <1% to 83% [28]. Table 2 gives an overview of the structural properties of maize starches with different amylose contents [28]. The amylose content has a great impact on the thermal, rheological, and processing properties [2,3,8,10,29].

[Insert Table 2 here]

2.2. *Gelatinisation/melting of native starch*

When native starch granules are heated in water, their semicrystalline nature and three-dimensional architecture are gradually disrupted, resulting in a phase transition from the ordered granular structure into a disordered state in water, which is known as "gelatinisation" [30-32]. Gelatinisation is an irreversible process that includes, in a broad sense and in time/temperature sequence, granular swelling, native crystalline melting (loss of birefringence), and molecular solubilisation [33]. Full gelatinisation of starch under shearless condition requires excess water (>63% for waxy maize starch for example [34]). With abundant water, the crystallites in starch might be pulled apart by swelling, leaving none to be melted at higher temperature. However, if the water content is limited, the swelling forces by water will be much less significant and the steric hindrance is high. In this case, higher temperature is required to facilitate the moibility of starch molecules and the destruturation of the crystalline regions [2,5,35,36]. The process of gelatinisation with low water content could more accurately be defined as the "melting" of starch [36]. The gelatinisation/melting behaviours of regular maize starch with different moisture contents are shown in Figure 2.

[Insert Figure 2 here]

The gelatinisation/melting behaviour of starch is quite different when shear treatment is imposed [37]. It has been shown that shear can enhance the destructuration of starch granules in abundant water [38,39] and the melting of crystallites with limited water [9,10,40]. The significance of such studies is that most processing techniques for starch involve shear treatment.

11

By gelatnisation/melting, native granular starch is thus converted into a molten state, which is known as "plasticised starch", or "thermoplastic starch".

2.3. Processing strategies for plasticised starch-based materials

The techniques that have been used to process starch, such as solution casting, internal mixing, extrusion, injection moulding, compression moulding, are similar to those widely used for conventional synthetic thermoplastics [1].

Water is indispensable for the thermal processing of starch. By reducing the moisture content, the melting temperature (T_m) of starch would progressively increase, and that of dry starch is often larger than its decomposition temperature (T_d), as extrapolated by Flory Law [41,42]. Water functions by lowering the T_m and plasticising the starch polymers, acting as a "plasticiser" in practical processing. However, the volatility of water could results in unstable processing or undesirable foaming. Besides, the final products based on starch containing only water usually have poor mechanical properties especially due to the brittleness, because of its final temperature usually lower than its glass transition temperature (T_g) [43-48], and/or resulting from the densification (happening below T_g) or retrogradation (also recrystallisation, happening above T_g) [32,49-51]. To overcome these issues, non-volatile (at the processing temperature) plasticisers such as polyols (glycerol, sorbitol, glycol, etc.) [43,47,48,52-59], nitrogen-based compounds (urea, ammonium derived, amines, etc.) [60-74], or citric acid (CA) [75-77] are utilised.

Chemical modification (e.g. hydroxylation [78-80] and acetylation [81-85]) of starch by substituting ester or ether groups for the hydroxyls is an effective way to improve the processing and product properties (mechanical properties, water resistance, etc.). However, chemical modification often decrease the polysaccharide

molecular weight, and also modify the biodegradability and generate some toxic chemical byproducts, which negatively impact the life-cycle assessment (LCA) of the final products.

To improve the performance such as moisture resistance, mechanical properties, and long-term stability, starch-based multiphase systems (blends or composites) have been developed. Starch is often blended with other polymers (mainly biodegradable) such as poly(lactic acid) (PLA), polycaprolactone (PCL), poly(butylene succinate adipate) (PBSA), poly(butylene adipate-*co*-terephthalate) (PBAT), and poly(vinyl alcohol) (PVA), as extensively reviewed in several papers [12-14]. Starch biocomposites can be produced with the reinforcement by cellulose fibres (potato pulp, bleached leafwood fibres, fibres from bleached eucalyptus pulp, and flax and jute fibres), and lignin fillers [15]. When the fillers become nano-scaled, nanocomposites could be obtained, which will be discussed in the next sections.

3. Starch-based nano-biocomposites reinforced by phyllosilicates

Phyllosilicates possess some strong advantages such as wide availability, low cost, versatility, eco-friendliness, and low toxicity. Along with the following discussion, the details of studies on starch-based nano-biocomposites reinforced by phyllosilicates are tabulated in Appendix 1 for readers' reference.

3.1. *Phyllosilicates*

Phyllosilicates, or layered silicates, are an important group of minerals that includes the clay minerals, the micas, chlorite, serpentine, talc, etc. They have different structure, texture, and/or morphology. The layered structure of phyllosilicates in detail can be found elsewhere [86-88]. Table 1 lists the most

13

commonly used phyllosilicates for starch-based nano-biocomposites. Particularly, some phyllosilicates do not display a normal layered structure. These include sepiolite, which displays a kind of fibrous structure [86,89], and halloysite, which has usual layered structure forms spheroidal aggregates [86].

Cationic exchange is the most common technique for chemical modification of the phyllosilicate surface, which increases the interlayer spacing (d_{001}) [90]; and by this technique, various organomodified MMTs (OMMTs) and hectorites used for starch-based nano-biocomposites (cf. Table 3) can be produced, which mainly differ in the counter-cation nature and the cationic exchange capacity (CEC). Nevertheless, most conventional organomodifiers increase the hydrophobicity of the phyllosilicate, resulting in reduced compatibility with the hydrophilic starch matrix. This is one of the key points to consider for devleoping starch-based nano-biocomposites.

[Insert Table 3 here]

The dispersion state of a typical phyllosilicate (except sepiolite and halloysite) in a polymer, which depends on the preparation conditions and the matrix–nanolayer affinity, determines the structure of the resulting composite, which can be either *phase separated composite (microcomposite)*, *intercalated nanocomposite*, or *exfoliated nanocomposite* [15-18,20,91].

3.2. *Preparation techniques*

Normally, incorporation of phyllosilicate nanolayers into a polymer matrix can be carried out with one of three main techniques, i.e. (a) *solution intercalation* (b) *in situ intercalative polymerisation*, or (c) *melt intercalation* [16-18,92,93].

3.2.1. *Solution intercalation*

Solution intercalation is based on a solvent system in which the polymer is soluble and the phyllosilicate is swellable and dispersible. For preparing nanocomposites based on other polymers, the polymer and the phyllosilicate are normally dissolved/swollen separately in solvent and then the two solutions are mixed allowing the intercalation to occur by the polymer chains replacing the solvent molecules within the interlayer spaces of the phyllosilicate [19]. However, the procedure would probably need to be adjusted flexibly to achive maximum polymer intercalation when starch is the matrix. It it not uncommon to first mix starch and the phyllosilicate followed by gelatinisation. In this case, the intercalation process will take place during gelatinisation as reflected by the rheological changes [94]. Besides, to minimise the intercalation of the plasticiser (glycerol) in the phyllosilicate (a typical issue), right mixing order of different ingredients (starch, nanofiller, and plasticiser) [95] or using an additional step of co-precipitation in ethanol [96] could help.

3.2.2. *In situ intercalative polymerisation*

During *in situ* polymerisation, a phyllosilicate is swollen in a monomer solution, and then the monomer polymerisation takes place, leading to a d_{001} increase, till in some cases a fully exfoliated morphology [17]. However, since starch molecular chains are synthesised during the plant growth, this technique is limited to nano-biocomposites with chemically modified starch such as starch graft copolymers as the matrix [97-101].

15

3.2.3. Melt intercalation

Melt intercalation involves processing a mixture of a polymer with a phyllosilicate in a melt processing unit (e.g. extruder or internal mixer). During processing, the chains diffuse into between the aggregated silicate layers to produce a (nano-)structured system that is controlled by the processing conditions such as temperature, shearing, and residence time. Shearing is necessary to induce platelets delamination from the phyllosilicate tactoids (a step-wise mechanism has been given by Fornes et al. [102]); and extended residence time is needed to allow the diffusion of polymer chains into the interlayer spaces and then to obtain an exfoliated morphology [103]. Nevertheless, the strong shear and long residence time would also contribute to the degradation of the starch molecules. Thus, it is necessary to balance the processing parameters to minimise the polymer chain degradation and to obtain a well exfoliated morphology.

3.3. Nano-biocomposites based on starch (without other polymers as the matrix)

3.3.1. Effect of phyllosilicate addition

Starch-based systems reinforced by phyllosilicates normally exhibit increases in tensile strength (σ) [96,104-133], Young's modulus (E) [95,96,105,107-111,115,118-120,122,124-127,130,132,134-139], storage modulus (E') (measured by dynamic mechanical analysis) [116,129,134,140], T_g [106,116,129,134,136,139,141-144], thermal stability [95,97,99,104,105,107-109,116,117,119,122,124,134,140,142,144,145], moisture resistance (i.e. moisture uptake, water vapour permeability [WVP], etc.) [95,104,105,108-110,112-119,123,126,127,133,141,145,146], oxygen barrier property [147], and biodegradation rate [148], generally meaning improved performance, even though the

16

elongation at break (ε_b) was observed to be reduced in most studies [95,96,104,107-110,112-117,119-121,123-125,128,130,134,136]. While these changes could usually be ascribed to the structural reasons such as (a) the homogeneous dispersion of silicate layers in the starch matrix [96,105,106,109,114,115,120,122-124,126,129,139,149,150], (b) the strong interactions (typically by hydrogen bonding) between the nanofiller and matrix [104,108,112,114,116,119-122,124-126], and (c) the high aspect (width-to-thickness) ratio and thus the vast exposed surface of the nanofiller [105,119,123], the specific mechanisms regarding the changes in the different properties are detailed below:

- Glass transition: an increase in the T_g (of the starch-rich domains, sic passim) indicates the restriction of chains mobility [129,144].

- Mechanical properties: increases in the E, E', and σ can be ascribed to (a) the facilitation of stress transfer from the matrix to the nanofiller [96,112,151], (b) the formation of a physical crosslinking network [116,125], (c) the stretching resistance of the oriented backbones of the chains in the interlayer spaces [119]. Besides, a decrease in the ε_b can be attributed to the decreased flexibility of the starch molecules [112,119,125].

- Moisture resistance: an increase is the result of (a) the introduction of tortuous and thus longer pathways through the matrix for the diffusion of water molecules [104,110-112,114,116,118,119,123,126], and (b) the shielding of the exposed water-sensitive –OH groups of the starch [114,126,127].

- Oxygen barrier property: an increase can be ascribed to the introduction of more tortuous and longer diffusion pathways for oxygen molecules [147].

- Thermal stability: improvement can be due to (a) the inorganic phase (phyllosilicate) having higher thermal stability, compared to the organic one

(starch), acting as a heat barrier [119,123], (b) the increase in the tortuosity of the diffusion pathways for oxygen and the combustion (pyrolysis) gas [16,97,119,122,144,145], and (c) the reorganisation of the starch structure with less exposed –OH groups, and thus less susceptibility to degradation [95,126,134],

In spite of the general trends mentioned above, discrepancies have also existed in certain cases over ε_b [95,96,105,106,120,122,129], breaking energy [105,107-109,124,126,136], thermal stability [128,152], T_g [115,133], T_m [129,153,154], moisture resistance [136]. To address these, it might be useful to consider the crystalline structures in the materials as influenced by the nanofillers. Crystallinity and/or crystal size could affect the biodegradation [148], mechanical properties [96,120,122,136], and moisture resistance [119]. Most typically, a higher crystallinity could embrittle materials with lower ε_b values [120,122,136]. Nevertheless, the literature shows no consistent trend of recrystallnisation as influenced by the phyllosilicate addition (restrained [96,108,109,114,125,148,149,152,153], unchanged [147], or enhanced [127,138]).

3.3.2. *Effects of phyllosilicate type and content*

3.3.2.1. *Montmorillonite*

Table 3 highlights various natural and organomodified MMT nanofillers that have been utilised in starch-based nano-biocomposites. It is important to note that the surface hydrophobicity of Cloisite MMT nanofillers follows the order, $Na^+ < 30B < 10A < 25A < 93A < 20A < 15A < 6A$. Although OMMT could provide much greater d_{001} than natural sodium MMT (MMT–Na^+, or Cloisite Na^+) to possibly facilitate starch molecular intercalation, the structure of the resulting composites is

demonstrated to be more depend on the hydrophilicity of MMT [149]. It has been

shown that incorporation of hydrophobic OMMT nanofillers such as Cloisite 15A, 6A,

and 10A, Nanomer I.30E, etc. led to the formation of microcomposites [94,112,117],

as evidenced by the unchanged d_{001}. When Cloisite 30B, a more hydrophilic OMMT,

was utilised, higher d_{001} values were obtained, corresponding to higher dispersion

[94,116,135,146]. Exfoliated nanocomposites have also been produced with MMT–

Na$^+$ due to the more hydrophilic character which makes it more compatible with

plasticised starch [94,95,108,112,116,117,119,135,145-147,149,155]. Uniform

dispersion of the MMT in the plasticised starch can be achieved in this case due to the

polar interactions especially hydrogen bonds formed between the –OH groups of the

MMT and of the starch molecules [108,112,116,117].

[Insert Table 3 here]

The high compatibility of MMT–Na$^+$ with a starch matrix and the corresponding

good dispersion could result in improved properties (cf. Section 3.3.1) compared with

those of other starch–OMMT hybrids. Typically, the tensile properties of starch-based

biocomposites filled by Cloisite Na$^+$, 30B, 10A, and 6A examined by Park et al.

[116,117] are shown in Appendix 1. In addition, these authors also showed that

MMT–Na$^+$ could shift the T_g to a higher temperature, whereas the OMMTs decreased

this relaxation temperature [116,117].

It is worth noting that that, more than the reason of surface polarity matching,

some other reasons could also account for the property changes (either deteriation or

improvement) when OMMT is used. For example, Zhang et al. [149] showed reduced

thermal stability of starch-based materials with Cloisite 93A while MMT–Na$^+$ could

result in a higher T_d. This reduction could rather be ascribed to the earlier decomposition of the organic alkyl ammounium on the clay [149] or the catalytic effect of acidic sites of the MMT [152]. Moreover, some studies [111,146,147] showed that the hydrophobicity of the clay could affect the water sensitivity of the whole system. For example, Table 4 shows that (except that urea–ethanolamine was used as the plasticiser, which will be discussed in Section 3.3.3) nanocomposites filled with MMT–Na$^+$ had higher moisture uptake than those with MMT–OH mainly due to the higher hydrophilic nature of MMT–Na$^+$ [147].

[Insert Table 4 here]

In certain cases, MMT with proper organomodification may still display better reinforcing ability than MMT–Na$^+$. Qiao et al. [128] showed that incorporation of OMMT based on trimethyl dodecyl ammonium into acetylated starch could result in a nano-biocomposite with higher σ and E' than the sample with MMT–Na$^+$. This was attributed to the higher dispersion and d_{001} of the OMMT in the acetylated starch matrix [128]. Chivrac et al. [115,121,136,137,141,156] used cationic starch (CS) as a new organomodifier to better match the polarity of a starch matrix. Remarkably, morphological analyses showed that MMT organomodified by CS (OMMT–CS) allowed preparation of well-exfoliated nano-biocomposites, compared to natural MMT–Na$^+$, which only led to the formation of an intercalated structure (cf. Figure 3) [121]. Consequently, the OMMT–CS could lead to greater stiffness without affecting the ε_b [121,137].

[Insert Figure 3 here].

Although Tang et al. [112] reported that the MMT content did not have any significant effect on the occurrence of intercalation or exfoliation, it is worth noting that there can be an optimised level of MMT addition for the greatest improvement in the properties such as mechanical properties [105,106,111,112,116,150], moisture barrier property [111,145], and thermal stabilities [116]. A higher content of MMT might contribute to aggregates and stacks of MMT in a starch matrix [96,108,116,120,150] and also to lower plasticisation of the starch phase [114].

3.3.2.2. Other phyllosilicates

Other clays (natural or synthetic) such as hectorite [129,134,135,140] and kaolinite [115,135,140], and halloysite [131,132] have also been experimented into starch-based materials. Non-swelling clays such as kaolinite [115] and halloysite [131] can hardly generate a well dispersed structure (intercalation/exfoliation for kaolinite), and thus variations in the properties could be very limited. Although dimethylsulphoxide (DMSO) could assist the dispersion of kaolinite [157], healthy and environmental problems might be arised; nonetheless, the problem with the easy aggregation of halloysite could be safely solved by ball-milling treatment with polyethylene glycol as the dispersing agent (also compatibliser), which results in improved σ and E [132]. Natural hectorite might perform better than kaolinite for the formation of a nanocomposite structure (as shown by the increased d_{001}) [135,140]; nevertheless, organomodified hectorite (Bentone 109) could only result in conventional composite just like kaolinite [135]. Again, this can be explained by the dominant role of the phyllosilicate hydrophilicity in determining the biocomposite

structure. In addition, a larger CEC could contribute to a stronger water retention property which also influences the mechanical properties [158].

Chivrac et al. [122] initiated the use of sepiolite in starch-based materials, and found its reinforcing effect was even better than that of MMT, as evidenced by the higher E, ε_b, and breaking σ, which was ascribed to the stronger nanofiller–matrix interactions. Nevertheless, when sepiolite was modified by CS for better interactions with starch, the thermal stability of the nano-biocomposites could be deteriorated, due to the fast thermal decomposition of CS [122].

3.3.3. Effect of plasticisers/additives

Glycerol has been a widely used plasticiser for preparing starch–phyllosilicate nano-biocomposites [95,96,108,110-123,127,134-137,141,142,145,147-153,156,159]. Because of the strong polar interactions between the –OH groups of the starch chains, of the glycerol, and of the silicate layers, glycerol and/or starch chains can enter into silicate interlayers [117,119]. However, high glycerol/clay ratio could contribute to intercalation of only glycerol (as observed by the d_{001} increasing to about 18.5 Å) instead of starch molecules (thus conventional composites), whereas total exfoliation could be obtained without the plasticiser [134,136,140,149]. Such a similar phenomenon has also been reported with sorbitol [124,136]. This may be because of, compared with those of starch, the smaller size of the plasticiser favouring its penetration [95] and/or the stronger interaction of the plasticiser with the nanoclays [136]. It is also necessary to note that, in this case, the trapping of the plasticiser in the interlayer spaces could also induce a reduced plasticisation effect on the starch phase [127,136].

Chiou et al. [145] and Tang et al. [113] found a granual increase in the degree of clay intercalation/exfoliation with the decreasing glycerol content (cf. Figure 4). As a result, the film with 5% glycerol exhibited the lowest WVP, and highest T_g and σ [113]. However, it was proposed from these studies that samples containing higher glycerol contents had an increase in the starch–glycerol interactions, which competed with the interactions with the nanoclay surfaces [113,120,145].

[Insert Figure 4 here]

Chiou et al. [145] proposed that the hydrophilic nature of glycerol could negate the improved water resistance of nano-biocomposites containing exfoliated MMT. This issue has been extensively addressed by Chivrac et al. [141], who showed that high plasticiser content (23 wt.% glycerol) could induce phase separation, with plasticiser-rich and starch-rich phases, resulting in the nanoclay being preferentially located in the latter (cf. Figure 5) [141]. Therefore, a preferential pathway for water transfer was more likely to be created in the very hydrophilic glycerol-rich domains where the nanoclay platelets were almost absent. In this case, even if exfoliated morphology was achieved, the heterogeneous clay distribution and phase separation phenomenon explained the lack of improvement and even the decline in the moisture barrier property [141].

[Insert Figure 5 here]

Other plasticisers such as sorbitol [124,129,136], CA [114], urea [105,106,113,125,126,147,155], formamide [106-109,113,124,126], *N*-(2-

23

hydroxyethyl)formamide [104], ethanolamine [105,107,109,125,147], 1-allyl-3-methylimidazolium chloride ([AMIM]Cl, a hydrophilic ionic liquid) [160], or their combinations have been proved to be effective in enhancing the dispersion and exfoliation of silicate layers in starch. Nevertheless, some systems mentioned above are eco-toxic and cannot be used to develop safe "green" materials. However, the use of these latter plasticisers may avoid the disturbance of small polyols in the intercalation/exfoliation process (as mentioned before). As a result, nano-biocomposites plasticised by these plasticisers usually have improved properties. For example, Tang et al. [112,113] demonstrated that a formamide- or urea-plasticised starch–MMT nano-biocomposite exhibited a lower WVP, higher T_g, and higher σ than the glycerol-plasticised counterpart (cf. Appendix 1 for the mechanical properties and Figure 6 for the X-ray diffraction [XRD] patterns). Zeppa et al. [147] showed that the use of urea–ethanolamine as the plasticiser could effectively reduce the moisture sensitivity and oxygen permeability (cf. Table 4) which might be due to the increased dispersion of the nanofiller.   Chen et al. [155] reported that the use of urea enhanced the dispersion of ammonium-treated MMT in a starch matrix, making exfoliation possible. This is because the $–NH_2$ groups of urea could develop strong interactions with the quaternary ammonium from the organoclay [155].

[Insert Figure 6 here]

For producing more desirable nano-biocomposites, phyllosilicates can be pretreated/activated with glycerol [114,142], ethanolamine [105,107,109], CA [106,120], urea [126], [AMIM]Cl [160,] etc. before compounding with starch. Pretreatment/activation can increase the d_{001} and destruct the stacked layered structure

of a phyllosilicate (cf. Table 5). For this purpose, a high speed emulsifying machine [114,142] or a single-screw extruder could be used [124,126,149]. As reported by Huang et al. [105-107,109], the d_{001} of the MMT–Na$^+$ was widened resulting from the intercalation of the CA or ethanolamine during activation, making the interaction with plasticised starch easier in a later stage to achieve total dispersion and exfoliation [105-107,109]. Nonetheless, the possible competition between the starch and the plasticiser for the intercalation might decrease the plasticisation of starch, because the intense interactions (the hydrogen bonding and the ion-dipole) existed in these multiphase systems [114,126].

[Insert Table 5 here]

Chitosan has been used as a new eco-friendly compatibiliser as this polycation could lead to fewer clay aggregates and improved mechanical properties, although intercalation of chitosan was not observed due to its high molecular mass [96,150]. In addition, polyethylene glycol was reported to be a good compatibliser for dispersing halloysite nanotubes in starch [132].

3.3.4. *Effects of starch type, amylose content and chemical modification*

The amylose content of starch or starch type was also reported to have a structural impact on starch-based biocomposites, even though the results were not consistent [111,112]. Mondragón et al. [111] suggested that plasticised waxy starch were easiser than either regular or high-amylose (70%) starch to form an intercalated/exfoliated structure. Corresonpondingly, the mechanical properties such as σ and E tended to increase with the MMT content with incremental improvement following the order,

25

high-amylose < regular < waxy maize starch [111]. In contrast, Tang et al. [112] reported that a regular maize starch–based nanocomposite film presented better moisture barrier and mechanical properties than either a waxy or high-amylose starch–based counterpart. Besides, the WVP, σ and ε_b of the films did not change significantly as the amylose content increased to > 50%. To account for these results, complicated reasons including the degree of gelatinisation and the crystallinity of the materials should be considered.

Various chemically modified starches have been experimented to develop nano-biocomposites [97,128-130,133,139,140,144]. Chemical modification can result in starch derivatives with varied properties such as the molecular chain length and hydrophilicity, influencing the interactions with a phyllosilicate. For example, Wilhelm et al. [140] showed that the use of oxidised starch instead of unmodified starch gave rise to the d_{001}, indicating the easier intercalation of the shorter oxidised starch chains. Besides, the plasticiser (glycerol) intercalation was minimised while the intercalation of the oxidised starch chains was preferred [140]. On the other hand, by replacing some hydroxyls of starch with less hydrophilic groups like acetate groups, the polarity matching between the starch and a specific phyllosilicate can differ [97,130,133,139]. For instance, Nejad et al. [130,139] reported that OMMT (Dellite 67G or 43B), compared with MMT–Na$^+$ (Dellite LVF), matched better with hydrophobic starch derivatives (acetate, propionate, and propionate acetate laurate). Therefore, very good dispersion and partially exfoliated structures were achieved.

3.3.5. *Effects of preparation techniques and processing conditions*

Namazi et al. [97] compared solution intercalation and *in situ* polymerisation methods for preparing starch-*g*-PCL nano-biocomposites reinforced by Cloisite 15A.

26

Their result showed that, although the d_{001} could be varied by the clay addition level and swelling/reaction time, the diffusion and intercalation of the copolymer into the interlayer spaces was generally better by solution intercalation than by *in situ* intercalation [97].

Chiou et al. [146] examined the effects of moisture content, temperature, screw speed, and specific mechanical energy in a twin-screw extrusion process of wheat starch–based biocomposites reinforced by MMT–Na^+. They found that only the moisture content played an important role in affecting the nanofiller dispersion, with the reason proposed to be the greater degree of gelatinisation at higher moisture content, allowing more leaching of hydrophilic molecules from the granules to penetrate into the interlayer spaces [146]. When Cloisite 30B was used, only the increased temperature produced slight intercalation due to the incompatibility of starch with the hydrophobic Cloisite 30B [146].

Dean et al. [158] investigated the effect of different mixing regimes prior to extrusion on the structure of starch-based nano-biocomposites. It was shown that, when the levels of the phyllosilicate, water, and starch were optimised, exfoliation could be achieved via conventional standard mixing without the use of ultrasonics [158]. Nevertheless, a recent study [120] reported that combined mechanical and ultrasonic mixing modes led to the most dispersion of the silicate layers in the nano-biocomposites prepared by solution casting and thus the highest E, irrespective of the clay type, compared to a process involving only one mixing mode. This is due to the contribution of both dispersive (the breakup of the silicate agglomerates to individual layers, provided by the ultrasonic device) and distributive (a spatial uniformity of all the components, provided by the mechanical mixer) mixing mechanisms [120].

3.3.6. Towards some applications

Recent studies have shown that the addition of a phyllosilicate abundant of –OH groups to a starch graft copolymer superabsorbent is expected to improve the morphological homogeneity, water absorbing property, and gel strength because the crosslinking network can be improved with homogeneous dispersion of MMT [100]. The crosslinking density could be influenced by the type [98] and content [99-101] of the phyllosilicate. Zhou et al. [144] found that the addition of OMMT could result in a decrease in the cell size and the compressibility of starch acetate–based foams prepared by melt extrusion. Wang et al. [160] discovered that the combined use of MMT and [AMIM]Cl could result in plasticised starch-based films with high electrical conductance ($10^{-0.3}$ S/cm). Moreover, studies [161,162] have shown that the electrorheological activity of a novel ternary kaolinite–DMSO–carboxymethyl starch nanocomposite could be influenced by the degree of intercalation.

3.4. Nano-biocomposites based on starch blends

In order to produce starch-based nano-biocomposites with better properties, starch has been blended with other polymers, including PLA [163-168], PCL [169-177], PVA [178-180], PBAT [181,182], PBSA [183,] some trademarked polyesters [176,184,185], and natural rubber [186]. Some of these studies [169-172,181,182], though quite interesting, will less be discussed here since the matrix contained starch as a minor component.

McGlashan and Halley [185] found that addition of MMT to a starch–polyester (the type not disclosed) matrix could make the extrusion processing more stable: the die and die lip temperature could be lowered without detrimentally affecting the film blowing process [185]. The reason could be the exfoliated MMT acting as a barrier

for plasticiser migration and evaporation. This also contributed to products with greater stability with storing time [185]. Ikeo et al. [177] suggested that addition of MMT–Na$^+$ could improve the compatibility between starch and PCL. Moreover, Dean et al. [180] suggested that starch recrystallisation in starch–PVA blends could be disrupted by addition of MMT–Na$^+$, which reduced the rate of embrittlement over time.

In some studies [168,178,179,183,185,187], the effects of different factors such as the second polymer content and the nanofiller type and content on the properties of nanocomposites were systematically investigated. These nanocomposites are expected to show improved characteristics (increases in the E' [177,183], E, [168,169,176,178,180,185-187], and σ [168,169,176,178,180,185-187]). However, it is quite significant to note that incorporation of another polymer (usually being relatively hydrophobic) would modify the hydrophilicity of the material. As a result, MMT–Na$^+$ might not match anymore the polarity of the blend. McGlashan and Halley [185] proposed that the organic constituents (alcohols and hydrogenated tallow) of the OMMT could be more thermodynamically compatible with the polyester. Lee and co-workers [163-167] compared addition of different MMTs in the melt processing of tapioca starch–PLA nanocomposite foams. Their results showed that Cloisite 30B, instead of MMT–Na$^+$, could result in the greatest extent of intercalation (cf. Table 6 for details) and also better functional properties [163]. This was caused by strong hydrogen bonding between the –OH groups of the matrix and those of the Cloisite 30B organomodifier [163]. A similar result was observed by Bocchini et al. [183] who used a starch–PBSA matrix. Majdzadeh-Ardakani and Nazari [179] showed that CA–modified MMT, compared with MMT–Na$^+$ and Cloisite 30B, led to better mechanical properties of starch–PVA nanocomposites because of strong interactions between the

CA and the starch/PVA polymer chains [179]. Moreover, Dean et al. [178] showed

that, for starch–PVA nanocomposites reinforced by MMT–Na$^+$, the relative

concentration of the PVA and MMT–Na$^+$ could be directly correlated to the change in

the d_{001} (cf. Figure 7) [178].

[Insert Table 6 here]

[Insert Figure 7 here]

Starch is known to regularly show problem of compatibility with another polymer.

Arroyo et al. [168] found that, in starch–PLA nanocomposites, MMT–Na$^+$ was

preferentially located in the starch phase or at the blend interface. Mondragón et al.

[186] revealed that, in starch–natural rubber nanocomposites, MMT–Na$^+$ nanolayers

were mainly dispersed in the natural rubber domains forming a well-ordered

intercalated structure. In these cases, MMT–Na$^+$ might have preferential polarity

matching with one of the two polymers in the matrix, and, as a result, interactions and

stress transfer between the phases could be tampered [168,186]. Of course, some

studies have addressed the compatibility issue, and methods such as high energy ball

milling (for starch–PCL [177]) and reactive processing (for starch–PCL [173-176]

and starch–PBAT [181,182]) have shown to be quite effective.

4. Starch-based nano-biocomposites reinforced by polysaccharide nanofillers

Polysaccharide nanofillers represent the second popular group of nanofillers used

for starch-based nano-biocomposites. Along with the following discussion, the details

of studies on this group of nano-biocomposites are tabulated in Appendix 2.

4.1. Polysaccharide nanofillers

A series of polysaccharides with similar chemical structures such as cellulose, starch, chitin, and chitosan can be produced into different forms of nanofillers (nanowhiskers and nanoparticles), which can be employed for fabricating starch-based nano-biocomposites (cf. Table 7). Cellulose nanowhiskers (CNWs) and starch nanoparticles (SNPs) have already been widely used whereas the use of chitin nanoparticles has been less investigated. One of the advantages in using them is the similar polysaccharide chemical structure of the nanofiller and the matrix, which could benefit the nanofiller–matrix interactions.

[Insert Table 7 here]

4.1.1. Cellulose nanowhiskers

CNWs (also cellulose nanofibres) can be isolated from biomass like flax [188], hemp [189], ramie [190], peal hull [191,192], cassava bagasse [193], and tunicate (a sea animal) [194-197], or from microcrystalline cellulose [129,198], through acid hydrolysis with a concentrated mineral acid (typically sulphuric acid) under strictly controlled conditions of time and temperature [188-194,196,199-202]. Acid action results in a decrease of the amorphous parts and thus the material with high crystallinity is obatined. Generally, the final geometrical characteristics depend on the cellulose origin and the acid hydrolysis process conditions such as time, temperature, and purity of the materials [22]. It can be seen from Table 7 that tunicin (animal cellulose) nanowhiskers have comparatively high aspect ratio (*L/D*: 50–200), which could enhance the nanofiller–matrix interfacial phenomena. Regarding the time, Chen et al. [192] found that 8 h of hydrolysis was long enough to remove all the

hemicellulose and lignin and most of the amorphous regions in the pea hull fibre,

when the CNWs showed the highest *L/D* value (36). However, if the hydrolysis time

was too long (particularly 24 h), the crystalline regions could also be destroyed (cf.

Table 8) [192].

[Insert Table 8 here]

Though direct acid hydrolysis is most frequently used to prepare CNWs, other

methods have also been employed (cf. Table 7), such as enzyme hydrolysis followed

by combined shear and pressure treatment [203-205]. Besides, a complementary (e.g.

mechanical) treatment in addition to the traditional hydrolysis have also been

practised [206]. Regardless of the preparation method, a high crystallinity of the

nanofiller is generally encouraging because of the higher *E* [22], which is beneficial to

mechanical property improvement in the resulting nano-biocomposites.

4.1.2. *Starch nanoparticles*

Le Corre et al. [207] have reviewed starch SNPs prepared by different methods,

mainly (a) starch nanocrystals resulting from the disruption of amorphous domains

from semicrystalline granules by acid hydrolysis, and (b) SNPs produced from

gelatinised starch.

Starch nanocrystals can be obtained by acid (normally sulphuric acid) hydrolysis

of native starch granules by strictly controlling the temperature, acid and starch

concentrations, hydrolysis duration, and stirring speed [208-212]. Figure 8 shows one

of the first observations of starch nanocrystals by transimission electron microscopy

(TEM). This kind of starch nanocrystals have a strong drawback since they gelatinise

in hot water which could be a problem when preparing plasticised starch nano-biocomposites.

[Insert Figure 8 here]

In the second method, SNPs were prepared by ethanol precipitation into a gelatinised starch solution with constant stirring. The resulting SNPs free from water were further modified by CA in a dry preparation technique. The so-formed amorphous SNPs could not be swelled or gelatinised in hot water because of the crosslinking induced by the CA (cf. Figure 9) [213]. Also, the reaction with the CA decreased the aggregation and the size of the SNPs [213].

[Insert Figure 9 here]

4.1.3. Chitin/chitosan nanowhiskers/nanoparticles

Chitin nanowhiskers can be made from different chitin sources by deproteinisation in a boiling alkaline (KOH) solution and then hydrolysing the sample with a boiling HCl solution with vigorous stirring [214-218]. Besides, Chang et al. [219] introduced a modified method with two identical acidic treatments followed by repeated sonication disruption/dispersion processes. In this case, chitin nanoparticles were obtained with a low crystallinity because acid hydrolysis converted some of the crystalline religions into amorphous parts [219].

For transforming chitosan into a nanofiller, a very simple and mild method based on ionotropic gelation between chitosan and sodium tripolyphosphate was used: chitosan was dissolved into an acetic acid solution, followed by the dropwise addition

33

of sodium tripolyphosphate into the solution with vigorous stirring and sonication [220-222]. This method involves physical crosslinking by electrostatic interactions (instead of chemical crosslinking), which avoids possible toxicity of reagents and other undesirable effects [222].

4.2. Preparation techniques

From Appendix 2, one can find that a solution casting method was predominantly usd in these studies (except that Teixeira et al. [193] used a melt mixing process). Several reasons might account:

- Nanowhiskers/nanoparticles tend to aggregate due to association by strong hydrogen bonding (especially CNWs [188,189,206] and SNPs [210,212,223,224]);

- The nanofiller structure may be destroyed at high temperature, which tampers the reinforcing ability (especially, SNPs may gelatinise [212,224]);

- The nanofiller is prepared in aqueous condition, with the resulting dispersion (without either sedimentation or flocculation, as a consequence of charge repulsion due to the surface sulphate groups created during the sulphuric acid treatment) easy to be incorporated into a starch solution [129,188-192,194,196,210,212,223,224].

For the dispersion of nanowhiskers/nanoparticles in a starch solution, some additional treatments such as ultrasonication and homogenisation might help [198,206]. If SNPs are used, they may be added at reduced temperature to avoid gelatinisation [212,224].

As far as bacterial cellulose nanowhiskers (BCNWs) are concerned, special preparation methods were practised. Wan et al. [225] incorporated BCNWs into

34

plasticised starch via a solution impregnation method [225]. Grande et al. [226,227] developed a bio-inspired bottom-up technique to produce self-assembled nano-biocomposites of cellulose synthesised by *Acetobacter* bacteria and native starch (cf. Figure 10). This method was reported to be able to result in nano-biocomposites with coherent morphology [226,227].

[Insert Figure 10 here]

4.3. Nano-biocomposites reinforced by cellulose nanowhiskers

4.3.1. Effect of cellulose nanowhiskers addition

According to the literature, the mechanical properties (σ, and E), thermal property (T_g), and moisture resistance generally show improvement with addition of CNWs to starch-based materials [129,188-198,205,206,225,226,228]. This can be linked to not only the good nanofiller dispersion in the matrix, resulting from the chemical similarity, but also the strong nanofiller–matrix adhesion by hydrogen bonding interactions [188,190,192]. Specific reasons for the improvement are summarised below:

- Mechanical properties: improvement (but usually at the expense of the ε_b) can be benefited by (a) the formation of a rigid network of the CNWs, the mutual entanglement between the nanofiller and the matrix, and the efficient stress transfer from the matrix to the nanofiller [206,229], and by (b) an increase in the overall crystallinity of the system resulting from the nucleating effect of the CNWs [196,197]. (The latter point has been in dispute since the hindrance of the lateral rearrangement of the starch chains, and hence that of the recrystallisation, was also observed [206]).

35

- Glass transition: an increase in the T_g can be ascribed to (a) the restriction of mobility of the amorphous starch chains by the contact with the CNW surface [189-191] or by the increased crystallinity [196,197], and to (b) the relocation of the plasticiser(s) (including water) from the starch matrix to the CNW surfaces (detailed in Section 4.3.3), which decreases the plasticisation effect on the amorphous regions [194,195].

- Moisture resistance: improvement can be contributed by (a) the less hydrophilic nature of cellulose and the geometrical impedance created by the CNWs, (b) the constraint of the starch swelling due to the presence of the CNW network, (c) the resistance of the diffusion of water molecules along the nanofiller–matrix interface [194,196,205,225,230,231], and (d) a decrease in the mobility of the starch chains, resulting from an increase in the T_g or the crystallinity [194].

It is noteworthy that high level of nanofiller addition is not necessarily good because of the aggregation, adversely affecting the properties [191]. Moreover, one controlling factor which needs to be emphasised here is the moisture content (usually related to the relative humidity [RH] during post-processing conditioning), which plays a key role in controlling the properties by assisting in the formation of the hydrogen bonding between the CNWs, and by (may together with the other plasticisers) increasing the mobility of the starch chains which is favourable either for its recrystallisation during the conditioning process or for the decrease in its T_g [194-197].

In addition to the properties mentioned above, Chen et al. [191,192] reported that nano-biocomposites filled with CNWs showed transparency very close to or even

slightly higher than that of the pure starch matrix, which was attributed to the nano-size and the homogeneous dispersion of the nanofiller.

In the meantime, addition of CNWs to a starch matrix could probably result in a decrease in the thermal stability (as observed by the T_d) [191,192,206]. The reason might be that the presence of acid sulphate groups (as a result of the preparation CNWs by sulphuric acid) decreased the thermal stability of the cellulose by dehydration, hence also reducing the thermal stability of the starch matrix after incorporation [191-193,232]. Such a phenomenon also occurred when hydrochloric acid was used for the acid hydrolysis [206]. In contrast, when a non–acid hydrolysis method was used, the nano-biocomposites showed improved thermal stability [198].

4.3.2. Effect of nanofiller preparation

Preparation can directly affect the quality of nanofiller, which then impacts the structure and performance of the resulting nanocomposites. Chen et al. [191,192] found that, while starch–CNWs nano-biocomposites (with CNWs prepared by acid hydrolysis of pea hull fibre for 4–24 h) generally exhibited much better properties, i.e. the higher σ, ε_b, E, T_g, transparency, moisture resistance (cf. Figure 11), than the microcomposites (with the native pea hull fibres without acid hydrolysis) [191], 8 h of acid hydrolysis could result in most homogeneous dispersion of the CNWs within the starch matrix and in this case the CNWs was wrapped most tightly by the matrix [192]. It was suggested that this stronger nanofiller–matrix adhesion resulted from the highest aspect ratio (cf. Table 8), and contributed to the superior properties of the nano-biocomposite such as transparency, σ, and ε_b (cf. Figure 11) [192]. Moreover, Woehl et al. [228] found that enzyme hydrolysis of bacterial cellulose for 60 min, compared with either shorter or longer time, could generate CNWs with which the

37

nano-biocomposites displaying the most improved mechanical properties. This is because 60 min is enough to disentangle the fibres and reduce the defects in the surface of the fibres without weakening the crystalline regions of the CNWs [228].

[Insert Figure 11 here]

A noteworthy fact is that, in certain cases, non-cellulose components may also be generated along with CNWs, which could also affect the properties of nano-biocomposites. Teixeira et al. [193] found that sugars co-originated from hydrolysis of cassava bagasse (containing also residual starch) caused considerable reduction in the T_g and inhibited the formation of V_H-type crystalline structure in the nano-biocomposites, as agreed by an increase in the ε_b [193]. This is because the interactions between the starch and the sugars reduced those between the starch and the CNWs, resulting in very high mobility of the starch chains [193].

4.3.3. Plasticiser relocation and transcrystallisation phenomena

Dufresne and co-workers [194,195], by undertaking a series of studies on plasticised waxy maize starch–based nano-biocomposites reinforced by tunicin nanowhiskers, have discovered some effects which could tamper the reinforcement by the CNWs [194,195]:

- The accumulation of the plasticiser in the vicinity of the CNW/amylopectin interfacial zone (because of the stronger interactions of either the water or glycerol with the cellulose than with the starch), enhanced in moist conditions;

- The formation of a highly oriented layer, i.e. transcrystalline zone, around the CNWs by the recrystallinsation of the amylopectin chains assisted by the plasticiser accumulation and the nucleating effect of the CNWs.

These effects could interfere with the inter-CNW hydrogen-bonding forces and hinder the stress transfer at the nanofiller–matrix interface, and thus compromise the mechanical properties of the ensuing nano-biocomposites [194,195].

The plasticiser relocation and transcrystallisation phenomena have also been observed in other CNWs-reinforced systems [193]. Using different plasticisers (e.g. using sorbitol instead of glycerol) may help restraining these phenomena [196,197].

4.4. *Nanocomposites reinforced by starch nanoparticles*

4.4.1. *Effect of starch nanoparticles addition*

With the addition of SNPs, starch-based nano-biocomposites generally showed increased values of the strength at break, E [212,213,224], and T_g [212,213,224], and decreased values of the WVP [210,213], indicating improved performance. However, some unfavourable property changes were also observed, e.g. higher water uptake [210] and lower T_d [210,223].

Due to the same chemical structure, good interfacial interactions (nanofiller–nanofiller and nanofiller–matrix) by hydrogen bonding and hence a strong reinforcing effect of SNPs could be expected [212,213,224]. Besides, the nucleating effect of SNPs could facilitate the recrystallisation of the starch chains at the interface, as demonstrated by increases in the T_m and melting enthalpy (ΔH_m) (although high SNPs content might hinder the recrystallinisation possibly because of an increase in the viscosity [212]). Starting from these points, the mechanisms accounting for the property changes are summarised below:

- Mechanical properties: increases in the E and breaking σ and a decrease in the ε_b results from (a) the reinforcing effect of the SNPs [212,213,224], and (b) the increased crystallinity in the starch matrix (which further increased during ageing, cf. Table 9) [212,224].

- Glass transition: an increase in the T_g was due to (a) the strengthened intermolecular interactions [212,213,224], and (b) the increased crystallinity in the matrix [212,224].

- Moisture resistance: a reduction is ascribed to (a) the less hydrophilic nature of the SNPs (especially CA–modified SNPs [213]), and to (b) the introduced tortuous pathways for water molecules to pass through [210,213]

- Thermal stability: a decrease is attributed to (a) the sulphate groups on the acid hydrolysed SNPs [210,223,232] (similarly discussed for CNWs before) and to (b) the strong interactions between the SNPs and the glycerol [210,223] (detailed hereafter).

[Insert Table 9 here]

4.4.2. *Effect of plasticiser*

Regarding some property deterioration and results discrepancy as shown in Appendix 2, it is believed that a starch–SNPs nano-biocomposite is a complex system governed by not only the nanofiller, but also the plasticiser.

Angellier et al. [224] proposed that, because of the same chemical nature of the filler and matrix and thus the same affinity of plasticisers for both components [224], "crystallisation" (co-crystallisation?), instead of trancrystallinisation (cf. Section 4.3.3), occurred at the nanofiller–matrix interface. These could explain [212,224] a

greater reinforcing effect of the SNPs when the plasticiser content (glycerol or sorbitol) was high (cf. Table 9). However, García et al. [210] suggested that the higher density of –OH groups on the surfaces of SNPs, which were mainly the crystalline zones of hydrolysed waxy starch, led to more association of the SNPs with glycerol molecules. Consequently, more –OH groups of the matrix available to interact with moisture [210] existed, and a nanometric fibrillar structure (possibly formed by the SNPs, glycerol, and transcrystallised amylopectin) (cf. Figure 12) which becoming a preferential path for water vapour diffusion was formed [223], resulting in an increase in the moisture sensitivity.

[Insert Figure 12 here]

4.5. Nanocomposites reinforced by chitin/chitosan nanoparticles

Chang and co-workers [219,220] found that chitin/chitosan nanoparticles could be uniformly dispersed in a starch matrix at low loading levels, resulting in improved properties (e.g. σ, E', T_g, and WVP; the mechanisms are similar to those for SNPs reinforced nano-biocomposites); however, when the nanofiller addition was high (5 wt.% for chitin [219], 6 wt% for chitosan [220]), conglomeration/aggration occurred. Nevertheless, good interfacial interactions between the nanofiller and the matrix could be still observed [219].

5. Starch-based nano-biocomposites reinforced by carbonaceous nanofillers

This group of nanofillers are highly interesting to be incorporated into starch-based materials though they have not been extensively studied so far. Along with the

41

following discussion, the details of studies on these materials are also tabulated in Appendix 3.

5.1. Carbonaceous nanofillers

Carbonaceous nanofillers such as carbon nanotubes (CNTs), graphite, and carbon black (CB) represent a promising group of nanofillers which not only induce performance improvement but also new functionalities especially electrical conductivity and electroactivity. CNTs-reinforced nanocomposites have already shown great potentials in biomedical applications such as sensors, stimulators of bone cells, etc. [233-236], although the toxicity of CNTs appears still controversial [237,238]. There have already been some exciting reports on starch–CNTs nano-biocomposites, whereas those reinforced by other carbon nanofillers scarcely exist.

5.1.1. Carbon nanotubes

CNTs can be either single-wall carbon nanotubes (SWCNTs) or multi-wall carbon nanotubes (MWCNTs). Despite of the wide use of CNTs in other polymer nanocomposite systems [21,22], the use of CNTs as the nanofiller for starch-based materials has just been initiated, and mostly MWCNTs were involved [237,239-241]. This may due to the lower price and more abundance of MWCNTs than SWCNTs. Besides, MWCNTs exhibit high aspect ratio (~1000), and excellent mechanical (E: ~1 TPa), thermal, and electrical properties [242-244].

The effectiveness of utilising CNTs for nanocomposites strongly depends on two main factors: (a) homogeneous dispersion of nanotubes throughout the matrix without destroying the integrity of them, and (b) adequate interfacial adhesion between the phases [22,245]. These are difficult to achieve especially in starch considering its

highly hydrophilic nature. Hence, modification of CNTs is highly necessary, as some methods reported includes:

- The treatment by a surfactant (e.g. sodium dodecyl sulphate [240] and sodium dodecyl benzene sulphonate [246]),

- The carboxylation by strong acids (e.g. sulphuric acid and nitric acid) [239,241], and

- The wrapping by an aqueous solution of a starch-iodine complex [237].

The last method is especially interesting here. Actually, this method has been extensively studied and shown to be effective in improving the dispersion stability of CNTs in aqueous solutions [247-253].

Compared with a non-covalent way (e.g. the wrapping with starch, and the modification by a surfactant), the covalent modification of CNT surfaces is more likely to provide strong interactions at the nanofiller–matrix interface. Regarding this, CNTs grafted by polysaccharides such as chitosan [254], cellulose acetate [255], and starch [256] would be interesting. Nevertheless, covalent sidewall functionalisation usually destroys the extended networks on the CNT surfaces, diminishing their mechanical and electronic properties [237].

5.1.2. *Graphite and graphite oxide*

Graphite combines the lower price and the layered structure of phyllosilicates with the superior thermal and electrical properties of CNTs [257-259]. While as-prepared graphite cannot be dispersed in water or organic solvent, which makes the fabrication of nanocomposites difficult, graphite oxide (GO) is hydrophilic and can form strong physical interactions with a polymer like starch due to its various oxygen functional groups including hydroxyls, epoxides, carbonyls, and carboxyls [260].

43

5.2. Preparation techniques

Starch–carbonaceous nanofiller nano-biocomposites were mostly prepared by a convenient solution process assisted by sonication and strong stirring. Much care should be taken to choose the sequence of addition of ingredients, which might affect the nanofiller dispersion, the gelatinisation/plasticisation, and thus the final structure and properties of the nano-biocomposite. Regarding this, it could be better if the nanofiller was dispersed in water which was then added to a gelatinised starch solution [239].

5.3. Nanocomposites reinforced by carbon nanotubes

5.3.1. Effect of carbon nanotubes addition

Incorporation of MWCNTs into starch-based materials generally increased the ultimate σ [237,239,240], E [237,239,240], T_g [237,239,261], and T_d [241], and decreased the water sensitivity [239,261], showing improved performance. Homogeneous dispersion of the nanofiller in the matrix and strong nanofiller–matrix interactions can account for the property enhancement [237,239-241,261], which relies on the proper MWCNTs modification. The specific reasons for the effect of MWCNTs on the property variations are summarised below:

- Glass transition: an increase in the T_g can be attributed to the reduced flexibility and mobility of the starch chains in contact with the MWCNT surfaces [239,261,262].

- Thermal melting: a reduction in the ΔH_m could reflect the restraint of the starch recrystallisation, with the reason being the MWCNTs spatially

preventing the starch molecules from moving, interacting and crystallising again [239,240].

- Mechanical properties: higher values of the σ and E can be ascribed to (a) the formation of an isotropic, three-dimensional nanotube network, which inhibits the crack propagation [240], and (b) the effective stress transfer from the matrix to the nanofiller [240], and (c) the increase in the T_g, which contributes to an increase in the stiffness [237,261]; meanwhile a decrease in the toughness or ε_b as usually observed was attributed to the spatial restraint of the slippage movement of the starch molecules, yielding increasingly brittle samples [240]

- Thermal stability: an increase can be accounted by (a) the higher thermal stability of MWCNTs, (b) a barrier effect of the nanotubes which hinders the diffusion of the degradation products [241,263,264], and (c) an increase in the degradation activation energy [241]

- Moisture sensitivity: a reduction can be associated with (a) the low water sensitivity of MWCNTs [239], (b) the suppression of swelling of the matrix when submitted to a highly moist atmosphere [239], and (c) the decrease in the free volume (as observed by the T_g) where the water diffusion occurs [261,265].

There could be an optimised level of nanofiller addition, which was, for example, 3.8% for surfactant-treated MWCNTs [240], and 1.5% for carboxylated MWCNTs [241].

5.3.2. *Effect of nanofiller modification*

For the carboxylated MWCNTs, the acid-treatment process can incorporate various polar groups (carboxylic, carbonyl, and hydroxyl groups), which can improve the hydrophilicity and reduce the MWCNTs agglomeration [239,241]. As a result of the hydrogen bonding interactions and thus the high starch–MWCNTs compatibility, the σ and E of the nanocomposites did not come at the expense of the ε_b, which increased from 30% to 42% with the MWCNTs addition level up to 1% [239].

Very recently, Famá et al. [237,261] used a same starch to wrap MWCNTs and to be as the matrix. The SEM results showed that the failure occurred within the matrix rather than between the MWCNTs and their starch coating, indicating strong nanofiller–matrix adhesion (cf. Figure 13) [237]. Therefore, efficient load transfer was attained, resulting in increases in not only the σ but also the toughness and ε_b [237]. This work is remarkable since very small content of MWCNTs, i.e. 0.055%, could result in great changes in the material performance [237].

[Insert Figure 13 here]

5.3.3. *Electrical conductivity*

Besides the properties discussed above, addition of CNTs into a starch matrix gives the resulting nano-biocomposite (preferably in amorphous state) electrical conductivity, which can be influenced by both the water and MWCNT contents [240,241]. Ma et al. [240] demonstrated that, while higher water content would result in an increase in the conductivity in a very sensitive way ($y = B_2x^2 + B_1x + B_0$, with y being the conductivity and x the water content), an increase in the MWCNT content decreased the sensitivity of conductivity to water (both the monomial coefficient B_1

46

and B_2 approached more to zero), until an electrical percolation threshold was reached when the effect of water content was eliminated (cf. Figure 14a). If the water content was fixed at 0%, the conductivity firstly observed a gradual increase with increasing the MWCNT content and then a stepwise increase when a specific level of MWCNT content was reached (cf. Figure 14b) [240,241]. The reasons accounting for these phenomena are:

(a) Water is advantageous to improve the conductivity by improving the movement of the starch chains [266], which, however, is spatially restrained by the introduction of MWCNTs [240].

(b) While the conductivity at low levels (<2.85 wt.%) of MWCNTs addition was due to the formation of a conductive network through hopping and tunnelling processes [267], the creation of an interconnected structure of the MWCNTs allows easy flow of electrons at an applied electric field at the MWCNTs content higher than a specific value [240].

[Insert Figure 14 here]

5.4. *Nanocomposites reinforced by graphite oxide*

Li et al. [260] pioneered the work on starch-based nano-biocomposites reinforced by GO, of which the content was up to 2 wt.%. They found that hydrogen bonding formed between the GO and matrix, and that the nanofiller was well dispersed (exfoliated) at low GO loading levels [260]. With increasing the GO loading level, the σ, E, and T_d were continuously increased, the ultraviolet (UV) transmittance and ε_b were decreased, and the moisture uptake first decreased to a lowest value and then

slightly increased [260]. The property variations can be explained by the similar reasons for phyllosilicate-reinforced nano-biocomposites.

5.5. *Nanocomposites reinforced by carbon black*

Ma et al. [268] revealed that CB-reinforced starch-based nano-biocomposites prepared by solution casting with microwave radiation contained the CB in good dispersion, whereas isolated agglomerates of the CB particles existed in those from melt extrusion. As a consequence, the former approach shows better σ, WVP, and conductivity. A following study [269] showed that the quality of the electrical conductive network could be better with lower glycerol content (and thus lower viscosity), which could facilitate the flocculation of the CB during the solution process.

6. Starch-based nano-biocomposites reinforced by other nanofillers

This section will discuss more nanofillers which have been used for the development of starch-based nano-biocomposites. Along with the discussion below, the details about these nano-biocomposites are summarised in Appendix 4.

6.1. *Nanocomposites reinforced by metalloid oxides, metal oxides, and metal chalcogenides*

6.1.1. *Nanofillers and preparation techniques*

Metalloid oxides (e.g. SiO_2 and Sb_2O_3), metal oxides (e.g. ZnO, TiO_2, and $ZrO_2 \cdot nH_2O$), and metal chalcogenides (e.g. CdS, CdSe) are grouped together here because of their similar chemical categories, preparation methods, and nanofiller reinforcement mechanisms. Novel applications are expected for nanocomposites

reinforced by this type of nanofillers. For example, metal oxides and chalcogenides are normally semiconductor materials. Incorporation of such a nanofiller into a polymer can result in nanocomposites to be used as components for photovoltaic solar cells, light emitting diodes, photodiodes, and gas sensors [270].

Only solution methods have been used to fabricate these starch-based nano-biocomposites:

(a) The nanoparticles (SiO_2 [143,271] and TiO_2 [272]) are directly added into a starch matrix dispersion;

(b) The nanoparticles (ZnO [273,274] and Sb_2O_3 [275,276]) are firstly synthesised with a stabilising template (e.g. native starch [277], soluble starch [274,278-282], and CMC [273,275,276,283]), and then the encapsulated nanoparticles are incorporated into a starch dispersion;

(c) The nanoparticles (SiO_2 [284,285], TiO_2 [286], CdS [278], and CdSe [162]) are directly synthesised in a starch dispersion, which acts not only as the stabiliser but also as the matrix (sol–gel method).

When the first method is used, intensive sonication and/or shearing is normally required to avoid large aggregates of nanoparticles [271,287]. The second and third methods may be better to achieve good dispersion of nanoparticles. Particularly, the third method has recently been extended to a reactive extrusion process for producing starch–PVA–SiO_2 nano-biocomposites [287].

6.1.2. *Effects of addition of metalloid oxides, metal oxides and chalcogenides*

Uniform dispersion of a nanofiller (especially for polysaccharide-encapsulated metal nanoparticles) in a starch matrix and strong interfacial adhesion through hydrogen bonding between them could usually be achieved (due to the similar

49

chemical structures of the stabiliser and the matrix) [273-276,283]. As a result, the resulting nanocomposites generally display increases in the mechanical properties (σ [271-276,283], E [273,274], and E' [273,274]), T_g [273,274], WVP [273,274,276,283], and also UV–vis absorbance (due to the quantum confinement effect of the nanofiller) [143,273,274,276] and light transparency [278,288]. However, an increase in the water sensitivity was observed which was ascribed to the higher exposed –OH groups of the matrix (CdS [278]), or the high surface energy and plenty of free –OH groups of the nanofiller (nano-SiO_2 [289]). In addition, there were a decrease in the T_d but an increase in the residual weight, which could be due to either the poor thermal stability of the stabiliser (e.g. CMC) in the nanoparticles [276,283], or the increased –OH groups which directed the reaction toward carbonisation instead of the formation of volatile components [278,288]. The crystallinity was observed to be either increased (CdS [278]) or decreased (SiO2 [143]).

A higher addition level of nanofiller may result in agglomeration of nanoparticles [273-276,283,289], which is unfavourable for the performance improvement. For example, Wu et al. [271] found that the best σ and wear resistance could be achieved when the nano-SiO_2 addition level was 4% and 3% respectively. Tang et al. [289] found that 3 wt.% was the optimised level of the nano-SiO_2 for the best σ and the lowest water absorption of starch–PVA based nanocomposites

6.2. *Nanocomposites reinforced by layered double hydroxides*

The LDH structure is referred to as the natural hydrotalcite and the structure consists of brucite-like layers constituted of edge-sharing $M(OH)_6$ octahedra [290,291]. In order to inhibit the staking of the clay sheets, LDH needs to be synthesised in a polysaccharide [292]. However, as shown in a previous study [293],

even synthesised in a starch matrix, LDH could hardly be intercalated by starch molecules. Alternatively, Wu et al. [294] used carboxymethyl cellulose sodium (CMC) as a stabiliser, which contributed to good dispersion of LDH stacks in the starch matrix and to good filler–matrix interactions [294]. The resulting biocomposites with a low LDH loading level (6 wt.%) showed obviously improved mechanical properties (increased σ) and water resistance (decreased WVP) [294]. Nevertheless, the weak thermal stability of the CMC could facilitate the decomposition of the starch upon heating [294].

6.3. Nanocomposites reinforced by α–zirconium phosphate

Synthetic α–ZrP (i.e. $Zr(HPO_4)_2 \cdot H_2O$,) exhibits similar structural characteristics to natural MMT clay but has advantages such as high purity and ion exchange capacity and ease of intercalation and exfoliation [295-298]. In addition, the particle size and aspect ratio can be manipulated by varying the reaction conditions [295]. Wu et al. [295] found that plasticised starch and α–ZrP could interact and form strong hydrogen bonds, meaning good compatibility. Compared with the neat plasticised starch, the nano-biocomposite films showed increases in the σ and ε_b, and decreases in the crystallinity and moisture uptake. Besides, the maximum T_d decreased with an increase in the α–ZrP content, which could be ascribed to the increase in the acidity of the α–ZrP with the increase in the temperature, which induces the decomposition of the glycoside bonds [295].

6.4. Nanocomposites reinforced by hydroxyapatite

The use of hydroxyapatite (HA) is mainly for making biomaterials for biomedical applications such as clinical orthopaedics [299]. The successful use of injection

moulding to produce HA-reinforced starch–EVA nanocomposites with high mechanical performance for temporary tissue replacement applications has been demonstrated [300]. Besides, rod-like nano-HA crystals can be synthesised with controlled shape and size using soluble starch as a template (via an *in situ* biomimetic process), and the bioactivity and biocompatibility of the resulting biocomposites were verified [301,302]. Sundaram et al. [303] reported the fabrication of a porous scaffold biomaterial made from nano-HA, gelatin, and starch displaying the appropriate enhanced mechanical properties for bone repair and regeneration.

7.   Summary and perspectives

A wide variety of nanofillers have been examined with starch. Phyllosilicates (especially MMT of the smectite group) have been mostly utilised due to their advantages such as wide availability, low cost, and high aspect ratio and thus vast exposed surface area (and also the swelling nature). In addition, polysaccharide nanofillers represent the second most popular group due to their abundance in nature, the biological sources, and the chemical similarity to starch. Nevertheless, the preparation of these bio-nanoparticles is time consuming and involves acid hydrolysis in multiple steps which is not eco-friendly. Furthermore, used have been many other nanofillers such as carbonaceous nanofillers, metalloid oxides, metal oxides, and metal chalcogenides. One of the advantages in utilising such nanofillers is that they can provide new functionalities to starch-based materials in addition to the general reinforcement.

With the incorporation of the nanofiller, starch-based materials generally show improvement in some of their properties such as mechanical properties (typically σ, E, and E'), T_g, thermal stability, moisture resistance, oxygen barrier property, and

biodegradation rate. The improvement can be fundamentally ascribed to the homogeneous dispersion of the nanofiller in the matrix and the strong interface adhesion, which can contribute to the formation of a rigid nanofiller network and influence the molecular and crystalline structures in the matrix. To realise these, the nanofiller–matrix compatibility is the key point to address, which mainly depends on the surface chemistry of the nanofiller and is usually achieved by hydrogen bonding, although more factors such as the plasticiser(s)/additive(s), the starch type and chemical modification, the presence of other polymer(s), and the processing and annealing conditions also have strong influences. But above all, a major role is played by the nanofiller itself, of which the aspect ratio/surface area, chemistry, and mechanical properties could be influenced by its preparation and modification.

Nevertheless, how the nanofiller affected the crystalline structure and crystallinity of the starch matrix has not been unambiguously elucidated across the literature. These can be highly affected by the formulation (e.g. the amylose content of the starch, and the type and content of the plasticiser), the processing conditions (e.g. temperature, pressure, shearing, and orientation), and the storing conditions (e.g. time, temperature, and RH). Besides, phase separation of the plasticiser, the starch, and/or the nanofiller may exist in the system, with the different domains showing different recrystallisation/anti-crystallisation behaviours. These reasons may account for the discrepancies in some of the results such as T_g and moisture resistance.

With improved properties that are comparable to those of traditional petroleum-based polymers such as polyethylene and polypropylene, the current applications of starch-based materials can be greatly enhanced and widened. The renewable resource and inherent environmental friendliness of such materials can justify its wide use for a sustainable future. Particularly, the use of starch-based nano-biocomposites as new

53

packaging materials would be based on their biodegradation and improved barrier and mechanical properties.

In the future research, it is still very important to test new nanofillers to be incorporated into starch for developing promising nano-biocomposites with excellent performance and new functionalities to be competitive in the materials world. In addition, the heterogeneous dispersion of the nanofiller and the phase separation issue existed in some of the past studies should be addressed in the future. While the manipulation of chemistry might help to some extent, the future research should also emphasise the importance in using processing techniques like extrusion which are more aligned to the efficient industrial production. Thus, research is also needed regarding how thermomechanical treatment in this kind of processing can assist in achieving a well dispersive structure without adding a detrimental effect to the final properties due to starch molecular degradation.

References

[1] Liu H, Xie F, Yu L, Chen L, Li L. Thermal processing of starch-based polymers. Prog Polym Sci 2009;34:1348-68.

[2] Liu H, Yu L, Xie F, Chen L. Gelatinization of cornstarch with different amylose/amylopectin content. Carbohydr Polym 2006;65:357-63.

[3] Liu P, Xie F, Li M, Liu X, Yu L, Halley PJ, Chen L. Phase transitions of maize starches with different amylose contents in glycerol-water systems. Carbohydr Polym 2011;85:180-7.

[4] Xie F, Liu W-C, Liu P, Wang J, Halley PJ, Yu L. Starch thermal transitions comparatively studied by DSC and MTDSC. Starch/Stärke 2010;62:350-7.

[5] Liu H, Xie F, Chen L, Yu L, Dean K, Bateman S. Thermal behaviour of high amylose cornstarch studied by DSC. Int J Food Eng 2005;1:Article 3/1-6.

[6] Xie F, Halley PJ, Avérous L. Rheology to understand and optimize processibility, structures and properties of starch polymeric materials. Prog Polym Sci 2012;37:595-623.

[7] Tajuddin S, Xie F, Nicholson TM, Liu P, Halley PJ. Rheological properties of thermoplastic starch studied by multipass rheometer. Carbohydr Polym 2011;83:914-9.

[8] Xie F, Yu L, Su B, Liu P, Wang J, Liu H, Chen L. Rheological properties of starches with different amylose/amylopectin ratios. J Cereal Sci 2009;49:371-7.

[9] Xue T, Yu L, Xie F, Chen L, Li L. Rheological properties and phase transition of starch under shear stress. Food Hydrocolloids 2008;22:973-8.

[10] Wang J, Yu L, Xie F, Chen L, Li X, Liu H. Rheological properties and phase transition of cornstarches with different amylose/amylopectin ratios under shear stress. Starch/Stärke 2010;62:667-75.

[11]   Martin O, Averous L, Della Valle G. In-line determination of plasticized wheat starch viscoelastic behavior: impact of processing. Carbohydr Polym 2003;53:169-82.

[12]   Avérous L. Biodegradable multiphase systems based on plasticized starch: a review. Polym Rev 2004;44:231-74.

[13]   Yu L, Dean K, Li L. Polymer blends and composites from renewable resources. Prog Polym Sci 2006;31:576-602.

[14]   Wang X-L, Yang K-K, Wang Y-Z. Properties of starch blends with biodegradable polymers. Polym Rev 2003;43:385-409.

[15]   Avérous L, Halley PJ. Biocomposites based on plasticized starch. Biofuels, Bioprod Biorefin 2009;3:329-43.

[16]   Alexandre M, Dubois P. Polymer-layered silicate nanocomposites: preparation, properties and uses of a new class of materials. Mater Sci Eng, R 2000;28:1-63.

[17]   Sinha Ray S, Okamoto M. Polymer/layered silicate nanocomposites: a review from preparation to processing. Prog Polym Sci 2003;28:1539-641.

[18]   Sinha Ray S, Bousmina M. Biodegradable polymers and their layered silicate nanocomposites: in greening the 21st century materials world. Prog Mater Sci 2005;50:962-1079.

[19]   Pavlidou S, Papaspyrides CD. A review on polymer–layered silicate nanocomposites. Prog Polym Sci 2008;33:1119-98.

[20]   Paul DR, Robeson LM. Polymer nanotechnology: nanocomposites. Polymer 2008;49:3187-204.

[21]   Spitalsky Z, Tasis D, Papagelis K, Galiotis C. Carbon nanotube-polymer composites: chemistry, processing, mechanical and electrical properties. Prog Polym Sci 2010;35:357-401.

[22]   Kumar AP, Depan D, Singh Tomer N, Singh RP. Nanoscale particles for polymer degradation and stabilization--trends and future perspectives. Prog Polym Sci 2009;34:479-515.

[23]   Pérez S, Baldwin PM, Gallant DJ. Structural features of starch granules I. In: James B, Roy W. editors. Starch (Third Edition). San Diego: Academic Press, 2009. p. 149-92.

[24]   Jane J-l. Structural features of starch granules II. In: James B, Roy W. editors. Starch (Third Edition). San Diego: Academic Press, 2009. p. 193-236.

[25]   Pérez S, Bertoft E. The molecular structures of starch components and their contribution to the architecture of starch granules: a comprehensive review. Starch/Stärke 2010;62:389-420.

[26]   Buléon A, Colonna P, Planchot V, Ball S. Starch granules: structure and biosynthesis. Int J Biol Macromol 1998;23:85-112.

[27]   Zobel HF. Molecules to granules: a comprehensive starch review. Starch/Stärke 1988;40:44-50.

[28]   Tan I, Flanagan BM, Halley PJ, Whittaker AK, Gidley MJ. A method for estimating the nature and relative proportions of amorphous, single, and double-helical components in starch granules by ^{13}C CP/MAS NMR. Biomacromolecules 2007;8:885-91.

[29]   Li M, Liu P, Zou W, Yu L, Xie F, Pu H, Liu H, Chen L. Extrusion processing and characterization of edible starch films with different amylose contents. J Food Eng 2011;106:95-101.

[30]   Ratnayake WS, Jackson DS, Steve LT. Starch gelatinization. Adv Food Nutr Res 2008;55:221-68.

[31]   Lelievre J. Starch gelatinization. J Appl Polym Sci 1974;18:293-6.

57

[32]   Atwell WA, Hood LF, Lineback DR, Varrianomarston E, Zobel HF. The
terminology and methodology associated with basic starch phenomena. Cereal
Foods World 1988;33:306-11.

[33]   Russo MAL, O'Sullivan C, Rounsefell B, Halley PJ, Truss R, Clarke WP. The
anaerobic degradability of thermoplastic starch: polyvinyl alcohol blends:
potential biodegradable food packaging materials. Bioresour Technol
2009;100:1705-10.

[34]   Wang SS, Chiang WC, Zhao B, Zheng XG, Kim IH. Experimental analysis
and computer simulation of starch-water interactions during phase transition. J
Food Sci 1991;56:121-4.

[35]   Donovan JW. Phase transitions of the starch-water system. Biopolymers
1979;18:263-75.

[36]   Lai LS, Kokini JL. Physicochemical changes and rheological properties of
starch during extrusion. Biotechnol Prog 1991;7:251-66.

[37]   Xie F, Liu H, Chen P, Xue T, Chen L, Yu L, Corrigan P. Starch gelatinization
under shearless and shear conditions. Int J Food Eng 2006;2:Article 6/1-29.

[38]   Yu L, Kealy T, Chen P. Study of starch gelatinization in a flow field using
simultaneous rheometric data collection and microscopic observation. Int Polym
Process 2006;21:283-9.

[39]   Chen P, Yu L, Kealy T, Chen L, Li L. Phase transition of starch granules
observed by microscope under shearless and shear conditions. Carbohydr Polym
2007;68:495-501.

[40]   Xie F, Yu L, Chen L, Li L. A new study of starch gelatinization under shear
stress using dynamic mechanical analysis. Carbohydr Polym 2008;72:229-34.

[41]   Liu X, Yu L, Liu H, Chen L, Li L. In situ thermal decomposition of starch with constant moisture in a sealed system. Polym Degrad Stab 2008;93:260-2.

[42]   Russell PL. Gelatinisation of starches of different amylose/amylopectin content. A study by differential scanning calorimetry. J Cereal Sci 1987;6:133-45.

[43]   Enrione J, Osorio F, Pedreschi F, Hill S. Prediction of the glass transition temperature on extruded waxy maize and rice starches in presence of glycerol. Food Bioprocess Technol 2010;3:791-6.

[44]   Liu P, Yu L, Wang X, Li D, Chen L, Li X. Glass transition temperature of starches with different amylose/amylopectin ratios. J Cereal Sci 2010;51:388-91.

[45]   Chaudhary DS, Adhikari BP, Kasapis S. Glass-transition behaviour of plasticized starch biopolymer system - a modified Gordon-Taylor approach. Food Hydrocolloids 2011;25:114-21.

[46]   Liu H, Chaudhary D, Ingram G, John J. Interactions of hydrophilic plasticizer molecules with amorphous starch biopolymer—an investigation into the glass transition and the water activity behavior. J Polym Sci, Part B: Polym Phys 2011;49:1041-9.

[47]   Lourdin D, Coignard L, Bizot H, Colonna P. Influence of equilibrium relative humidity and plasticizer concentration on the water content and glass transition of starch materials. Polymer 1997;38:5401-6.

[48]   Forssell PM, Mikkilä J, M., Moates GK, Parker R. Phase and glass transition behaviour of concentrated barley starch-glycerol-water mixtures, a model for thermoplastic starch. Carbohydr Polym 1997;34:275-82.

[49]   Gudmundsson M. Retrogradation of starch and the role of its components. Thermochim Acta 1994;246:329-41.

[50]   Liu Q, Thompson DB. Effects of moisture content and different gelatinization heating temperatures on retrogradation of waxy-type maize starches. Carbohydr Res 1998;314:221-35.

[51]   Bulkin BJ, Kwak Y, Dea ICM. Retrogradation kinetics of waxy-corn and potato starches; a rapid, raman-spectroscopic study. Carbohydr Res 1987;160:95-112.

[52]   Da Róz AL, Carvalho AJF, Gandini A, Curvelo AAS. The effect of plasticizers on thermoplastic starch compositions obtained by melt processing. Carbohydr Polym 2006;63:417-24.

[53]   Mathew AP, Dufresne A. Plasticized waxy maize starch: effect of polyols and relative humidity on material properties. Biomacromolecules 2002;3:1101-8.

[54]   Gaudin S, Lourdin D, Le Botlan D, Ilari JL, Colonna P. Plasticisation and mobility in starch-sorbitol films. J Cereal Sci 1999;29:273-84.

[55]   Kirby AR, Clark SA, Parker R, Smith AC. The deformation and failure behaviour of wheat starch plasticized with water and polyols. J Mater Sci 1993;28:5937-42.

[56]   van Soest JJG, de Wit D, Tournois H, Vliegenthart JFG. The influence of glycerol on structural changes in waxy maize starch as studied by Fourier transform infra-red spectroscopy. Polymer 1994;35:4722-7.

[57]   Shi R, Liu Q, Ding T, Han Y, Zhang L, Chen D, Tian W. Ageing of soft thermoplastic starch with high glycerol content. J Appl Polym Sci 2007;103:574-86.

[58]   Yan Q, Hou H, Guo P, Dong H. Effects of extrusion and glycerol content on properties of oxidized and acetylated corn starch-based films. Carbohydr Polym 2012;87:707-12.

[59]   Qiao X, Tang Z, Sun K. Plasticization of corn starch by polyol mixtures. Carbohydr Polym 2011;83:659-64.

[60]   Ma XF, Yu JG, Wan JJ. Urea and ethanolamine as a mixed plasticizer for thermoplastic starch. Carbohydr Polym 2006;64:267-73.

[61]   Ma X, Yu J. The plastcizers containing amide groups for thermoplastic starch. Carbohydr Polym 2004;57:197-203.

[62]   Ma X, Yu J. The effects of plasticizers containing amide groups on the properties of thermoplastic starch. Starch/Stärke 2004;56:545-51.

[63]   Ma X, Yu J, Ma YB. Urea and formamide as a mixed plasticizer for thermoplastic wheat flour. Carbohydr Polym 2005;60:111-6.

[64]   Yang J-h, Yu J-g, Ma X-f. Study on the properties of ethylenebisformamide and sorbitol plasticized corn starch (ESPTPS). Carbohydr Polym 2006;66:110-6.

[65]   Yang J-h, Yu J-g, Ma X-f. Preparation of a novel thermoplastic starch (TPS) material using ethylenebisformamide as the plasticizer. Starch/Stärke 2006;58:330-7.

[66]   Yang J-H, Yu J-G, Ma X-F. Preparation and properties of ethylenebisformamide plasticized potato starch (EPTPS). Carbohydr Polym 2006;63:218-23.

[67]   Dai H, Chang P, Peng F, Yu J, Ma X. *N*-(2-hydroxyethyl)formamide as a new plasticizer for thermoplastic starch. J Polym Res 2009;16:529-35.

[68]   Zheng P, Chang PR, Yu J, Ma X. Formamide and 2-hydroxy-*N*-[2-(2-hydroxy-propionylamino)-ethyl] propionamide (HPEP) as a mixed plasticizer for thermoplastic starch. Carbohydr Polym 2009;78:296-301.

[69]   Dai H, Chang PR, Geng F, Yu J, Ma X. Preparation and properties of starch-based film using *N,N*-bis(2-hydroxyethyl)formamide as a new plasticizer. Carbohydr Polym 2010;79:306-11.

[70]   Dai H, Chang PR, Yu J, Geng F, Ma X. *N*-(2-hydroxypropyl)formamide and *N*-(2-hydroxyethyl)-*N*-methylformamide as two new plasticizers for thermoplastic starch. Carbohydr Polym 2010;80:139-44.

[71]   Zhang J-s, Chang PR, Wu Y, Yu J-g, Ma X-f. Aliphatic amidediol and glycerol as a mixed plasticizer for the preparation of thermoplastic starch. Starch/Stärke 2008;60:617-23.

[72]   Ma X, Yu J, Feng J. Urea and formamide as a mixed plasticizer for thermoplastic starch. Polym Int 2004;53:1780-5.

[73]   Ma X, Yu J. Formamide as the plasticizer for thermoplastic starch. J Appl Polym Sci 2004;93:1769-73.

[74]   Shogren RL, Swanson CL, Thompson AR. Extrudates of cornstarch with urea and glycols: structure/mechanical property relations. Starch/Stärke 1992;44:335-8.

[75]   Shi R, Zhang Z, Liu Q, Han Y, Zhang L, Chen D, Tian W. Characterization of citric acid/glycerol co-plasticized thermoplastic starch prepared by melt blending. Carbohydr Polym 2007;69:748-55.

[76]   Yu J, Wang N, Ma X. The effects of citric acid on the properties of thermoplastic starch plasticized by glycerol. Starch/Stärke 2005;57:494-504.

[77]   Wang N, Yu J, Chang PR, Ma X. Influence of citric acid on the properties of glycerol-plasticized dry starch (DTPS) and DTPS/poly(lactic acid) blends. Starch/Stärke 2007;59:409-17.

[78]   Chaudhary AL, Miler M, Torley PJ, Sopade PA, Halley PJ. Amylose content

and chemical modification effects on the extrusion of thermoplastic starch from

maize. Carbohydr Polym 2008;74:907-13.

[79]   Lafargue D, Pontoire B, Buléon A, Doublier JL, Lourdin D. Structure and

mechanical properties of hydroxypropylated starch films. Biomacromolecules

2007;8:3950-8.

[80]   Vorwerg W, Dijksterhuis J, Borghuis J, Radosta S, Kröger A. Film properties

of hydroxypropyl starch. Starch/Stärke 2004;56:297-306.

[81]   Fringant C, Desbrières J, Rinaudo M. Physical properties of acetylated starch-

based materials: relation with their molecular characteristics. Polymer

1996;37:2663-73.

[82]   Fringant C, Rinaudo M, Foray MF, Bardet M. Preparation of mixed esters of

starch or use of an external plasticizer: two different ways to change the properties

of starch acetate films. Carbohydr Polym 1998;35:97-106.

[83]   Jarowenko W. Acetylated starch and miscellaneous organic esters. In:

Wurzburg OB. editor Modified starches: properties and uses. Boca Raton, FL:

CRC Press, 1986. p. 55-77.

[84]   Volkert B, Lehmann A, Greco T, Nejad MH. A comparison of different

synthesis routes for starch acetates and the resulting mechanical properties.

Carbohydr Polym 2010;79:571-7.

[85]   Zamudio-Flores PB, Torres AV, Salgado-Delgado R, Bello-Pérez LA.

Influence of the oxidation and acetylation of banana starch on the mechanical and

water barrier properties of modified starch and modified starch/chitosan blend

films. J Appl Polym Sci 2010;115:991-8.

[86]   Bergaya F, Jaber M, Lambert J-F. Clays and clay minerals as layered nanofillers for (bio)polymers. In: Avérous L, Pollet E. editors. Environmental Silicate Nano-Biocomposites (Green Energy and Technology). London: Springer-Verlag, 2012. p. 41-75.

[87]   Hendricks SB. Lattice structure of clay minerals and some properties of clays. J Geol 1942;50:276-90.

[88]   Jozja N, Baillif P, Touray J-C, Pons C-H, Muller F, Burgevin C. Impacts « multi-échelle » d'un échange (Mg,Ca)–Pb et ses conséquences sur l'augmentation de la perméabilité d'une bentonite. C R Geosci 2003;335:729-36.

[89]   Duquesne E, Moins S, Alexandre M, Dubois P. How can nanohybrids enhance polyester/sepiolite nanocomposite properties? Macromol Chem Phys 2007;208:2542-50.

[90]   Lagaly G. Interaction of alkylamines with different types of layered compounds. Solid State Ionics 1986;22:43-51.

[91]   Sinha Ray S, Okamoto K, Okamoto M. Structure−property relationship in biodegradable poly(butylene succinate)/layered silicate nanocomposites. Macromolecules 2003;36:2355-67.

[92]   Giannelis EP. Polymer layered silicate nanocomposites. Adv Mater 1996;8:29-35.

[93]   Mallapragada SK, Narasimhan B. Handbook of biodegradable polymeric materials and applications, Volume 1. American Scientific Publishers, 2006.

[94]   Chiou B-S, Yee E, Glenn GM, Orts WJ. Rheology of starch-clay nanocomposites. Carbohydr Polym 2005;59:467-75.

[95]   Pandey JK, Singh RP. Green nanocomposites from renewable resources: effect of plasticizer on the structure and material properties of clay-filled starch. Starch/Stärke 2005;57:8-15.

[96]   Chung Y-L, Ansari S, Estevez L, Hayrapetyan S, Giannelis EP, Lai H-M. Preparation and properties of biodegradable starch-clay nanocomposites. Carbohydr Polym 2010;79:391-6.

[97]   Namazi H, Mosadegh M, Dadkhah A. New intercalated layer silicate nanocomposites based on synthesized starch-*g*-PCL prepared via solution intercalation and in situ polymerization methods: as a comparative study. Carbohydr Polym 2009;75:665-9.

[98]   Wu J, Lin J, Zhou M, Wei C. Synthesis and properties of starch-*graft*-polyacrylamide/clay superabsorbent composite. Macromol Rapid Commun 2000;21:1032-4.

[99]   Zhou M, Zhao J, Zhou L. Utilization of starch and montmorrilonite for the preparation of superabsorbent nanocomposite. J Appl Polym Sci 2011;121:2406-12.

[100]   Luo W, Zhang Wa, Chen P, Fang Ye. Synthesis and properties of starch grafted poly[acrylamide-*co*-(acrylic acid)]/montmorillonite nanosuperabsorbent via *γ*-ray irradiation technique. J Appl Polym Sci 2005;96:1341-6.

[101]   Al E, Güçlü G, Banuİyim T, Emik S, Özgümü S. Synthesis and properties of starch-graft-acrylic acid/Na-montmorillonite superabsorbent nanocomposite hydrogels. J Appl Polym Sci 2008;109:16-22.

[102]   Fornes TD, Yoon PJ, Keskkula H, Paul DR. Nylon 6 nanocomposites: the effect of matrix molecular weight. Polymer 2001;42:09929-40.

[103]   Dennis HR, Hunter DL, Chang D, Kim S, White JL, Cho JW, Paul DR. Effect of melt processing conditions on the extent of exfoliation in organoclay-based nanocomposites. Polymer 2001;42:9513-22.

[104]   Dai H, Chang P, Geng F, Yu J, Ma X. Preparation and properties of thermoplastic starch/montmorillonite nanocomposite using *N*-(2-hydroxyethyl)formamide as a new additive. J Polym Environ 2009;17:225-32.

[105]   Huang M, Yu J. Structure and properties of thermoplastic corn starch/montmorillonite biodegradable composites. J Appl Polym Sci 2006;99:170-6.

[106]   Huang M, Yu J, Ma X. High mechanical performance MMT-urea and formamide-plasticized thermoplastic cornstarch biodegradable nanocomposites. Carbohydr Polym 2006;63:393-9.

[107]   Huang MF, Yu JG, Ma XF. Preparation of the thermoplastic starch/montmorillonite nanocomposites by melt-intercalation. Chin Chem Lett 2005;16:561-4.

[108]   Huang M-F, Yu J-G, Ma X-F. Studies on the properties of Montmorillonite-reinforced thermoplastic starch composites. Polymer 2004;45:7017-23.

[109]   Huang M-f, Yu J-g, Ma X-f, Jin P. High performance biodegradable thermoplastic starch-EMMT nanoplastics. Polymer 2005;46:3157-62.

[110]   Maksimov RD, Lagzdins A, Lilichenko N, Plume E. Mechanical properties and water vapor permeability of starch/montmorillonite nanocomposites. Polym Eng Sci 2009;49:2421-9.

[111]   Mondragón M, Mancilla JE, Rodríguez-González FJ. Nanocomposites from plasticized high-amylopectin, normal and high-amylose maize starches. Polym Eng Sci 2008;48:1261-7.

[112] Tang X, Alavi S, Herald TJ. Barrier and mechanical properties of starch-clay nanocomposite films. Cereal Chem 2008;85:433-9.

[113] Tang X, Alavi S, Herald TJ. Effects of plasticizers on the structure and properties of starch-clay nanocomposite films. Carbohydr Polym 2008;74:552-8.

[114] Wang N, Zhang X, Han N, Bai S. Effect of citric acid and processing on the performance of thermoplastic starch/montmorillonite nanocomposites. Carbohydr Polym 2009;76:68-73.

[115] de Carvalho AJF, Curvelo AAS, Agnelli JAM. A first insight on composites of thermoplastic starch and kaolin. Carbohydr Polym 2001;45:189-94.

[116] Park H-M, Lee W-K, Park C-Y, Cho W-J, Ha C-S. Environmentally friendly polymer hybrids Part I mechanical, thermal, and barrier properties of thermoplastic starch/clay nanocomposites. J Mater Sci 2003;38:909-15.

[117] Park H-M, Li X, Jin C-Z, Park C-Y, Cho W-J, Ha C-S. Preparation and properties of biodegradable thermoplastic starch/clay hybrids. Macromol Mater Eng 2002;287:553-8.

[118] Lilichenko N, Maksimov R, Zicans J, Merijs Meri R, Plume E. A biodegradable polymer nanocomposite: mechanical and barrier properties. Mech Compos Mater 2008;44:45-56.

[119] Cyras VP, Manfredi LB, Ton-That M-T, Vazquez A. Physical and mechanical properties of thermoplastic starch/montmorillonite nanocomposite films. Carbohydr Polym 2008;73:55-63.

[120] Majdzadeh-Ardakani K, Navarchian AH, Sadeghi F. Optimization of mechanical properties of thermoplastic starch/clay nanocomposites. Carbohydr Polym 2010;79:547-54.

[121] Chivrac F, Pollet E, Schmutz M, Avérous L. New approach to elaborate
exfoliated starch-based nanobiocomposites. Biomacromolecules 2008;9:896-900.

[122] Chivrac F, Pollet E, Schmutz M, Avérous L. Starch nano-biocomposites based
on needle-like sepiolite clays. Carbohydr Polym 2010;80:145-53.

[123] Ibrahim SM. Characterization, mechanical, and thermal properties of gamma
irradiated starch films reinforced with mineral clay. J Appl Polym Sci
2011;119:685-92.

[124] Ma X, Yu J, Wang N. Production of thermoplastic starch/MMT-sorbitol
nanocomposites by dual-melt extrusion processing. Macromol Mater Eng
2007;292:723-8.

[125] Ren P, Shen T, Wang F, Wang X, Zhang Z. Study on biodegradable
starch/OMMT nanocomposites for packaging applications. J Polym Environ
2009;17:203-7.

[126] Wang N, Zhang X, Han N, Liu H. A facile method for preparation of
thermoplastic starch/urea modified montmorillonite nanocomposites. J Compos
Mater 2010;44:27-39.

[127] Müller CMO, Laurindo JB, Yamashita F. Effect of nanoclay incorporation
method on mechanical and water vapor barrier properties of starch-based films.
Ind Crops Prod 2011;33:605-10.

[128] Qiao X, Jiang W, Sun K. Reinforced thermoplastic acetylated starch with
layered silicates. Starch/Stärke 2005;57:581-6.

[129] Kvien I, Sugiyama J, Votrubec M, Oksman K. Characterization of starch
based nanocomposites. J Mater Sci 2007;42:8163-71.

[130]   Hassan Nejad M, Ganster J, Bohn A, Volkert B, Lehmann A. Nanocomposites of starch mixed esters and MMT: Improved strength, stiffness, and toughness for starch propionate acetate laurate. Carbohydr Polym 2011;84:90-5.

[131]   Xie Y, Chang PR, Wang S, Yu J, Ma X. Preparation and properties of halloysite nanotubes/plasticized Dioscorea opposita Thunb. starch composites. Carbohydr Polym 2011;83:186-91.

[132]   He Y, Kong W, Wang W, Liu T, Liu Y, Gong Q, Gao J. Modified natural halloysite/potato starch composite films. Carbohydr Polym 2012;87:2706-11.

[133]   Gao W, Dong H, Hou H, Zhang H. Effects of clays with various hydrophilicities on properties of starch–clay nanocomposites by film blowing. Carbohydr Polym 2012;88:321-8.

[134]   Wilhelm HM, Sierakowski MR, Souza GP, Wypych F. Starch films reinforced with mineral clay. Carbohydr Polym 2003;52:101-10.

[135]   Chen B, Evans JRG. Thermoplastic starch-clay nanocomposites and their characteristics. Carbohydr Polym 2005;61:455-63.

[136]   Chivrac F, Pollet E, Dole P, Avérous L. Starch-based nano-biocomposites: plasticizer impact on the montmorillonite exfoliation process. Carbohydr Polym 2010;79:941-7.

[137]   Chivrac F, Pollet E, Avérous L. Shear induced clay organo-modification: application to plasticized starch nano-biocomposites. Polym Adv Technol 2009;21:578-83.

[138]   Chaudhary DS. Understanding amylose crystallinity in starch-clay nanocomposites. J Polym Sci, Part B: Polym Phys 2008;46:979-87.

[139]   Nejad MH, Ganster J, Volkert B. Starch esters with improved mechanical properties through melt compounding with nanoclays. J Appl Polym Sci 2010;118:503-10.

[140]   Wilhelm H-M, Sierakowski M-R, Souza GP, Wypych F. The influence of layered compounds on the properties of starch/layered compound composites. Polym Int 2003;52:1035-44.

[141]   Chivrac F, Angellier-Coussy H, Guillard V, Pollet E, Avérous L. How does water diffuse in starch/montmorillonite nano-biocomposite materials? Carbohydr Polym 2010;82:128-35.

[142]   Wang X, Zhang X, Liu H, Wang N. Impact of pre-processing of montmorillonite on the properties of melt-extruded thermoplastic starch/ montmorillonite nanocomposites. Starch/Stärke 2009;61:489-94.

[143]   Xiong H, Tang S, Tang H, Zou P. The structure and properties of a starch-based biodegradable film. Carbohydr Polym 2008;71:263-8.

[144]   Xu Y, Zhou J, Hanna MA. Melt-intercalated starch acetate nanocomposite foams as affected by type of organoclay. Cereal Chem 2005;82:105-10.

[145]   Chiou B-S, Wood D, Yee E, Imam SH, Glenn GM, Orts WJ. Extruded starch-nanoclay nanocomposites: effects of glycerol and nanoclay concentration. Polym Eng Sci 2007;47:1898-904.

[146]   Chiou BS, Yee E, Wood D, Shey J, Glenn G, Orts W. Effects of processing conditions on nanoclay dispersion in starch-clay nanocomposites. Cereal Chem 2006;83:300-5.

[147]   Zeppa C, Gouanvé, Espuche E. Effect of a plasticizer on the structure of biodegradable starch/clay nanocomposites: thermal, water-sorption, and oxygen-barrier properties. J Appl Polym Sci 2009;112:2044-56.

[148]   Magalhães NF, Andrade CT. Thermoplastic corn starch/clay hybrids: effect of clay type and content on physical properties. Carbohydr Polym 2009;75:712-8.

[149]   Zhang Q-X, Yu Z-Z, Xie X-L, Naito K, Kagawa Y. Preparation and crystalline morphology of biodegradable starch/clay nanocomposites. Polymer 2007;48:7193-200.

[150]   Kampeerapappun P, Aht-ong D, Pentrakoon D, Srikulkit K. Preparation of cassava starch/montmorillonite composite film. Carbohydr Polym 2007;67:155-63.

[151]   Chivrac F, Gueguen O, Pollet E, Ahzi S, Makradi A, Averous L. Micromechanical modeling and characterization of the effective properties in starch-based nano-biocomposites. Acta Biomater 2008;4:1707-14.

[152]   Magalhães NF, Andrade CT. Calcium bentonite as reinforcing nanofiller for thermoplastic starch. J Braz Chem Soc 2010;21:202-8.

[153]   Liu H, Chaudhary D, Yusa S-i, Tadé MO. Glycerol/starch/Na$^+$-montmorillonite nanocomposites: A XRD, FTIR, DSC and ^{1}H NMR study. Carbohydr Polym 2011;83:1591-7.

[154]   Chaudhary D, Liu H, John J, Tadé MO. Morphological investigation into starch bio-nanocomposites via synchrotron radiation and differential scanning calorimetry. J Nanotechnol 2011.

[155]   Chen M, Chen B, Evans JRG. Novel thermoplastic starch-clay nanocomposite foams. Nanotechnology 2005;16:2334.

[156]   Chivrac F, Gueguen O, Pollet E, Avérous L, Ahzi S, Belouettar S. Micromechanically-based formulation of the cooperative model for the yield behavior of starch-based nano-biocomposites. J Nanosci Nanotechnol 2010;10:2949-55.

[157] Mbey JA, Hoppe S, Thomas F. Cassava starch–kaolinite composite film. Effect of clay content and clay modification on film properties. Carbohydr Polym 2012;88:213-22.

[158] Dean K, Yu L, Wu DY. Preparation and characterization of melt-extruded thermoplastic starch/clay nanocomposites. Compos Sci Technol 2007;67:413-21.

[159] Bagdi K, Müller P, Pukánszky B. Thermoplastic starch/layered silicate composites: structure, interaction, properties. Compos Interfaces 2006;13:1-17.

[160] Wang N, Zhang X, Wang X, Liu H. Communications: Ionic liquids modified montmorillonite/thermoplastic starch nanocomposites as ionic conducting biopolymer. Macromol Res 2009;17:285-8.

[161] Wang B-X, Zhao X-P. The influence of intercalation rate and degree of substitution on the electrorheological activity of a novel ternary intercalated nanocomposite. J Solid State Chem 2006;179:949-54.

[162] Zhao X, Wang B, Li J. Synthesis and electrorheological activity of a modified kaolinite/carboxymethyl starch hybrid nanocomposite. J Appl Polym Sci 2008;108:2833-9.

[163] Lee SY, Xu YX, Hanna MA. Tapioca starch-poly (lactic acid)-based nanocomposite foams as affected by type of nanoclay. Int Polym Process 2007;22:429-35.

[164] Lee SY, Chen H, Hanna MA. Preparation and characterization of tapioca starch-poly(lactic acid) nanocomposite foams by melt intercalation based on clay type. Ind Crops Prod 2008;28:95-106.

[165] Lee SY, Hanna MA, Jones DD. An adaptive neuro-fuzzy inference system for modeling mechanical properties of tapioca starch-poly(lactic acid) nanocomposite foams. Starch/Stärke 2008;60:159-64.

[166] Lee S-Y, Hanna MA. Preparation and characterization of tapioca starch-poly(lactic acid)-Cloisite Na$^+$ nanocomposite foams. J Appl Polym Sci 2008;110:2337-44.

[167] Lee SY, Hanna MA. Tapioca starch-poly(lactic acid)-Cloisite 30B nanocomposite foams. Polym Compos 2009;30:665-72.

[168] Arroyo OH, Huneault MA, Favis BD, Bureau MN. Processing and properties of PLA/thermoplastic starch/montmorillonite nanocomposites. Polym Compos 2010;31:114-27.

[169] Pérez CJ, Alvarez VA, Mondragón I, Vázquez A. Mechanical properties of layered silicate/starch polycaprolactone blend nanocomposites. Polym Int 2007;56:686-93.

[170] Perez C, Vázquez A, Alvarez V. Isothermal crystallization of layered silicate/starch-polycaprolactone blend nanocomposites. J Therm Anal Calorim 2008;91:749-57.

[171] Pérez CJ, Alvarez VA, Mondragón I, Vázquez A. Water uptake behavior of layered silicate/starch-polycaprolactone blend nanocomposites. Polym Int 2008;57:247-53.

[172] Pérez CJ, Alvarez VA, Vázquez A. Creep behaviour of layered silicate/starch-polycaprolactone blends nanocomposites. Mater Sci Eng, A 2008;480:259-65.

[173] Kalambur SB, Rizvi SS. Starch-based nanocomposites by reactive extrusion processing. Polym Int 2004;53:1413-6.

[174] Kalambur S, Rizvi SSH. Biodegradable and functionally superior starch-polyester nanocomposites from reactive extrusion. J Appl Polym Sci 2005;96:1072-82.

[175] Kalambur S, Rizvi SSH. Rheological behavior of starch-polycaprolactone (PCL) nanocomposite melts synthesized by reactive extrusion. Polym Eng Sci 2006;46:650-8.

[176] Ikeo Y, Aoki K, Kishi H, Matsuda S, Murakami A. Nano clay reinforced biodegradable plastics of PCL starch blends. Polym Adv Technol 2006;17:940-4.

[177] Vertuccio L, Gorrasi G, Sorrentino A, Vittoria V. Nano clay reinforced PCL/starch blends obtained by high energy ball milling. Carbohydr Polym 2009;75:172-9.

[178] Dean KM, Do MD, Petinakis E, Yu L. Key interactions in biodegradable thermoplastic starch/poly(vinyl alcohol)/montmorillonite micro- and nanocomposites. Compos Sci Technol 2008;68:1453-62.

[179] Majdzadeh-Ardakani K, Nazari B. Improving the mechanical properties of thermoplastic starch/poly(vinyl alcohol)/clay nanocomposites. Compos Sci Technol 2010;70:1557-63.

[180] Dean KM, Petinakis E, Goodall L, Miller T, Yu L, Wright N. Nanostabilization of thermally processed high amylose hydroxylpropylated starch films. Carbohydr Polym 2011;86:652-8.

[181] Nayak SK. Biodegradable PBAT/starch nanocomposites. Polym-Plast Technol Eng 2010;49:1406-18.

[182] Raquez J-M, Nabar Y, Narayan R, Dubois P. Preparation and characterization of maleated thermoplastic starch-based nanocomposites. J Appl Polym Sci 2011;122:639-47.

[183] Bocchini S, Battegazzore D, Frache A. Poly (butylensuccinate co-adipate)-thermoplastic starch nanocomposite blends. Carbohydr Polym 2010;82:802-8.

[184]   Park H-M, Kim G-H, Ha C-S. Preparation and characterization of biodegradable aliphatic polyester/thermoplastic starch/organoclay ternary hybrid nanocomposites. Compos Interfaces 2007;14:427-38.

[185]   McGlashan SA, Halley PJ. Preparation and characterisation of biodegradable starch-based nanocomposite materials. Polym Int 2003;52:1767-73.

[186]   Mondragón M, Hernández EM, Rivera-Armenta JL, Rodríguez-González FJ. Injection molded thermoplastic starch/natural rubber/clay nanocomposites: morphology and mechanical properties. Carbohydr Polym 2009;77:80-6.

[187]   Avella M, De Vlieger JJ, Errico ME, Fischer S, Vacca P, Volpe MG. Biodegradable starch/clay nanocomposite films for food packaging applications. Food Chem 2005;93:467-74.

[188]   Cao X, Chen Y, Chang PR, Muir AD, Falk G. Starch-based nanocomposites reinforced with flax cellulose nanocrystals. Express Polym Lett 2008;2:502-10.

[189]   Cao X, Chen Y, Chang PR, Stumborg M, Huneault MA. Green composites reinforced with hemp nanocrystals in plasticized starch. J Appl Polym Sci 2008;109:3804-10.

[190]   Lu Y, Weng L, Cao X. Morphological, thermal and mechanical properties of ramie crystallites--reinforced plasticized starch biocomposites. Carbohydr Polym 2006;63:198-204.

[191]   Chen Y, Liu C, Chang PR, Anderson DP, Huneault MA. Pea starch-based composite films with pea hull fibers and pea hull fiber-derived nanowhiskers. Polym Eng Sci 2009;49:369-78.

[192]   Chen Y, Liu C, Chang PR, Cao X, Anderson DP. Bionanocomposites based on pea starch and cellulose nanowhiskers hydrolyzed from pea hull fibre: effect of hydrolysis time. Carbohydr Polym 2009;76:607-15.

[193] Teixeira EdM, Pasquini D, Curvelo AAS, Corradini E, Belgacem MN, Dufresne A. Cassava bagasse cellulose nanofibrils reinforced thermoplastic cassava starch. Carbohydr Polym 2009;78:422-31.

[194] Angles MN, Dufresne A. Plasticized starch/tunicin whiskers nanocomposites. 1. Structural analysis. Macromolecules 2000;33:8344-53.

[195] Angles MN, Dufresne A. Plasticized starch/tunicin whiskers nanocomposite materials. 2. Mechanical behavior. Macromolecules 2001;34:2921-31.

[196] Mathew AP, Dufresne A. Morphological investigation of nanocomposites from sorbitol plasticized starch and tunicin whiskers. Biomacromolecules 2002;3:609-17.

[197] Mathew AP, Thielemans W, Dufresne A. Mechanical properties of nanocomposites from sorbitol plasticized starch and tunicin whiskers. J Appl Polym Sci 2008;109:4065-74.

[198] Chang PR, Jian R, Zheng P, Yu J, Ma X. Preparation and properties of glycerol plasticized-starch (GPS)/cellulose nanoparticle (CN) composites. Carbohydr Polym 2010;79:301-5.

[199] Azizi Samir MAS, Alloin F, Dufresne A. Review of recent research into cellulosic whiskers, their properties and their application in nanocomposite field. Biomacromolecules 2005;6:612-26.

[200] Azizi Samir MAS, Alloin F, Sanchez J-Y, El Kissi N, Dufresne A. Preparation of cellulose whiskers reinforced nanocomposites from an organic medium suspension. Macromolecules 2004;37:1386-93.

[201] Bondeson D, Mathew A, Oksman K. Optimization of the isolation of nanocrystals from microcrystalline cellulose by acid hydrolysis. Cellulose 2006;13:171-80.

[202] Dong XM, Kimura T, Revol J-F, Gray DG. Effects of ionic strength on the isotropic−chiral nematic phase transition of suspensions of cellulose crystallites. Langmuir 1996;12:2076-82.

[203] Mohanty AK, Misra M, Drzal LT. Natural fibers, biopolymers, and their biocomposites. Boca Raton: CRC Press, 2005.

[204] Paakko M, Ankerfors M, Kosonen H, Nykanen A, Ahola S, Osterberg M, Ruokolainen J, Laine J, Larsson PT, Ikkala O, Lindstrom T. Enzymatic hydrolysis combined with mechanical shearing and high-pressure homogenization for nanoscale cellulose fibrils and strong gels. Biomacromolecules 2007;8:1934-41.

[205] Svagan AJ, Hedenqvist MS, Berglund L. Reduced water vapour sorption in cellulose nanocomposites with starch matrix. Compos Sci Technol 2009;69:500-6.

[206] Kaushik A, Singh M, Verma G. Green nanocomposites based on thermoplastic starch and steam exploded cellulose nanofibrils from wheat straw. Carbohydr Polym 2010;82:337-45.

[207] Le Corre Db, Bras J, Dufresne A. Starch nanoparticles: a review. Biomacromolecules 2010;11:1139-53.

[208] Angellier H, Choisnard L, Molina-Boisseau S, Ozil P, Dufresne A. Optimization of the preparation of aqueous suspensions of waxy maize starch nanocrystals using a response surface methodology. Biomacromolecules 2004;5:1545-51.

[209] Putaux J-L, Molina-Boisseau S, Momaur T, Dufresne A. Platelet nanocrystals resulting from the disruption of waxy maize starch granules by acid hydrolysis. Biomacromolecules 2003;4:1198-202.

[210] García NL, Ribba L, Dufresne A, Aranguren MI, Goyanes S. Physico-
mechanical properties of biodegradable starch nanocomposites. Macromol Mater
Eng 2009;294:169-77.

[211] Zeng M, Huang Y, Lu L, Fan L, Lourdin D. Effects of filler-matrix
morphology on mechanical properties of corn starch-zein thermo-moulded films.
Carbohydr Polym 2011;84:323-8.

[212] Viguié J, Molina-Boisseau S, Dufresne A. Processing and characterization of
waxy maize starch films plasticized by sorbitol and reinforced with starch
nanocrystals. Macromol Biosci 2007;7:1206-16.

[213] Ma X, Jian R, Chang PR, Yu J. Fabrication and characterization of citric acid-
modified starch nanoparticles/plasticized-starch composites. Biomacromolecules
2008;9:3314-20.

[214] Gopalan Nair K, Dufresne A, Gandini A, Belgacem MN. Crab shell chitin
whiskers reinforced natural rubber nanocomposites. 3. Effect of chemical
modification of chitin whiskers. Biomacromolecules 2003;4:1835-42.

[215] Sriupayo J, Supaphol P, Blackwell J, Rujiravanit R. Preparation and
characterization of α-chitin whisker-reinforced chitosan nanocomposite films with
or without heat treatment. Carbohydr Polym 2005;62:130-6.

[216] Paillet M, Dufresne A. Chitin whisker reinforced thermoplastic
nanocomposites. Macromolecules 2001;34:6527-30.

[217] Saito Y, Putaux JL, Okano T, Gaill F, Chanzy H. Structural aspects of the
swelling of β chitin in HCl and its conversion into α chitin. Macromolecules
1997;30:3867-73.

[218] Morin A, Dufresne A. Nanocomposites of chitin whiskers from riftia tubes and
poly(caprolactone). Macromolecules 2002;35:2190-9.

[219]   Chang PR, Jian R, Yu J, Ma X. Starch-based composites reinforced with novel chitin nanoparticles. Carbohydr Polym 2010;80:421-6.

[220]   Chang PR, Jian R, Yu J, Ma X. Fabrication and characterisation of chitosan nanoparticles/plasticised-starch composites. Food Chem 2010;120:736-40.

[221]   Tsai ML, Bai SW, Chen RH. Cavitation effects versus stretch effects resulted in different size and polydispersity of ionotropic gelation chitosan–sodium tripolyphosphate nanoparticle. Carbohydr Polym 2008;71:448-57.

[222]   Shu XZ, Zhu KJ. A novel approach to prepare tripolyphosphate/chitosan complex beads for controlled release drug delivery. Int J Pharm 2000;201:51-8.

[223]   García NL, Ribba L, Dufresne A, Aranguren M, Goyanes S. Effect of glycerol on the morphology of nanocomposites made from thermoplastic starch and starch nanocrystals. Carbohydr Polym 2011;84:203-10.

[224]   Angellier H, Molina-Boisseau S, Dole P, Dufresne A. Thermoplastic starch-waxy maize starch nanocrystals nanocomposites. Biomacromolecules 2006;7:531-9.

[225]   Wan YZ, Luo H, He F, Liang H, Huang Y, Li XL. Mechanical, moisture absorption, and biodegradation behaviours of bacterial cellulose fibre-reinforced starch biocomposites. Compos Sci Technol 2009;69:1212-7.

[226]   Grande CJ, Torres FG, Gomez CM, Troncoso OP, Canet-Ferrer J, Martínez-Pastor J. Development of self-assembled bacterial cellulose-starch nanocomposites. Mater Sci Eng, C 2009;29:1098-104.

[227]   Grande CJ, Torres FG, Gomez CM, Troncoso OP, Canet-Ferrer J, Martinez-Pastor J. Morphological characterisation of bacterial cellulose-starch nanocomposites. Polym Polym Compos 2008;16:181-5.

[228]   Woehl MA, Canestraro CD, Mikowski A, Sierakowski MR, Ramos LP,
Wypych F. Bionanocomposites of thermoplastic starch reinforced with bacterial
cellulose nanofibres: effect of enzymatic treatment on mechanical properties.
Carbohydr Polym 2010;80:866-73.

[229]   Siqueira G, Bras J, Dufresne A. Cellulose whiskers versus microfibrils:
influence of the nature of the nanoparticle and its surface functionalization on the
thermal and mechanical properties of nanocomposites. Biomacromolecules
2008;10:425-32.

[230]   Sreekala MS, Goda K, Devi PV. Sorption characteristics of water, oil and
diesel in cellulose nanofiber reinforced corn starch resin/ramie fabric composites.
Compos Interfaces 2008;15:281-99.

[231]   Luo HL, Lian JJ, Wan YZ, Huang Y, Wang YL, Jiang HJ. Moisture
absorption in VARTMed three-dimensional braided carbon-epoxy composites
with different interface conditions. Mater Sci Eng, A 2006;425:70-7.

[232]   Roman M, Winter WT. Effect of sulfate groups from sulfuric acid hydrolysis
on the thermal degradation behavior of bacterial cellulose. Biomacromolecules
2004;5:1671-7.

[233]   Harrison BS, Atala A. Carbon nanotube applications for tissue engineering.
Biomaterials 2007;28:344-53.

[234]   Wang J. Carbon-nanotube based electrochemical biosensors: a review.
Electroanalysis 2005;17:7-14.

[235]   Lahiff E, Lynam C, Gilmartin N, O'Kennedy R, Diamond D. The increasing
importance of carbon nanotubes and nanostructured conducting polymers in
biosensors. Anal Bioanal Chem 2010;398:1575-89.

[236]   Xiao Y, Li CM. Nanocomposites: from fabrications to electrochemical bioapplications. Electroanalysis 2008;20:648-62.

[237]   Famá LM, Pettarin V, Goyanes SN, Bernal CR. Starch/multi-walled carbon nanotubes composites with improved mechanical properties. Carbohydr Polym 2011;83:1226-31.

[238]   Valdés M, Valdés González A, García Calzón J, Díaz-García M. Analytical nanotechnology for food analysis. Microchim Acta 2009;166:1-19.

[239]   Cao X, Chen Y, Chang PR, Huneault MA. Preparation and properties of plasticized starch/multiwalled carbon nanotubes composites. J Appl Polym Sci 2007;106:1431-7.

[240]   Ma X, Yu J, Wang N. Glycerol plasticized-starch/multiwall carbon nanotube composites for electroactive polymers. Compos Sci Technol 2008;68:268-73.

[241]   Liu Z, Zhao L, Chen M, Yu J. Effect of carboxylate multi-walled carbon nanotubes on the performance of thermoplastic starch nanocomposites. Carbohydr Polym 2011;83:447-51.

[242]   Curran SA, Ajayan PM, Blau WJ, Carroll DL, Coleman JN, Dalton AB, Davey AP, Drury A, McCarthy B, Maier S, Strevens A. A Composite from poly(*m*-phenylenevinylene-*co*-2,5-dioctoxy-*p*-phenylenevinylene) and carbon nanotubes: a novel material for molecular optoelectronics. Adv Mater 1998;10:1091-3.

[243]   Ajayan PM. Nanotubes from carbon. Chem Rev 1999;99:1787-800.

[244]   Qi HJ, Teo KBK, Lau KKS, Boyce MC, Milne WI, Robertson J, Gleason KK. Determination of mechanical properties of carbon nanotubes and vertically aligned carbon nanotube forests using nanoindentation. J Mech Phys Solids 2003;51:2213-37.

[245]   Ruan SL, Gao P, Yang XG, Yu TX. Toughening high performance ultrahigh molecular weight polyethylene using multiwalled carbon nanotubes. Polymer 2003;44:5643-54.

[246]   Bonnet P, Albertini D, Bizot H, Bernard A, Chauvet O. Amylose/SWNT composites: from solution to film – synthesis, characterization and properties. Compos Sci Technol 2007;67:817-21.

[247]   Star A, Steuerman DW, Heath JR, Stoddart JF. Starched carbon nanotubes. Angew Chem Int Edit 2002;41:2508-12.

[248]   Casey A, Farrell GF, McNamara M, Byrne HJ, Chambers G. Interaction of carbon nanotubes with sugar complexes. Synth Met 2005;153:357-60.

[249]   Lii C-y, Stobinski L, Tomasik P, Liao C-d. Single-walled carbon nanotube--potato amylose complex. Carbohydr Polym 2003;51:93-8.

[250]   Stobinski L, Tomasik P, Lii C-Y, Chan H-H, Lin H-M, Liu H-L, Kao C-T, Lu K-S. Single-walled carbon nanotube-amylopectin complexes. Carbohydr Polym 2003;51:311-6.

[251]   Kim O-K, Je J, Baldwin JW, Kooi S, Pehrsson PE, Buckley LJ. Solubilization of single-wall carbon nanotubes by supramolecular encapsulation of helical amylose. J Am Chem Soc 2003;125:4426-7.

[252]   Yang L, Zhang B, Liang Y, Yang B, Kong T, Zhang L-M. In situ synthesis of amylose/single-walled carbon nanotubes supramolecular assembly. Carbohydr Res 2008;343:2463-7.

[253]   Fu C, Meng L, Lu Q, Zhang X, Gao C. Large-scale production of homogeneous helical amylose/SWNTs complexes with good biocompatibility. Macromol Rapid Commun 2007;28:2180-4.

[254] Wu Z, Feng W, Feng Y, Liu Q, Xu X, Sekino T, Fujii A, Ozaki M. Preparation and characterization of chitosan-grafted multiwalled carbon nanotubes and their electrochemical properties. Carbon 2007;45:1212-8.

[255] Ke G. A novel strategy to functionalize carbon nanotubes with cellulose acetate using triazines as intermediated functional groups. Carbohydr Polym 2010;79:775-82.

[256] Yan L, Chang PR, Zheng P. Preparation and characterization of starch-grafted multiwall carbon nanotube composites. Carbohydr Polym 2011;84:1378-83.

[257] Kim H, Macosko CW. Processing-property relationships of polycarbonate/graphene composites. Polymer 2009;50:3797-809.

[258] Wei T, Luo G, Fan Z, Zheng C, Yan J, Yao C, Li W, Zhang C. Preparation of graphene nanosheet/polymer composites using in situ reduction–extractive dispersion. Carbon 2009;47:2296-9.

[259] Jiang L, Shen X-P, Wu J-L, Shen K-C. Preparation and characterization of graphene/poly(vinyl alcohol) nanocomposites. J Appl Polym Sci 2010;118:275-9.

[260] Li R, Liu C, Ma J. Studies on the properties of graphene oxide-reinforced starch biocomposites. Carbohydr Polym 2011;84:631-7.

[261] Famá L, Rojo PG, Bernal C, Goyanes S. Biodegradable starch based nanocomposites with low water vapor permeability and high storage modulus. Carbohydr Polym 2012;87:1989-93.

[262] Rao Y, Pochan JM. Mechanics of polymer−clay nanocomposites. Macromolecules 2006;40:290-6.

[263] Chatterjee A, Deopura BL. Thermal stability of polypropylene/carbon nanofiber composite. J Appl Polym Sci 2006;100:3574-8.

[264]   Yang J, Lin Y, Wang J, Lai M, Li J, Liu J, Tong X, Cheng H. Morphology, thermal stability, and dynamic mechanical properties of atactic polypropylene/carbon nanotube composites. J Appl Polym Sci 2005;98:1087-91.

[265]   Pinnavaia TJ, Beall GW. Polymer-clay nanocomposites (Wiley series In polymer science). Chichester-New York-Weinheim-Brisbane-Singapore-Toronto: John Wiley & Sons, Ltd, 2000.

[266]   Meyer WH. Polymer electrolytes for lithium-ion batteries. Adv Mater 1998;10:439-48.

[267]   Lee SH, Cho E, Jeon SH, Youn JR. Rheological and electrical properties of polypropylene composites containing functionalized multi-walled carbon nanotubes and compatibilizers. Carbon 2007;45:2810-22.

[268]   Ma X, Chang PR, Yu J, Lu P. Characterizations of glycerol plasticized-starch (GPS)/carbon black (CB) membranes prepared by melt extrusion and microwave radiation. Carbohydr Polym 2008;74:895-900.

[269]   Ma X, Chang PR, Yu J, Lu P. Electrically conductive carbon Black (CB)/glycerol plasticized-starch (GPS) composites prepared by microwave radiation. Starch/Stärke 2008;60:373-5.

[270]   Godovsky D. Device applications of polymer-nanocomposites. In: Springer Berlin / Heidelberg, 2000. p. 163-205.

[271]   Wu M, Wang M, Ge M. Investigation into the performance and mechanism of SiO_2 nanoparticles and starch composite films. J Text Inst 2009;100:254-9.

[272]   Yun Y-H, Hwang K-J, Wee Y-J, Yoon S-D. Synthesis, physical properties, and characterization of starch-based blend films by adding nano-sized TiO_2/poly(methyl metacrylate-*co*-acrylamide). J Appl Polym Sci 2011;120:1850-8.

[273]   Yu J, Yang J, Liu B, Ma X. Preparation and characterization of glycerol plasticized-pea starch/ZnO-carboxymethylcellulose sodium nanocomposites. Bioresour Technol 2009;100:2832-41.

[274]   Ma X, Chang PR, Yang J, Yu J. Preparation and properties of glycerol plasticized-pea starch/zinc oxide-starch bionanocomposites. Carbohydr Polym 2009;75:472-8.

[275]   Zheng P, Chang PR, Yu J, Ma X. Preparation of Sb_2O_3-carboxymethyl cellulose sodium nanoparticles and their reinforcing action on plasticized starch. Starch/Stärke 2009;61:665-8.

[276]   Chang PR, Yu J, Ma X. Fabrication and characterization of Sb_2O_3/carboxymethyl cellulose sodium and the properties of plasticized starch composite films. Macromol Mater Eng 2009;294:762-7.

[277]   Rodriguez P, Muñoz-Aguirre N, San-Martín Martinez E, González de la Cruz G, Tomas SA, Zelaya Angel O. Synthesis and spectral properties of starch capped CdS nanoparticles in aqueous solution. J Cryst Growth 2008;310:160-4.

[278]   Radhakrishnan T, Georges MK, Sreekumari Nair P, Luyt AS, Djokovi, V. Study of sago starch-CdS nanocomposite films: fabrication, structure, optical and thermal properties. J Nanosci Nanotechnol 2007;7:986-93.

[279]   Vigneshwaran N, Sampath K, Kathe AA, Varadarajan PV, Prasad V. Functional finishing of cotton fabrics using zinc oxide–soluble starch nanocomposites. Nanotechnology 2006;17:5087-95.

[280]   Li JH, Ren CL, Liu X, De Hu Z, Xue DS. "Green" synthesis of starch capped CdSe nanoparticles at room temperature. Mater Sci Eng, A 2007;458:319-22.

[281]   Wei Q, Kang S-Z, Mu J. "Green" synthesis of starch capped CdS nanoparticles. Colloids Surf, A 2004;247:125-7.

[282] Chairam S, Poolperm C, Somsook E. Starch vermicelli template-assisted synthesis of size/shape-controlled nanoparticles. Carbohydr Polym 2009;75:694-704.

[283] Liu D, Chang PR, Deng S, Wang C, Zhang B, Tian Y, Huang S, Yao J, Ma X. Fabrication and characterization of zirconium hydroxide-carboxymethyl cellulose sodium/plasticized *Trichosanthes Kirilowii* starch nanocomposites. Carbohydr Polym 2011;86:1699-704.

[284] Tang S, Zou P, Xiong H, Tang H. Effect of nano-SiO_2 on the performance of starch/polyvinyl alcohol blend films. Carbohydr Polym 2008;72:521-6.

[285] Yao K, Cai J, Liu M, Yu Y, Xiong H, Tang S, Ding S. Structure and properties of starch/PVA/nano-SiO_2 hybrid films. Carbohydr Polym 2011;86:1784-9.

[286] Liao H-T, Wu C-S. New biodegradable blends prepared from polylactide, titanium tetraisopropylate, and starch. J Appl Polym Sci 2008;108:2280-9.

[287] Frost K, Barthes J, Kaminski D, Lascaris E, Niere J, Shanks R. Thermoplastic starch-silica-polyvinyl alcohol composites by reactive extrusion. Carbohydr Polym 2011;84:343-50.

[288] Božanić DK, Djoković V, Bibić N, Sreekumari Nair P, Georges MK, Radhakrishnan T. Biopolymer-protected CdSe nanoparticles. Carbohydr Res 2009;344:2383-7.

[289] Tang H, Xiong H, Tang S, Zou P. A starch-based biodegradable film modified by nano silicon dioxide. J Appl Polym Sci 2009;113:34-40.

[290] Leroux F, Besse J-P. Polymer interleaved layered double hydroxide: a new emerging class of nanocomposites. Chem Mater 2001;13:3507-15.

[291] Hofmeister W, Platen HV. Crystal chemistry and atomic order in brucite-related double-layer structures. Crystallogr Rev 1992;3:3-26.

[292]   Taubert A, Wegner G. Formation of uniform and monodisperse zincite crystals in the presence of soluble starch. J Mater Chem 2002;12:805-7.

[293]   Chung Y-L, Lai H-M. Preparation and properties of biodegradable starch-layered double hydroxide nanocomposites. Carbohydr Polym 2010;80:526-33.

[294]   Wu D, Chang PR, Ma X. Preparation and properties of layered double hydroxide-carboxymethylcellulose sodium/glycerol plasticized starch nanocomposites. Carbohydr Polym 2011;86:877-82.

[295]   Wu H, Liu C, Chen J, Chang PR, Chen Y, Anderson DP. Structure and properties of starch/α−zirconium phosphate nanocomposite films. Carbohydr Polym 2009;77:358-64.

[296]   Clearfield A, Berman JR. On the mechanism of ion exchange in zirconium phosphates—XXXIV. Determination of the surface areas of α-$Zr(HPO_4)_2 \cdot H_2O$ by surface exchange. J Inorg Nucl Chem 1981;43:2141-2.

[297]   Clearfield A, Duax WL, Garces JM, Medina AS. On the mechanism of ion exchange in crystalline zirconium phosphates - IV Potassium ion exchange of α-zirconium phosphate. J Inorg Nucl Chem 1972;34:329-37.

[298]   Sun L, Boo WJ, Browning RL, Sue H-J, Clearfield A. Effect of crystallinity on the intercalation of monoamine in α-zirconium phosphate layer structure. Chem Mater 2005;17:5606-9.

[299]   Murugan R, Ramakrishna S. Crystallographic study of hydroxyapatite bioceramics derived from various sources. Cryst Growth Des 2004;5:111-2.

[300]   Reis RL, Cunha AM, Allan PS, Bevis MJ. Structure development and control of injection-molded hydroxylapatite-reinforced starch/EVOH composites. Adv Polym Technol 1997;16:263-77.

[301] Meskinfam M, Sadjadi MAS, Jazdarreh H, Zare K. Biocompatibility evaluation of nano hydroxyapatite-starch biocomposites. J Biomed Nanotechnol 2011;7:455-9.

[302] Sadjadi MS, Meskinfam M, Sadeghi B, Jazdarreh H, Zare K. In situ biomimetic synthesis, characterization and in vitro investigation of bone-like nanohydroxyapatite in starch matrix. Mater Chem Phys 2010;124:217-22.

[303] Sundaram J, Durance TD, Wang R. Porous scaffold of gelatin-starch with nanohydroxyapatite composite processed via novel microwave vacuum drying. Acta Biomater 2008;4:932-42.

Figure captions

Figure 1   Chemical structures of amylose (a) and amylopectin (b).

Figure 2   Thermal endotherms of regular maize starch with different water contents (a–g: 74.57%, 65.3%, 51.8%, 40%, 29.9%, 16.15%, and 9%) measured by differential scanning calorimetry.
Reprinted from Reference [2], Copyright (2006), with permission from Elsevier.

Figure 3   XRD patterns of OMMT–CS and wheat starch-based nanocomposites reinforced by OMMT–CS, with different inorganic fraction (1, 3 and 6 wt.%).
Reprinted with permission from Reference [121]. Copyright (2008) American Chemical Society.

Figure 4   Effects of glycerol content on the XRD patterns of starch–MMT nanocomposites (1–5), compared with that of natural montmorillonite (6).
Reprinted from Reference [113], Copyright (2008), with permission from Elsevier.

Figure 5   TEM image of wheat starch–based nanocomposites reinforced by OMMT–CS at 3 wt.% loading level, highlighting the phase separation phenomenon.
Reprinted from Reference [141], Copyright (2010), with permission from Elsevier.

Figure 6   XRD patterns of maize starch-based nanocomposites with 6% MMT, plasticised using 15% glycerol (1), urea (2), and formamide (3).
Reprinted from Reference [113], Copyright (2008), with permission from Elsevier.

Figure 7 d_{001} as a function of the mass ratio of PVA and MMT–Na$^+$ at different

moisture contents (error based on the thickness variation of the extruded

starch films).

Figure 8   TEM images of starch nanocrystals: longitudinal and planar views.

Figure 9   Reaction scheme of CA and SNPs (SN–OH) for preparing CA-modified

SNPs.

Figure 10   Scheme of the bottom-up process for fabricating starch–BCNWs

nanocomposites: (a) starch granules are in suspension in the culture

medium; (b) after autoclaving, starch is partially gelatinised, amylose

leaches, and granules swell; (c) BCNWs grow in presence of the partially

gelatinised starch; and (d) after hot pressing, the nanocomposite shows

interpenetrating networks (IPN) of amylose and cellulose.

Figure 11   Mechanical properties (a) and moisture uptake (b) of the pea starch (PS)

film, the pea starch–pea hull fibre composite film (PS/PHF), and the pea

starch–nanowhiskers nanocomposite films (PS/PHFNW-t, where t

represents the acid hydrolysis time for the CNWs preparation).

Figure 12   SEM images of the fractured surface of glycerol plasticised composite film (a) and unplasticised composite film (b) both containing 2.5 wt.% starch nanocrystals.

Reprinted from [223], Copyright (2011), with permission from Elsevier.

Figure 13   SEM images of the fracture surface of the nanocomposite with 0.055 wt% MWCNTs: (a) an agglomerate of MWCNTs ($\times$5k) and (b) a single carbon nanotube wrapped with the starch–iodine complex ($\times$200k).

Reprinted from [237], Copyright (2011), with permission from Elsevier.

Figure 14   The electrical conductivity of glycerol-plasticised starch with different MWCNT contents: (a) the effect of water contents on the conductivity of nanocomposites with different MWCNT contents; (b) the conductivity of nanocomposites filled with various MWCNT contents at 0% water content (calculated).

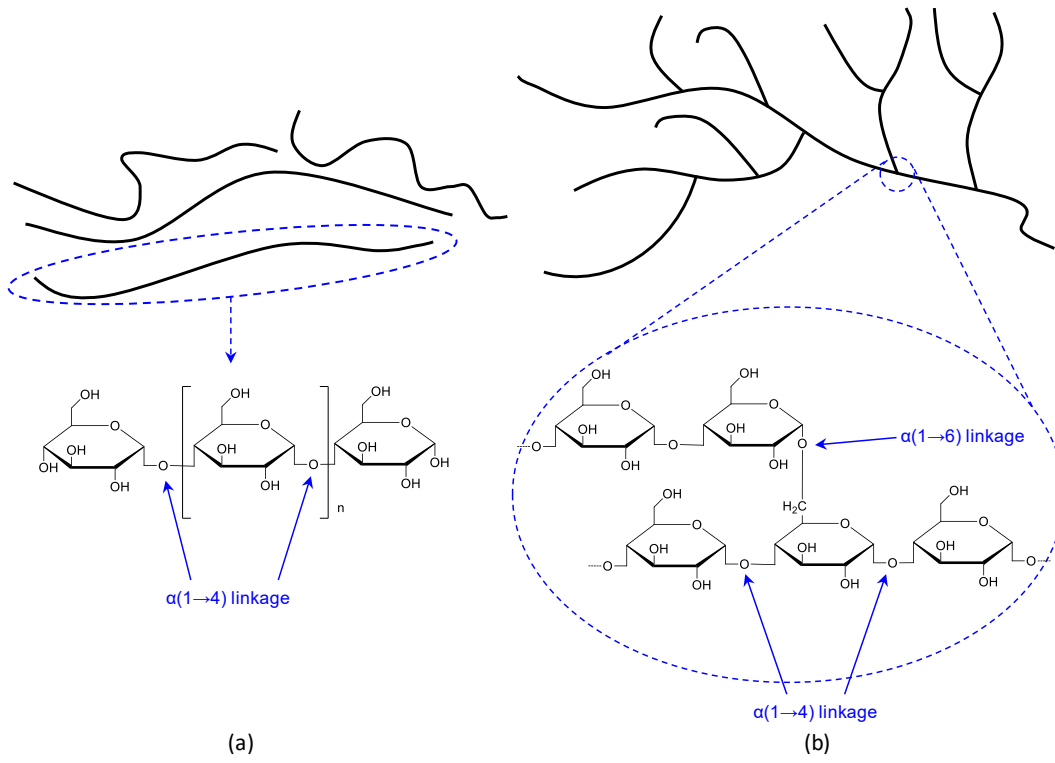Reprinted from [240], Copyright (2008), with permission from Elsevier.

α(1→4) linkage

(a)

α(1→6) linkage

α(1→4) linkage

(b)
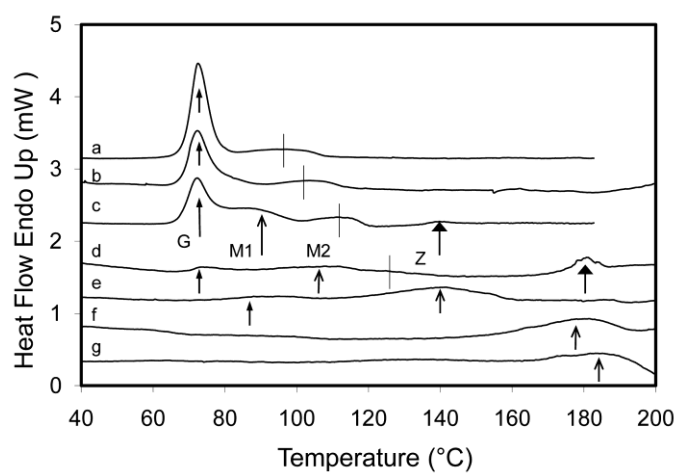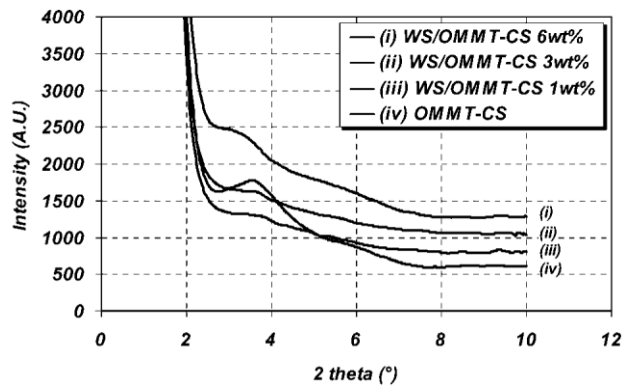
Figure 1

Figure 2

Figure 3
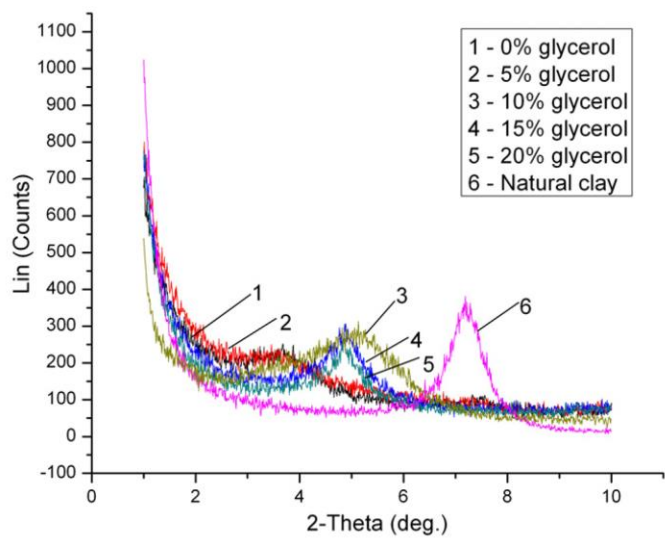
Figure 4
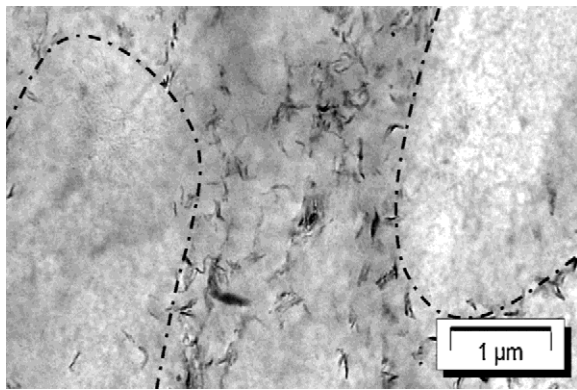
Figure 5

Figure 6

Figure 7

Longitudinal view

5-7 nm

9-10 nm

crystalline
amorphous

Planar view
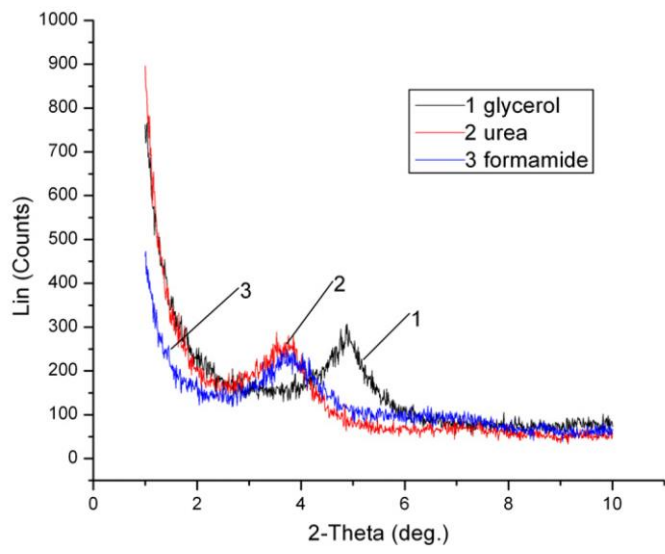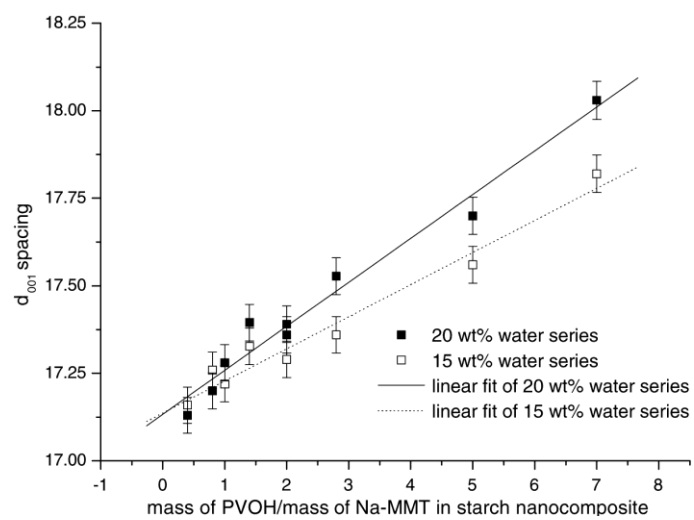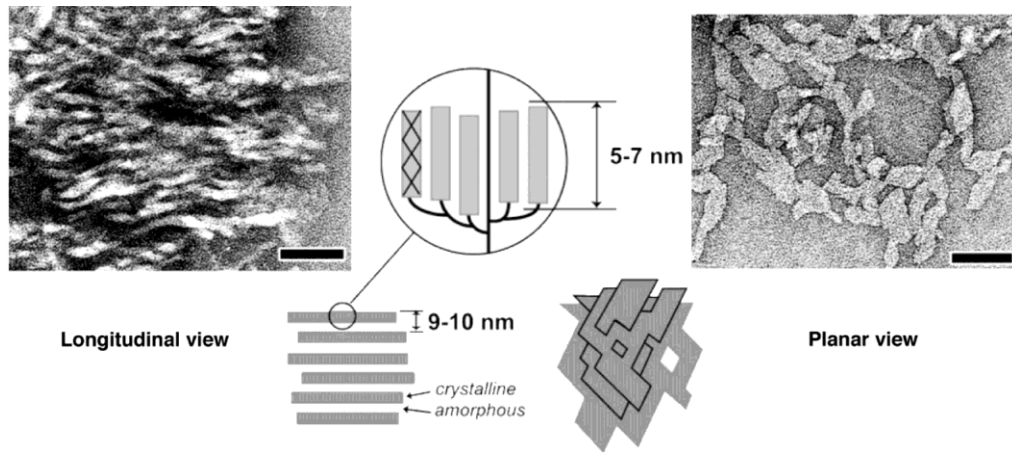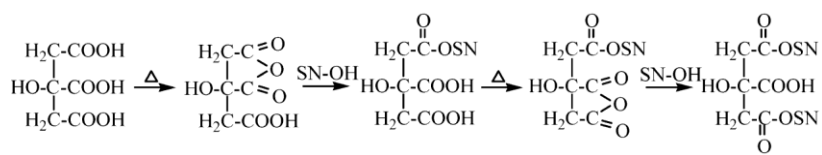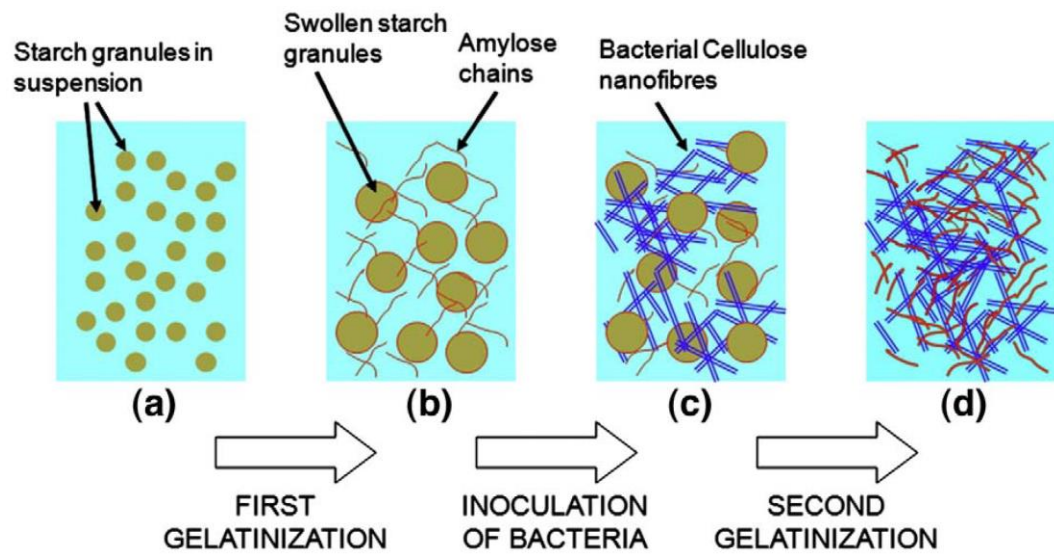
Figure 8

Figure 9

Figure 10
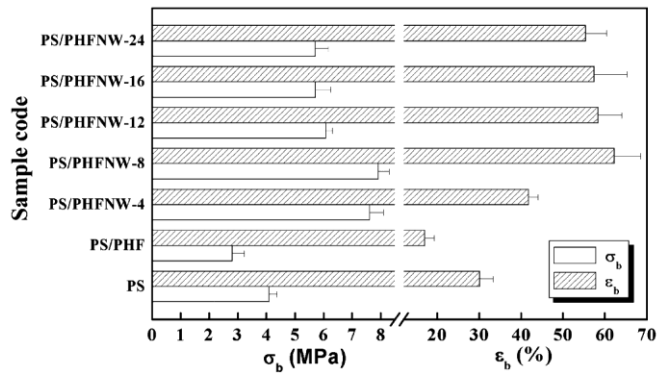
(a)
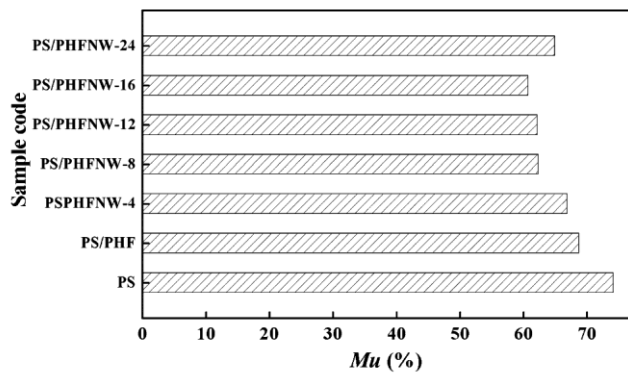
(b)

Figure 11

(a)

(b)

Figure 12

Figure 13

a

CNT0%: y=-9.39+19.95x-16.43x^2 R^2=0.99
CNT0.95%: y=-7.28+12.95x-9.76x^2 R^2=0.99
CNT1.9%: y=-5.95+10.37x-8.74x^2 R^2=0.99
CNT2.85%: y=-5.02+7.88x-6.76x^2 R^2=0.98
CNT3.8%: y=-2.47+1.40x-1.04x^2 R^2=0.97
CNT4.75%: y=-0.14+0.17x-0.07x^2 R^2=0.90

b
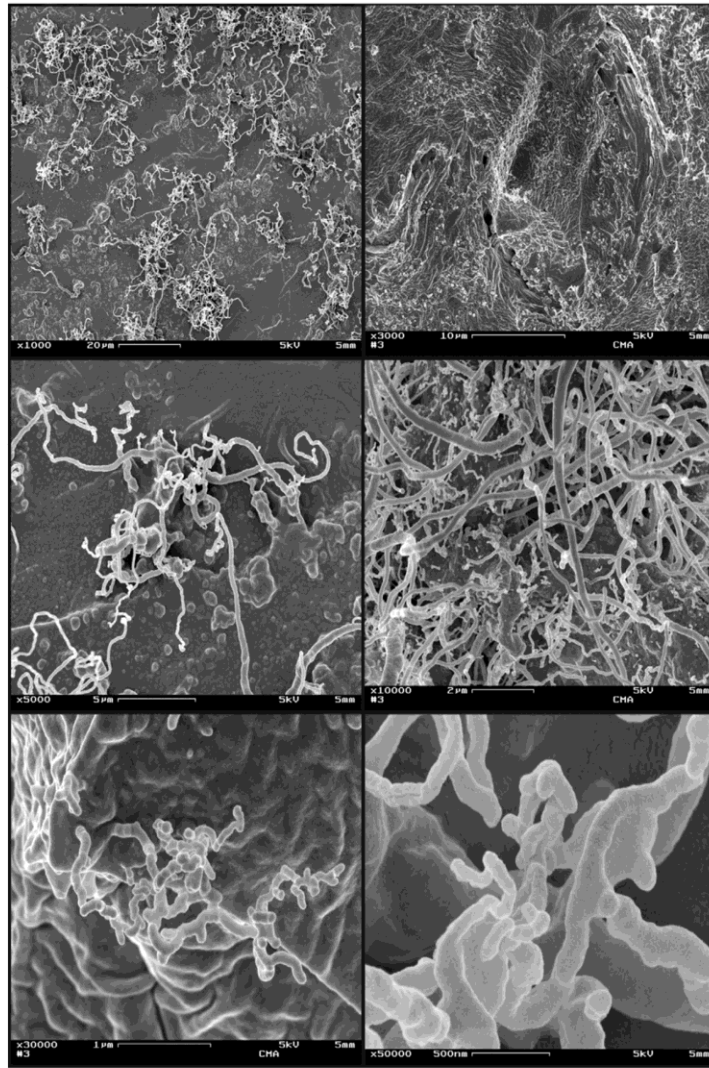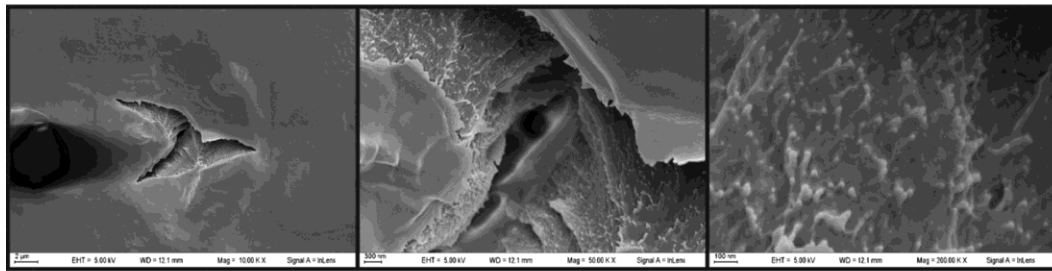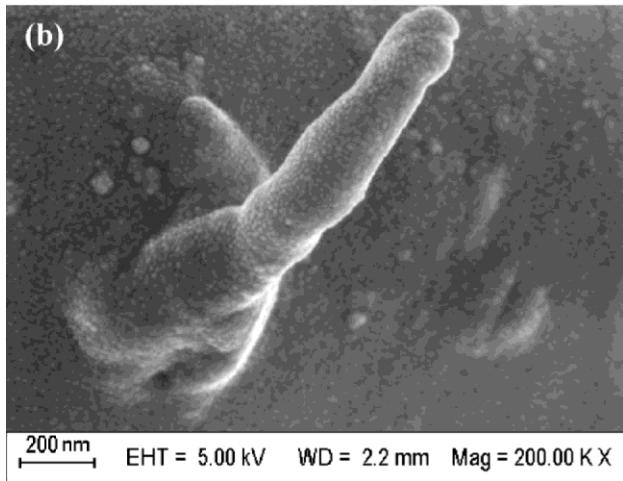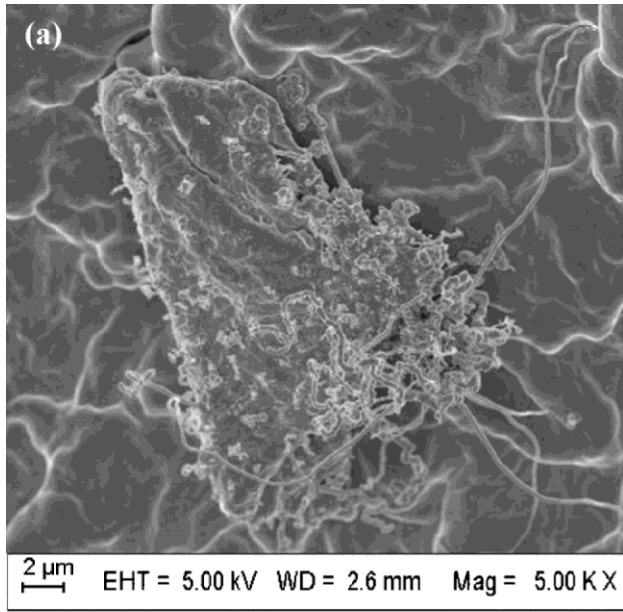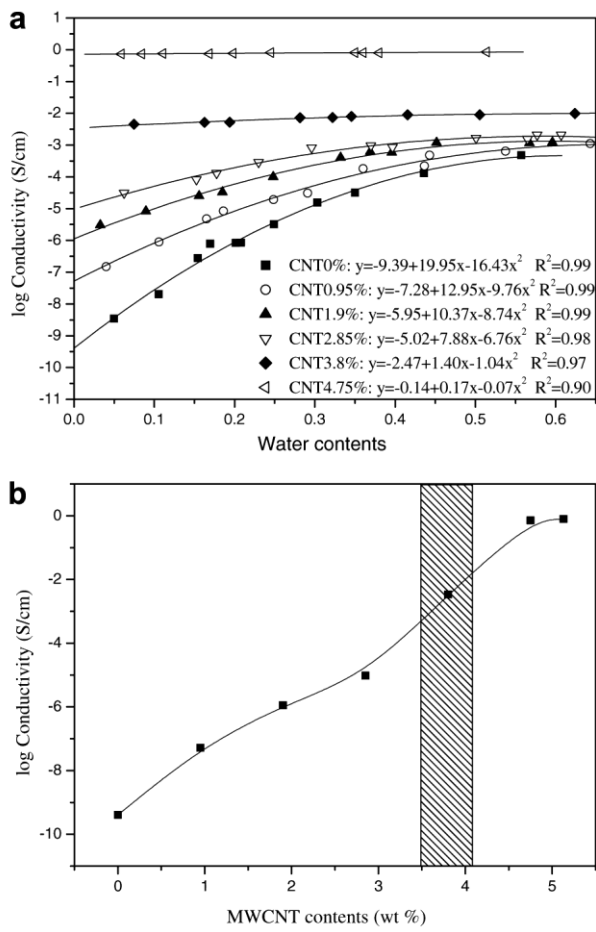
Figure 14

Tables

Table 1   Overview of the nanofillers used for starch-based nanocomposites

Group	Nanofiller	Dimensional Type	Remark
Phyllosilicates			
Clay minerals			
Kaolinite Group	Kaolinite	Nanolayer	Non-expandable
	Halloysite	Nanolayer (actually in cylindrical shape)	Non-expandable
Smectite Group	Montmorillonite	Nanolayer	Most expandable; most frequently used; natural sodium montmorillonite being a preferable choice due to the matching of polarity with starch
	Hectorite	Nanolayer	Expandable
Sepiolite Group	Sepiolite	Nanolayer (actually in needle shape)	–
Synthetic Clays	Somasif™ ME 100 fluorohectorite / fluoromica	Nanolayer	Montmorillonite- or hectorite-type synthetic clay

	Laponite® B, Laponite® RD	Nanolayer	Hectorite-type synthetic clay
Mica Group	Muscovite	Nanolayer	Non-expandable
	Paragonite	Nanolayer	Non-expandable
	Illite (hydrous mica)	Nanolayer	Non-expandable
Polysaccharides	Nanowhiskers / nanofibrils / nanofibres from cellulose	Nanotube / nanoparticle	Size and shape dependant on the preparation method and conditions
	Nanoparticles / nanocrystals from starch	Nanoparticle	–
	Nanoparticles from chitin / chitosan	Nanoparticle	–
Carbonaceous materials	Carbon nanotubes	Nanotube	–
	Graphite oxide	Nanolayer	–
	Carbon black	Nanoparticle	–
Metalloid oxides	Silicon dioxide (also silica) [SiO_2]	Nanoparticle	–
	Antimony trioxide [Sb_2O_3]	Nanoparticles	–
Metal oxides and chalcogenides	Zinc oxide [ZnO]	Nanoparticle	–
	Hydrous zirconium dioxide (also zirconia) [$ZrO_2 \cdot nH_2O$]	Nanoparticle	–
	Titanium dioxide (also titania) [TiO_2]	Nanoparticle	–
	Cadmium sulphide [CdS]	Nanoparticle	–

	Cadmium selenide [CdSe]	Nanoparticle	–
Metal phosphates	α–zirconium phosphate [Zr(HPO$_4$)·H$_2$O]	Nanolayer	–
Layered double hydroxides	[M$^{II}_{1-x}$M$^{III}_x$(OH)$_2$]$_{intra}$ [A$^{m-}_{x/m}$·nH$_2$O]$_{inter}$ [a]	Nanolayer	–
Non-silicate minerals	Brucite [Mg(OH)$_2$]	Nanolayer	–
	Hydroxyapatite [Ca$_{10}$(PO$_4$)$_6$(OH)$_2$]	Nanoparticle	–

[a] "M^{II}" and "M^{III}" are metal cations, "A" is the anion, and "intra" and "inter" denote the intralayer domain and the interlayer space, respectively.

Somasif™ is a trademark of CBC Co., Ltd. Japan; Laponite® is a registered trademark of Laporte Ind. Ltd. (SCP).

Table 2   The relative proportions of amorphous, single, and double-helix conformations for maize starches of varying amylose content along with their XRD patterns and degrees of crystallinity.

Adapted with permission from [28]. Copyright 2007 American Chemical Society.

Starch	Amylose content [a] (%)	Relative proportion [b] (%)			Degree of crystallinity [c]	XRD pattern
		V-type polymorph	Double-helix	Amorphous		
Waxy maize	3.4	0	47	53	29	A
Regular maize	24.4	3	33	64	21	A
Amylomaize (Gelose 50)	56.3	7	18	75	13	B
Amylomaize (Gelose 80)	82.9	14	38	68	15	B

[a] The maximum error for amylose content determination was 6%. [b] The maximum standard deviation for the ^{13}C NMR analysis calculation was 2.4%. [c] The maximum error for the calculation of degree of crystallinity was 3.5%.

Table 3　　　Unmodified and organomodified smectite group clays used for starch-based nanocomposites with the corresponding chemical

structures of counter-ions and their commercial trade names

Clay type	Counter-cation	Name
Montmorillonite (MMT)	Na^+	Natural sodium MMT; MMT–Na^+; Cloisite® Na^+; Dellite® LVF; Dellite® HPS; Nanofil® 757; BH Natural
	Methyl-tallow-bis-2-hydroxyethyl ammonium	Cloisite® 30B
	Dimethyl-benzyl-hydrogenated tallow ammonium	Cloisite® 10A; Bentone® 111; Dellite® 43B
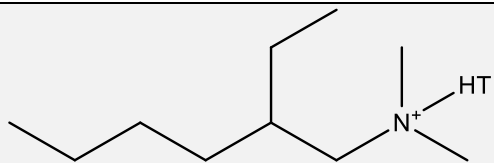
Dimethyl-hydrogenated tallow-2-ethylhexyl ammonium

Cloisite® 25A
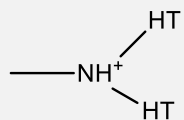
Methyl-dihydrogenated tallow ammonium

Cloisite® 93A
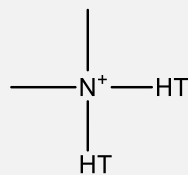
Dimethyl-dihydrogenated-tallow ammonium

Cloisite® 20A; Cloisite® 15A;

Cloisite® 6A; Dellite® 67G;

Dellite® 72T
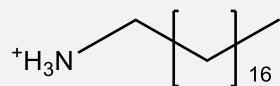
Octadecyl ammonium

Nanomer® I.30E
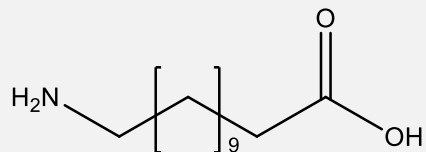
Nanofil® 784

Aminododecanoic acid
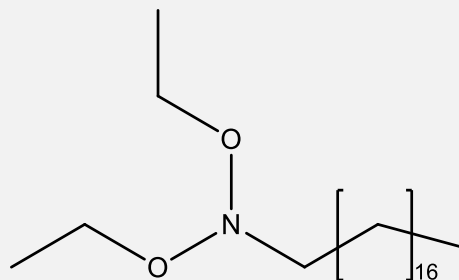
Nanofil® 804

Stearyl dihydroxyethyl ammonium
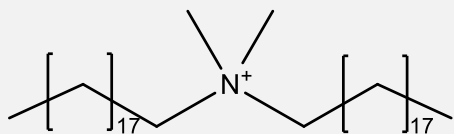
Nanofil® 948

Distearyl dimethyl ammonium chloride

–
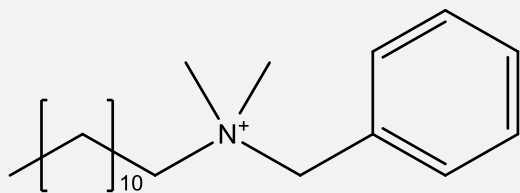
Dodecyl benzyl dimethyl ammonium bromide
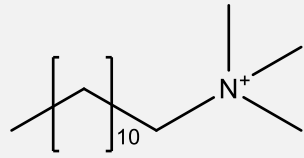
Dodecyl trimethyl ammonium

–
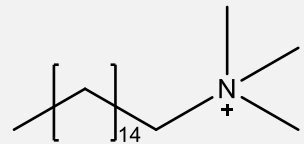
Hexodecyl trimethyl ammonium

–

Cationic starch

–
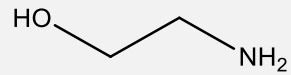
Ethanolamine

–
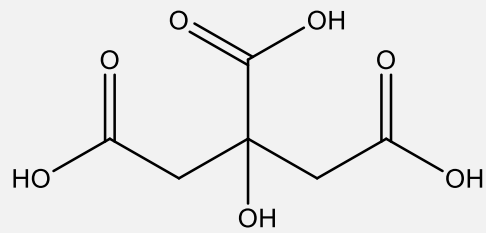
Citric acid

–

Hectorite Ca^{2+} Natural calcium hectorite;

99

|
——N$^+$——HT
|
HT

Bentone EA-163
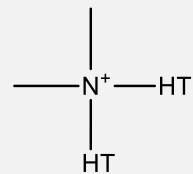
Bentone 109

Dimethyl-dihydrogenated-tallow ammonium

Cloisite® is a trademark of South Clay Products, Inc. (USA); Nanomer® is a trademark of Nanocor, Inc.; Dellite® is a trademark of Laviosa Chimica Mineraria , S.p.A. (Italy);

Nanofil® is a trademark of Süd Chemie AG (Germany); BH Natural is a product from Blackhill Bentonite LLC (USA); Bentone® is a trademark of Elementis Specialties

(USA); Nanomer® is a trademark of Nanocor, Inc. (USA).

T = tallow ($\approx$ 65% C18, $\approx$ 30% C16, $\approx$ 5% C14), HT = hydrogenated tallow.

The surface hydrophobicity of Cloisite clays: Na$^+$ < 30B < 10A < 25A < 93A < 20A < 15A.

Table 4   Water vapour sorption properties and oxygen transport properties of the different matrix and nanocomposite films.

Copyright © 2009 Wiley Periodicals, Inc.. Reproduced from [147] with permission.

Sample	M (%)	P (cm3 (STP) μm/(m^2 day)	$P_{composite}/P_{matrix}$	τ
S	13.3	187		
S/MMT–OH 6.25 wt.%	11.9	162	0.87	1.12
S/MMT–Na$^+$ 6.55 wt.%	12.9	105	0.56	1.71
SG	10.8	273		
SG/MMT–OH 5.6 wt.%	9.8	239	0.88	1.12
SG/MMT–Na$^+$ 6.1 wt.%	10.1	158	0.58	1.67
SUE	10.3	203		
SUE/MMT–OH 5.5 wt.%	8.2	136	0.67	1.47
SUE/MMT–Na$^+$ 6.4 wt.%	7.4	66	0.32	3.00

Abbreviations: M: equilibrium water content of the films on a dry basis; P: oxygen permeability coefficient at 20°C and 50% RH; $P_{composite}/P_{matrix}$: relative permeability; τ: tortuosity value deduced from Nielsen law.

Table 5   Changes in the interlayer spacing (d_{001}) of natural sodium montmorillonite as a result of pretreatment/activation

	Technique	d_{001} (nm)	References
Urea	Extrusion	1.01→1.86	[126]
Glycerol	High-speed emulsion	1.01→1.85	[114,142]
Sorbitol	Extrusion	1.01→1.80	[124]
Glycerol	Solution	1.01→1.63	[114,142]
Citric acid	Solution	1.01→1.55	[124]
N-(2-hydroxyethyl)formamide	Solution	1.01→1.37 [a]	[104]
1-ally1-3-methylimidazolium chloride	Solution	1.01→1.34	[160]
Ethanolamine	Solution	1.01→1.25	[109,173]

[a] The d_{001} of pretreated MMT–Na^+ was not shown in the reference thus that of MMT–Na^+ in the nanocomposite is shown here.

Table 6   Changes in the interlayer spacing (d_{001}) of pristine MMT nanofillers and starch–PLA nanocomposites reinforced by different MMT nanofillers (the weight ratio of starch and PLA was 9:1; and the MMT content was fixed at 3 wt.%.).

Nanofiller	d_{001} (nm)	Δd_{001} (nm)	References
Cloisite 30B	1.839→3.434	1.595	[163]
Cloisite 10A	1.896→3.424	1.528	[164]
Cloisite Na$^+$	1.222→2.398	1.175	[163]
Cloisite 25A	1.946→2.925	0.979	[164]
Cloisite 93A	2.337→3.201	0.864	[164]
Cloisite 20B	2.461→3.227	0.766	[163]
Cloisite 15A	2.832→3.178	0.346	[164]

Table 7   Summary of the polysaccharide nanofillers for starch-based nanocomposites

Source	Preparation method	Morphology	Dimensional characteristics	Remark	Reference
Plant cellulose				–	
Flax	Acid hydrolysis by H_2SO_4	Slender rods	L: 100 nm–500 nm; D: 10 nm–30 nm	Partly in the form of aggregates	Cao et al. [188]
Hemp	Acid hydrolysis by H_2SO_4	–	D: 30±10 nm	In the form of aggregates	Cao et al. [189]
Ramie	Acid hydrolysis by H_2SO_4	Spindle shape	L: 350 nm–700 nm; D: 70 nm–120 nm; L/D: 6	–	Lu et al. [190]
Wood	Mechanical shearing, enzymatic treatment, mechanical shearing, and high-pressure homogenisation	Fibres	L: several μm; D: 30±10 nm	–	Svagan et al. [205]
Pea hull	Acid hydrolysis by H_2SO_4	Needles or rod shape with one or two sharpened ends	L: 400±200 nm; D: 12±6 nm	Cellulose-I-type crystalline structure	Chen et al. [191,192]
Cassava bagasse	Acid hydrolysis by H_2SO_4	Long and curved	L: 360–1700 nm;	Low crystallinity: 54.1%;	Teixeira et al.

		elongated particles	D: 2–11 nm		[193]
Wheat straw	Steam explosion (with NaOH), acidic treatment by HCl, and high shear mechanical treatment	Fibre	D: 10–60 nm (most in the range of 30–40 nm)	The percentage of α-cellulose increased up to 86.38±3.12, and those of hemicellulose and lignin decreased to 8.13±0.8 and 6.34±1.25 respectively. The crystallinity increased to 79.87%. The tendency to agglomerate was also observed.	Kaushik et al. [206]
Microcrystalline cellulose (MC, commercially available)	Acid hydrolysis by H_2SO_4	Needle shape	L: ~200 nm; D: ~5 nm	–	Kvien et al. [129]
	Coagulated from a NaOH/urea/H_2O solution of MC by ethanol/HCl aqueous solution	Particles	D: 50–100 nm	The crystalline structure was composed of cellulose I and II, with the latter as newly formed.	Chang et al. [198]
Tunicin (animal cellulose)	Acid hydrolysis by H_2SO_4	Slender parallelepiped rods	L: 500 nm–2 μm; D: 10 nm; L/D: 50–200	Cellulose-I-type crystalline structure	Angles et al. [194,195] & Mathew et al.

					[196,197]
Bacteria cellulose	Bioinspired bottom-up process by *Acetobacter sp.* bacteria during the gelatinisation of starch	Coherent network of interconnected nanofibrils	D: 100–150 nm	High crystallinity, i.e. 74.8%	Grande et al. [226]
	Enzymatic hydrolysis of the *Acetobacter xylinum* bacterial cellulose by *Trichoderma reesei* endoglucanase	Fibre	D: 90 nm	Enzymatic hydrolysis smoothens the initially sharp profile of the fibres	Woehl et al. [228]
Starch					
Waxy maize	Acid hydrolysis by H_2SO_4	Platelet-like particles	L: 40–60 nm; W: 15–30 nm; T: 6–8 nm	Compact aggregates few micrometers long were observed.	Viguié et al. [212]
	Acid hydrolysis by H_2SO_4	Particle	D: 50 nm	Tend to form aggregates of around 1–5 μm; A-type crystalline structure	Angellier, et al. [224] & García et al. [210,223]
Regular maize	Treatments of gelatinised starch paste by ethanol and citric acid	Particles	D: 50–100 nm	Crosslinking and V_H-crystallinity were shown in starch nanoparticles	Ma et al. [213]
Chitin	Acid hydrolysis by HCl; repeated	Particles	D: 50–100 nm	α-chitin; lower crystallinity	Chang et al. [219]

				comparing to conventional chitin nanowhiskers	
	sonication processes				
Chitosan	Physical crosslinking between tripolyphosphate and protenised chitosan	Particles	D: 50–100 nm		Chang et al. [220]

L: length; *D*: diameter; *W*: width; *T*, thickness; *L/D*: aspect ratio

Table 8   Length (*L*), diameter (*D*), and aspect ratio (*L/D*) of pea hull fibre (PHF)

and the nanowhiskers hydrolysed from PHF by sulphuric acid (PHFNW-*t*) with

different acid hydrolysis times (*t*).

Reprinted from Reference [192], Copyright (2008), with permission from Elsevier.

| Sample code | *t* (h) | Size (average ± standard deviation) | | |
		L (nm)	*D* (nm)	*L*/D
PHF	0	34,000±21,000	14,000±6000	2.43
PHFNW-4	4	400±130	12±6	33.33
PHFNW-8	8	360±120	10±3	36.00
PHFNW-12	12	290±80	9±3	32.22
PHFNW-16	16	270±80	8±3	33.75
PHFNW-24	24	240±50	7±3	34.29

Table 9   Mechanical properties (E, Young's modulus; σ_b; strength at break; ε_b, elongation at break) of glycerol-plasticised waxy maize starch-based films with different plasticiser (glycerol or sorbitol) and nanofiller (SNPs) contents. Adapted with permission from [224] and [212]. Copyright 2006 and 2007 American Chemical Society.

Plasticiser type	Plasticiser content [a] (%)	Nanofiller content [a] (%)	Ageing [b]	E (MPa)	σ_b (MPa)	ε_b (%)
Glycerol	20	0	No	49 ± 12	2.4 ± 0.5	182 ± 52
		5	No	298 ± 54	13.2 ± 3.3	8.2 ± 1.5
		10	No	333 ± 54	13.6 ± 1.6	8.6 ± 1.5
		15	No	–	7.6 ± 2.9	4.5 ± 1.4
	25	0	No	11 ± 3.6	1.0 ± 0.1	297 ± 64
			Yes	59 ± 11	4.6 ± 0.7	61 ± 11
		2	No	75 ± 17	3.3 ± 0.4	122 ± 31
			Yes	147 ± 13	7.6 ± 0.7	57 ± 13
		5	No	80 ± 3.5	3.6 ± 0.4	97 ± 18
			Yes	154 ± 20	8.0 ± 0.7	52 ± 8.5
		10	No	82 ± 30	4.2 ± 1	57 ± 21
			Yes	173 ± 22	8.0 ± 0.4	33 ± 3.5
		15	No	241 ± 46	9.8 ± 1.4	20 ± 8
			Yes	$259 \pm ?$	$10.8 \pm ?$	$9 \pm ?$
	30	0	No	0.46 ± 0.3	0.26 ± 0.1	551 ± 80
		5	No	3.4 ± 1.1	1.3 ± 0.5	236 ± 40
		10	No	25 ± 14	2.7 ± 0.5	236 ± 40
		15	No	44 ± 5	3.6 ± 0.3	82 ± 13
Sorbitol	20	0	No	46.8 ± 2.5	1.06 ± 0.05	23 ± 2
	25	0	No	17.2 ± 1.1	0.38 ± 0.02	63 ± 4
			Yes	116.9 ± 2.5	4.46 ± 0.27	35 ± 3
	25	5	No	36.6 ± 1.6	0.99 ± 0.05	57 ± 8

		Yes	120.7 ± 6.0	4.47 ± 0.22	28 ± 2
	10	No	38.3 ± 3.6	1.37 ± 0.95	58 ± 5
		Yes	108.6 ± 3.3	3.81 ± 0.26	18 ± 2
	15	No	46.2 ± 7.0	1.59 ± 0.14	41 ± 12
		Yes	110.0 ± 0.6	4.42 ± 0.15	23 ± 2
35	0	No	6.02 ± 0.52	0.18 ± 0.05	107 ± 5
		Yes	51.1 ± 2.3	3.05 ± 0.05	42 ± 4
	5	No	9.93 ± 1.73	0.47 ± 0.03	92 ± 4
		Yes	69.1 ± 5.5	3.66 ± 0.11	26 ± 4
	10	No	18.8 ± 1.15	1.09 ± 0.02	64 ± 5
		Yes	24.9 ± 6.3	1.71 ± 0.35	29 ± 2
	15	No	42.5 ± 2.5	2.22 ± 0.14	45 ± 3
		Yes	58.4 ± 7.1	3.10 ± 0.10	28 ± 3
	25	No	103.0 ± 7.0	4.31 ± 0.21	31 ± 2

[a] based on the total weight of starch and plasticiser

[b] carried out at 88% RH for one week in addition to conditioning at 43% RH for one week

Appendices

Appendix 1   Preparation techniques, structures, and properties of starch-based nanocomposites reinforced by phyllosilicates

References	Plasticiser (/additive) type and content [a]	Preparation technique and conditioning	Matrix (type of starch)	Nanofiller type and content [a]	Composite structure and d_{001} (nm)	Matrix crystallinity	Thermal properties T_g (°C); T_d (°C)	Mechanical properties σ_u (MPa); σ_b (MPa); σ_y (MPa); E (MPa); ε_b (%)	Moisture sensitivity [b] M (%); M_∞ (%); D (mm$^2 \cdot$s^{-1}); P (g·m$^{-1}\cdot$s$^{-1}\cdot$Pa^{-1}); θ_c (°)
	No plasticiser								
Xu et al. [144]	Ethanol, 12% (s)	ME	Amylomaize (AC ≈ 70%) SA (DS = 1.78)	Cloisite 30B, 5% (?)	Intercalated, 1.87→3.95	–	T_g: 139→153; T_d: 370→386	–	–
				Cloisite 10A, 5% (?)	Intercalated, 1.99→3.81	–	T_g: 139→148; T_d: 370→387	–	–
				Cloisite 25A,	Intercalated,	–	T_g: 139→145;	–	–

				5% (?)	1.86→3.46		T_d: 370→387		
				Cloisite 20A, 5% (?)	Intercalated, 2.40→3.75	–	T_g: 139→147; T_d: 370→393	–	–
	Only water								
Zeppa et al. [147]	20% (s+p)	SC; vacuum, 6 w	Potato	MMT–Na$^+$, 5.6% (s+p+f)	Intercalated / exfoliated, 1.17→?	B, unchanged	T_d: 313→314	–	M_∞: 13.3→12.9 (?)
				Cloisite 30B, 6.1% (s+p+f)	CC, 1.85→?	B, unchanged	T_d: 313→312	–	M_∞: 13.3→11.9 (?)
	Glycerol	**Solution**							
Wilhelm et al. [134]	20% (s)	SC; 43% RH, 3 w	Cará	Hectorite–Ca$^+$, 30% (s+f)	Intercalated by glycerol, 1.44→1.86	–	T_g: 31→38	E: 815→1406; ε_b: 11→5	–
Pandey and Singh [95]	20% (s+p+f)	SC; ASTM E 104-02	Maize	MMT–Na$^+$, 5% (s+p+f)	Intercalated, ?→2.68 (increased)	–	–	E: 790→825; ε_b: 10→12	M^*: 34→23 (98% RH, 50 h)
Cyras et al. [119]	30% (s)	SC (sonicated);	Potato	MMT–Na$^+$, 5% (s+f)	Intercalated, 1.21→?	–	T_d^*: 287→312	σ_u: 3.3→5.2; σ_b: 3.1→4.1;	θ_c: 49.46→32.16 (ethylene glycol) / 43.71→42.63

Reference	Plasticizer	Method	Source	Filler	Structure		Thermal	Mechanical	Other
		vacuum, 6 w			(increased)			E: 30→196; ε_b: 62.6→46.8	(diiodomethane) M: decreased (75% RH) D: 2.00×10^8→1.73×10^8
Zeppa et al. [147]	20% (s+p)	SC; vacuum, 6 w	Potato	MMT–Na$^+$, 5.6% (s+p+f)	Intercalated / exfoliated, 1.17→?	B, unchanged	T_d: 315→318	–	M: 10.8→10.1 (?)
				Cloisite 30B, 6.1% (s+p+f)	CC, 1.85→?	B, unchanged	T_d: 315→315	–	M: 10.8→9.8 (?)
Chung et al. [96]	30% (s+f)	Solution, precipitated by ethanol, and CM	Maize	MMT–Na$^+$, 5% (s)	Exfoliated	B, decreased	–	σ_u: 11.8→15.5; E: 840→1390; ε_b: 4.62→4.34	–
				MMT–Na$^+$, (modified with chitosan), 5% (s)	Exfoliated	B, decreased	–	σ_u: 11.8→12.5; E: 840→805; ε_b: 4.62→5.35	–
				Laponite RD, 5% (s)	Exfoliated	B, decreased	–	σ_u: 11.8→15.5; E: 840→1406;	–

Author	Plasticizer	Process	Starch	Filler	Morphology / d-spacing		Thermal	Mechanical	Moisture / Other
								ε_b: 4.62→3.34	
Mondragón et al. [111]	30% (s)	SC; dried, 16 h	Amylomaize / regular maize/ waxy maize	Natural MMT (PGW G105), 10% (s+p)	Intercalated, 1.29→1.75 / 1.29→1.69 / 1.29→1.76	–	–	σ_u^*: 11.2→14.2; E^*: 380→435; ε_b^*: 24→22 / σ_u^*: 5.3→13.0; E^*: 245→325; ε_b^*: 35→29 / σ_u^*: 1.3→7.7; E^*: 55→370; ε_b^*: 25→14	M^*: 48→35 / M^*: 47→40 / M^*: 48→48 (98% RH, 2 w)
	Glycerol	**Melt**	**Unmodified starch**						
De Carvalho et al. [115]	30% (s)	MM, and CM; 60–70%	Maize	Kaolinite, 50% (s)	–	–	T_g: decreased (seen from the trend)	σ_u: 5.0→7.4; E: 125→293; ε_b: 31→14	M: 27.0→13.4 (100% RH, 3 d)
Park et al. [116,117]	30% (s+w+p)	MM, and IM	Potato	MMT–Na$^+$, 5% (?)	Intercalated, 1.17→1.78	–	T_g: 7→12 T_d: 305→336	σ_u: 2.61→3.32; ε_b: 47.0→57.2	P: decreased
				Cloisite 30B,	Slightly	–	T_g: 7→5.3	σ_u: 2.61→2.80;	P: decreased

				5% (?)	intercalated			ε_b: 47.0→44.5	
				Cloisite 10A, 5% (?)	CC	–	T_g: 7→0.1	σ_u: 2.61→2.14; ε_b: 47.0→34.9	P: decreased
				Cloisite 6A, 5% (?)	CC	–	T_g: 7→−3.8	σ_u: 2.61→2.51; ε_b: 47.0→38.0	P: decreased
Huang et al. [108]	30% (s)	ME; 39% RH, 2 w	Maize	MMT–Na$^+$, 30% (?)	–	A and V_H, almost disappeared	T_g: increased	σ_u: 5.5→27.3; σ_y: 3.5→25.5; E: 38→207; ε_b: 85.3→17.8	M_∞^*: 23.0→19.4 (50% RH)
Chen and Evans, [135]	30% (s)	MM and CM	Potato	MMT–Na$^+$, 13% (s+f+p)	Intercalated / exfoliated, 1.23→1.8	–	–	E^*: 5→8.8	–
				Natural hectorite, 13% (s+f+p)	Intercalated, 1.23→1.8	–	–	E^*: 5→7.8	–
				Bentone 109, 13% (s+f+p)	CC	–	–	E^*: 5→6.3	–
				Kaolinite,	CC	–	–	E^*: 5→6.4	–

				11% (s+f+p)					
Zhang et al. [149]	37.5% (s+p+f)	ME, and CM	Amylomaize (AC ≈70%)	MMT–Na$^+$, 3.125% (s+p+f)	Intercalated by glycerol, 1.2→1.8	V_a, 13→10%	T_d: 344→349	–	–
				Cloisite 93A, 3.125% (s+p+f)	Intercalated, 2.6→3.4	V_a, 13→11%	T_d: 344→335	–	–
Tang et al. [112]	15% (?)	ME, milling grinding, and SC	Maize / wheat / potato	MMT–Na$^+$, 9% (?)	Intercalated, 1.23→1.77	–	–	σ_u: 14.2→23.6; ε_b: 5.26→4.82 / σ_u: 14.1→21.3; ε_b: 6.08→5.09 / σ_u: 14.6→22.3; ε_b: 5.47→6.06 /	P: 4.47×10^{-10}→2.14×10^{-10} / P: 4.81×10^{-10}→2.28×10^{-10} / P: 5.03×10^{-10}→2.33×10^{-10}
				Nanomer I30E, 9% (?)	CC with tactoids, 2.23 (unchanged)	–	–	σ_u: 14.2→13.2; ε_b: 5.26→4.99 (maize)	P: 4.47×10^{-10}→4.33×10^{-10} (maize)
Magalhães et. al. [152]	25% (?)	ME	Maize	Natural Ca bentonite	Exfoliated, with tactoids,	B and V_H, decreased	T_d: decreased	E: 88.7→115.4; ε_b: decreased	–

Chivrac et al. [121,122,137,141]	23% (s+p+w)	MM; 57%RH, 1 m	Wheat	(NT25), 11.65% (?)	1.53→nil				
				MMT–Na⁺, 6% (s+p)	Intercalated by glycerol, 1.2→1.8	–	T_g: 11.7→23.9	σ_b^*: 2.3→1.8; E^*: 28→39; ε_b^*: 32→21	P: 4.68×10^{-10}→3.96×10^{-10}
				OMMT–CS, (prepared in solution), 6% (s+p)	Intercalated / exfoliated, with tactoids, 2.45→2.75	–	T_g: 11.7→21.7	σ_b^*: 2.3→2.6; E^*: 28→47; ε_b^*: 32→33	P: 4.68×10^{-10}→5.58×10^{-10}
				OMMT–CS, (prepared under shear condition), 3% (s+p)	Exfoliated	–	–	E^*: 28→45; ε_b^*: 32→34	–
				SEP–Na⁺, 6% (s+p)	–	E_H and V_H, new crystal structure appeared	T_d: 318→326	σ_b: 2.24→2.99; E: 28.3→67.3; ε_b: 31.7→31.0	–

Reference	Content	Method	Source	Filler	Ratio	Barrier	Thermal	Mechanical	Permeability
				OSEP–CS, 6% (s+p)	–	E_H and V_H, new crystal structure appeared	T_d: 318→306	σ_b: 2.24→3.19; E: 28.3→74.8; ε_b: 31.7→34.6	–
Wang et al. [114,142]	30% (s)	ME, and CM; airtight, 1 w	Maize	MMT–Na$^+$, 7% (s)	Intercalated, 1.01→1.90	–	T_g: 37.9→50.8	–	P^*: 5.0×10^{-10}→2.6×10^{-10}
				MMT–Na$^+$ (pretreated with glycerol by HSEM), 7% (s)	Intercalated, 1.01→2.17	–	T_g: 37.9→53.4; T_d: decreased (seen from the trend)	σ_u^*: 5.2→8.4; ε_b^*: 72→52	P^*: 5.0×10^{-10}→2.2×10^{-10}
Müller et al. [127]	25% (s)	ME, and CM	Cassava	Natural sodium bentonite, 3%	1.37→1.76	V_A, 14→21%	–	σ_u: 0.96→1.45; E: 16→42; ε_b: 63.3→72.93	P: 2.1×10^{-10}→1.7×10^{-10}
				Natural sodium bentonite (pre-	1.37→1.73	V_A, 14→16%	–	σ_u: 0.96→16.47; E: 16→789	P: 2.1×10^{-10}→0.83×10^{-10}

				dispersed with glycerol), 3%				ε_b: 63.3→2.60	
	Glycerol	**Melt**	**Modified starch**						
Qiao et al. [128]	50% (s)	MM, and CM; airtight, 3 d	Potato SA	MMT–Na$^+$, 5% (s)	Intercalated, 1.42→1.75	–	T_g: increased; T_d: unchanged	σ_u: 5.48→8.75; ε_b: 49.6→38.4	
				OMMT (DTA as the cation), 5% (s)	Intercalated, 2.63→3.10	–	T_g: increased; T_d: unchanged	σ_u: 5.48→10.36; ε_b: 49.6→28.0	
	Sorbitol								
Kvien et al. [129]	29.4% (s+p+w+f)	SC; 53% RH, 3 w	HP (DS = 0.11) and oxidised (DS = 0.04) potato	Laponite B, 5.2% (s+p+w+f)	–	–	T_g: 55→79; T_m: 134→160	σ_u: 370→470; σ_y: 11.3→12.5; ε_b: 25→31	–
	Triacetin								
Nejad et al. [130]	10% (s)	ME and IM;	Amylomaize	Dellite LVF,	–	–	T_g: 88→96	σ_u: 19.5→25.1;	–

Reference		Process	Starch	Clay, loading			T_g	Mechanical	Permeability
	50% RH, 24 h			(AC ≈ 50%) 5% (s) SPAL				E: 0.97→1.33; ε_b: 25.4→18.2	
			Amylomaize (AC ≈ 50%) 5% (s) SPAL	Dellite 43B,	–	–	T_g: 88→96	σ_u: 19.5→24.0; E: 0.97→1.64; ε_b: 25.4→16.8	–
			Amylomaize (AC ≈ 50%) 5% (s) SAPL	Dellite LVF,	–	–	T_g: 108→114	σ_u: 19.5→25.1; E: 1.51→1.71; ε_b: 25.2→20.1	–
			Amylomaize (AC ≈ 50%) 5% (s) SAPL	Dellite 43B,	–	–	T_g: 108→109	σ_u: 19.5→24.0; E: 1.51→2.11; ε_b: 25.2→27.1	–
Urea									
Tang et al. [112,113]	15% (?)	ME, milling grinding, and SC	Maize	MMT–Na+, 6% (?)	–	–	–	σ_u: 14.2→21.2; ε_b: 5.26→2.49	P: 4.47×10⁻¹⁰→2.50×10⁻¹⁰
Formamide									
Tang et al. [112,113]	15% (?)	ME, milling grinding,	Maize	MMT–Na+, 6% (?)	–	–	–	σ_u: 14.2→26.4 ε_b: 5.26→3.25	P: 4.47×10⁻¹⁰→1.61×10⁻¹⁰

and SC

N-(2-hydroxylethyl formamide

Dai et al. [104]	30% (s)	ME; 44% RH, 28 d	Maize	MMT–Na$^+$ (pretreated with the plasticiser), 8% (?)	1.01→1.37	V$_A$	T_d: increased	σ_u^*: 2.6→4.5; ε_b^*: 54→33	M^*: 14.6→12.6 (68% RH, 25 d)

Glycerol and citric acid

Wang et al. [114]	30% and 3% (s) respectively	ME, and CM, airtight, 1 w	Maize	MMT–Na$^+$ (pretreated with glycerol by a HSEM), 9% (s)	Intercalated, 1.01→2.21	–	–	σ_u^*: 4.0→9.2; ε_b^*: 108→53	P^*: 5.0×10^{-10}→1.9×10^{-10}

Sorbitol + formamide

Reference	Plasticizer	Method	Starch	Clay	Morphology / d-spacing		Thermal	Mechanical	Barrier
Ma et al. [124]	20% and 10% (s) respectively	ME	Maize	MMT–Na$^+$ (pretreated with sorbitol by extrusion), 6% (s)	Intercalated, 1.01→2.07	–	T_d: 325→338	σ_u^*: 4.2→7.2; E^*: 20→38; ε_b^*: 138→117	–
	Urea + Formamide								
Huang et al. [106]	20% and 10% (?) respectively	ME	Maize	MMT–Na$^+$ (activated by citric acid), 5% (?)	Exfoliated, 1.01→nil	–	T_g: 29.4→37.4	σ_u: 4.5→21.1; ε_b: 110→135	–
Ren et al. [125]	15% and 15% (?) respectively	ME, and CM	Sweet potato	OMMT (modified by 12-OREC), % (?)	–	A and V$_H$, decreased	–	σ_u: 4.2→6.8; E, 42→102; ε_b: 90→50	–
Wang et al. [126]	20% and 10% (s) respectively	ME, and CM	Maize	MMT–Na$^+$ (pretreated with urea by	Intercalated / exfoliated, 1.01→2.13	–	T_d: 337→341	σ_u^*: 4.5→10.6; E^*, 25→119; ε_b^*: 110→66	M_∞^*: 38→36 (75% RH); P^*: 5.0×10^{-10}→2.4×10^{-10}

				extrusion), 6% (s)						
	Urea + Ethanolamine									
Zeppa et al. [147]	10% and 10% (s+p) respectively	SC; vacuum, 6 w	Potato	MMT–Na$^+$, 5.6% (s+p+f)	Intercalated / exfoliated, 1.17→?	B, unchanged	T_d: 318→315	–		M_∞: 10.3→7.4 (?)
				Cloisite 30B, 6.1% (s+p+f)	CC, 1.85→?	B, unchanged	T_d: 318→317	–		M_∞: 10.3→8.2 (?)
Huang and Yu [105]	15% and 15% (?) respectively	ME	Maize	MMT–Na$^+$ (activated by ethanolamine), 8% (?)	exfoliated, 1.01→nil	–	T_d: increased	σ_u: 6.4→23.5; σ_y: 4.3→18.3; E: 125→599; ε_b: 116→145	M: 43.5→39.8 (100% RH, 14 d)
	Formamide + Ethanolamine									
Huang et al. [109]	15% and 15% (s) respectively	ME; 25% RH, 14 d	Maize	MMT–Na$^+$ (activated by ethanolamine),	Intercalated, 1.01→2.08	V_H and A, decreased	T_d: increased	σ_u: 5.6→7.5; σ_y: 3.7→6.0; E: 47→145;	M_∞^*: 45→33 (100% RH)

5% (?)	ε_b: 96.4→85.2

Abbreviations: AC, amylose content; DS, degree of substitution; SA, starch acetate; HP, hydroxypropylated; SPAL: starch propionate acetate laurate (DS = 2.31, 0.59, and 0.1, respectively); SAPL, starch acetate propionate laurate (DS = 2.27, 0.63, and 0.1, respectively); ME/MM: melt extrusion/mixing; CM/IM: compression/injection moulding; SC, solution casting, HSEM, high-speed emulsifying machine; CC: conventional composite; 12-OREC, dodecyl benzyl dimethyl ammonium bromide; DTA: dodecyl trimethyl ammonium; σ_u: ultimate tensile strength; σ_y: yield tensile strength; σ_b: breaking tensile strength; M (M_∞): moisture uptake at specific RH after a specific time (at equilibrium); D: water diffusion coefficient; P: water vapour permeability; θ_c: contact angle; h: hour(s); d: day(s); w: week(s); m, month(s); Refer to Nomenclature for other abbreviations.

Readers should note that some changes are not monotonic.

[a] The numbers denote the weight percentages with the following brackets denoting the bases for calculation (s: starch (whether moisture is contained depends on the reference); p: plasticiser (excluding water); w: water; f: nanofiller); the formulations are thus chosen to display the most performance variation. The nanofiller content was either the content of addition or the inorganic content determined by thermogravimetric analysis, depending on the reference.

[b] The brackets next to the results show the measurement conditions.

[*] Read from the figures in the original references to provide readers the rough values.

Appendix 2   Preparation techniques, structures, and properties of starch-based nanocomposites reinforced by polysaccharide nanofillers

Reference	Nanofiller type and content [a]	Matrix (type of starch)	Plasticiser type and content [a]	Preparation technique and conditioning	Matrix crystallinity	Thermal properties T_g (°C); T_m (°C); ΔH_m (J/g); T_d (°C)	Mechanical properties σ_u (MPa); σ_b (MPa); σ_y (MPa); E (MPa); ε_b (%)	Moisture sensitivity [b] M (%); M_∞ (%); D (mm$^2\cdot$s^{-1}); P (g$\cdot$m$^{-1}\cdot$s$^{-1}\cdot$Pa^{-1}); θ_c (°)
Cellulose nanowhiskers								
Lu et al. [190]	Ramie, 40% (s+p)	Wheat	Glycerol, 30% (s+p)	SC; 50% RH	–	T_g: 26.8→55.7; T_m: not observed	σ_u: 2.8→6.9 E: 56→480 ε_b: 94.2→13.6	M_∞: 63→45 (98% RH)
Cao et al. [188]	Flax, 30% (s+p)	Pea	Glycerol, 36% (s)	SC; 43% RH, 1 w	C, increased	T_g: 43.3→48.8	σ_u: 3.9→11.9 E: 32→498 ε_b: 98.2→7.2	M: 70→57 (98% RH, 72 h)
Cao et al.	Hemp, 30%	Pea	Glycerol,	SC;	C,	T_g: 43.3→48.7	σ_u: 3.9→11.5	M: 70→50

[189]	(s+p)		36% (s)	43% RH, 1 w	increased		E: 32→824 ε_b: 68.2→7.5	(98% RH, 3 d) θ_c: 39.5→66.5 (deionized water)
Chen et al. [191,192]	Pea hull, 10% (s+f)	Pea	Glycerol, 30% (s+p+f)	SC; 43% RH, 7 d	C	T_g: 30.8→42.6; T_d: 311.5→310.7	σ_b: 4.1→7.6 E: 40→415 ε_b: 30.1→41.8	–
Teixeira et al. [193]	Cassava bagasse, 10% (s+p+w+f)	Cassava	Glycerol, 30% (s+p+w+f))	MM (140 °C, 60 rpm, 6 min) and CM (140 °C)	B, V_H, 35→32%	T_g: 45→20	σ_u: 1.8→2.8 E: 16.8→25.8 ε_b: 29.8→76.5	M: 11.24→7.30 (53% RH, 10 d)
Kaushik et al. [206]	Wheat straw, 15% (?)	Wheat	Glycerol, 30% (?)	SC (sonicated; homogenised); 43% RH, 15 d	B, increased	T_g: 102→142; T_m: 118.7→98.6; ΔH_m: 171→169; T_d: 273→255	σ_y: 4.8→224 E: 76→224	M_∞: 5.93→6.24; D: 7.71×10⁻⁴→1.47×10⁻⁴ (75% RH)
Kvien et al. [129]	MC, 5% (s+p+f)	Potato	Sorbitol, 28% (s+p+f)	SC; 53% RH, 3 w	–	T_g: 55→70	σ_u: 370→460 σ_y: 11.3→13.7 ε_b: 25→32	–
Chang et al.	MC, 5% (s)	Wheat	Glycerol,	SC (sonicated);	–	T_d: 310→322	σ_u: 3.2→11.0	P: 5.75×10⁻¹⁰→3.43×10⁻¹⁰

Reference	Nanocellulose	Starch	Plasticizer	Processing	Crystallinity	Thermal	Mechanical	Water
[198]			30% (s)	50% RH, 48 h			ε_b^*: 111→32	
Grande et al. [226]	BC	Potato / maize	–	Solution (bottom-up) and hot-press	–	–	σ_u: 18.4→228.9 / 19.4→206.7 E: 285→6080 / 138→5650 ε_b: 12.6→5.7 / 22.5→4.8	–
Wan et al. [225]	BC, 22.0% (s+p)	Wheat	Glycerol, 30% (s)	Solution impregnation; dried	–	–	σ_u: 13.1→31.1 E: 155→361 ε_b: 39.4→5.3	M_∞: 13.86→12.23; D: 1.16×10^{-4}→0.56×10^{-4} (75% RH)
Woehl et al. [228]	BC (enzyme hydrolysed), 2.5% (s)	Cassava	Glycerol, 30% (s)	SC; 43% RH, 10 d	–	–	σ_u: 1.1→8.5 E: 33→575	–
Angles et al. [194,195]	Tunicin, 25% (s+g)	Waxy maize	Glycerol, 33% (s)	SC; 43% RH, 2 w	B, increased	T_g: 0.9→57.9; T_m: 132.4→134.4	σ_u^*: 1.2→2.0 E^*: 23→105 ε_b^*: 19→10	M_∞: 62→40; D: 1.76×10^{-7}→1.59×10^{-7} (98% RH)
Mathew et al. [196,197]	Tunicin, 25% (s+g)	Waxy maize	Sorbitol, 33%	SC; 43% RH, 2 w	B, increased	T_g: -27.6→-31.4; T_m: 146.5→143.2;	σ_u^*: 4→42 E^*: 50→760	M_∞: roughly unchanged; D: 10.1×10^{-6}→7.9×10^{-6}

					and then decreased	ΔH_m: 486→883	ε_b^*: 11→15	(98% RH)
	Starch nanoparticles							
Angellier et al. [224]	Waxy maize, 15% (s+p)	Waxy maize	Glycerol, 25% (s+p)	SC; 50% RH, 1 w	B, decreased	T_g: 3→39.8	σ_b: 1.0→9.8; E: 11→241; ε_b: 297→20	–
Viguié et al. [212]	Waxy maize, 15% (s+p)	Waxy maize	Sorbitol, 25% (s+p)	SC; 50% RH, 1 w	increased	T_g: 59→70; T_m: 150.1→169.7; ΔH_m: 99.8→165.2	σ_b: 0.38→1.59; E: 17.2→46.2; ε_b: 63→41	–
Ma et al. {Ma, 2008 #333]	Regular maize, 4% (s)	Pea	Glycerol, 30% (s)	SC; 50% RH, 48 h	–	T_g: 34.7→41.5	σ_y: 3.94→8.12; E: 50→125; ε_b^*: 42→35	P : 4.76×10^{-10}→2.72×10^{-10}
García et al. [210]	Waxy starch, 2.5% (s+p+f)	Cassava	Glycerol, 50% (s)	SC; 43% RH, 2 w	B and V, decreased	T_d: decreased	–	M_∞: 35→50 (98% RH); P : 4.5×10^{-10}→2.7×10^{-10}
García et al. [223]	Waxy maize, 2.5% (s+p+f)	Waxy maize	Glycerol, 50% (s)	SC; 43% RH, 2 w	B	T_g: increased; T_d: decreased	–	P : 3.8×10^{-10}→6.8×10^{-10}
	Chitin							

	nanoparticles							
Chang et al. [219]	Chitin, 5% (s)	Potato	Glycerol, 30% (s)	SC; 50% RH, 48 h	–	T_g: increased	σ_u: 2.84→7.79; ε_b: 59.3→19.3	P: 5.62×10⁻¹⁰→3.41×10⁻¹⁰
	Chitosan							
	nanoparticles							
Chang et al. [220]	Chitosan, 6% (s)	Potato	Glycerol, 30% (s)	SC; 50% RH, 48 h	–	$T_g{}^*$: 85→98 T_d: decreased (seen from the trend)	σ_u: 2.84→10.80; ε_b: 59.3→22.7	P: 5.80×10⁻¹⁰→3.15×10⁻¹⁰

Abbreviations: MC: microcrystalline cellulose; BC: bacteria cellulose.

Refer to Nomenclature and the foodnotes of Appendix 1 for other abbreviations and notes applicable here.

Appendix 3   Preparation techniques, structures, and properties of starch-based nanocomposites reinforced by carbonaceous nanofillers

Reference	Nanofiller type, modification, and content [a]	Matrix (type of starch)	Plasticiser type and content [a]	Preparation technique and conditioning	Matrix crystallinity	Thermal properties T_g (°C); T_m (°C); ΔH_m (J/g); T_d (°C)	Mechanical properties σ_u (MPa); σ_b (MPa); E (MPa); ε_b (%)	Moisture sensitivity [b] M_∞ (%); P (g·m^{-1}·s^{-1}·Pa^{-1})	Electrical conductivity κ (S/cm)
Ma et al. [240]	MWCNTs (D_o = 10 nm, D_i = 3–5 nm), treated by HNO$_3$ and NaDS, 3.8% (?)	Maize	Glycerol, 30% (s)	SC; 50% RH, 1 w	V→ nil	–	σ_u^*: 4.8→7.5 E^*: 181→248 ε_b^*: 50→30	–	κ^*: 10$^{-6.4}$→10$^{-4.1}$
Cao et al. [239]	MWCNTs (D_o = ~25 nm), carboxylated	Pea	Glycerol, 36% (s+p)	SC; 43% RH, 1 w	C	T_g: 16.5→25.3; T_m: 160.8→160.9; ΔH_m: 17.4→15.4	σ_u: 2.85→4.73; E: 20.7→39.2; ε_b: 29.7→32.0	M_∞: 65→56 (98% RH)	–

	by H_2SO_4 and HNO$_3$, 3.0% (?)								
Liu et al. [241]	MWCNTs (D_o = 10 nm, D_i = 3–5 nm, L = 0.5–500 µm), carboxylated, 1.5% (?)	Maize	Glycerol, 30% (s)	SC; 50% RH, 48 h	–	T_d: slightly increased	σ_u: 4.5→7.7; ε_b: 5.5→4.0	–	κ^*: $10^{-6.4}$→$10^{-4.1}$
Famá et al. [237,261]	MWCNTs (D_o = 15–20 nm, L = 1 µm), wrapped by tapioca starch–iodine complex, 0.055% (s+p)	Tapioca	Glycerol, 34.2% (s+p)	SC (sonicated); 57% RH, 4 w	–	T_g: 0→40	σ_u: 1.1→1.5; E: 2.5→4.2; ε_b: 80→90	P: increased by 43%	–
Li et al.	GO, 2% (s)	Pea	Glycerol,	SC	C,	T_d: 311.5→318.4	σ_b: 4.6→13.8;	M_∞: 63.0→41.5 (98%	–

[260]			25% (s)	(sonicated)	decreased		E : 110→1050; ε_b: 36.1→12.1	RH)	
Ma et al. [268,269]	CB, 3.8% (s+p)	Maize	Glycerol, 30% (s)	SC (sonicated; microwave irradiated); 50% RH, 1 w	–	–	σ_y^*: 3.8→10.6; ε_b^*: 34→8	P^*: 5.7×10^{-10}→2.6×10^{-10}	κ^*: $10^{-8.6}$→$10^{-0.1}$

Abbreviations: NaDBS, sodium dodecyl benzene sulphonate [$C_{12}H_{25}C_6H_4SO_3Na$]; NaDS: sodium dodecyl sulphate [$CH_3(CH_2)_{11}OSO_3Na$]; D_o: outer diameter; D_i: inner diameter; L: length.

Refer to Nomenclature and the foodnotes of Appendix 1 for other abbreviations and notes applicable here.

Appendix 4   Preparation techniques, structures, and properties of starch-based nanocomposites reinforced by other nanofillers

Reference	Nanofiller type, modification, and content [a]	Matrix	Plasticiser type and content, and other additives [a]	Preparation technique and conditioning	Matrix crystallinity	Thermal properties T_g (°C); T_m (°C); ΔH_m (J/g); T_d (°C)	Mechanical properties σ_u (MPa); σ_b (MPa); σ_y (MPa); E (MPa); ε_b (%)	Moisture sensitivity [b] M (%); M_∞ (%); P (g·m^{-1}·s^{-1}·Pa^{-1}) WA (%) WS (%)
	Nanolayers							
Chung and Lai [293]	LDH [c] ($L =$ 60±18 nm, $T =$ 5.5–5.8 nm, $d_{001} = 0.77$– 0.79 nm), 11.7% (s+f, in unmodified maize starch) /	Unmodified maize starch / acid- modified maize starch	–	SC (sol–gel); 53% RH, 9 h	B (24.9→23.3% / 23.4→22.9%) and V_H (4−5%, no significant decrease)		σ_u: 35.7→27.51 / 31.1→31.9; E: 2805→2841 / 2424→3316 ε_b: 2.77→1.80 / 3.55→1.81	M_∞: roughly unchanged (11, 33, 53, 75, and 97% RH)

	10.5% (s+f, in acid-modified starch)							
Wu et al. [294]	LDH [d] ($L =$ 30–60 nm, $T =$ 5.8–6.2 nm, $d_{001} = 0.75$–0.79 nm), stabilised by CMC, 6% (s)	Potato starch	Glycerol, 30% (s)	SC (sonicated); 50% RH, 48 h	–	T_d: 315→297	σ_u: 3.2→6.8; ε_b^*: 8→43	P^*: 17.1×10⁻¹¹→9.4×10⁻¹¹
Wu et al. [295]	ZrP, treated by n-butylamine, 0.3% (?)	Pea starch	Glycerol, 25% (?)	SC; 43% RH, 1 w	C, decreased	T_d: 316.6→316.6	σ_b^*: 4.1→9.4; ε_b^*: 31.3→47.5	M_∞^*: 69.6→63.0 (92% RH)
Nanoparticles								
Wu et al. [271]	SiO₂ ($D =$ 35 nm), treated by SHMP, 4% (?)	Modified starch (TB-225)	–	SC; 65% RH, 24 h	–	–	σ_u: 25.9→36.2;	–

Reference	Filler	Matrix	Additives	Processing	Crystallinity	Thermal	Mechanical	Barrier
Xiong et al. [143]	SiO_2, (D = 60 nm), 2.1% (m)	Maize starch / PVA: 10/4	Glycerol, 10.7% (m), HTM, Tweenum-80, liquid paraffin	SC (sonicated); dried	41.2→33.0%	T_m: from two to one peak, increased	σ_u: 10.2→18.3; ε_b: 13.6→16.5	WA: 48.3→14.5
Tang et al. [289]	SiO_2, 3% (m)	Maize starch / PVA: 6/4	Glycerol, 15% (m), HTM, Tweenum-80, liquid paraffin	SC (sonicated); dried	–	–	σ_u^*: 9.0→15.3; ε_b^*: 156→142	WA: 207.7→37.1
Tang et al. [284] and Yao et al. [285]	SiO_2, 2.5% (m)	Maize starch / PVA: 6/4	Glycerol, 25% (m), TEOS (precursor), HCl	SC (sol–gel); dried	increased	–	σ_u, 9.0→15.0; ε_b^*: 150→120	WA: 109.3→27.0; WS: 2.1→1.1; P^*: 1.9×10^{-10}→1.3×10^{-10}
Frost et al. [287]	SiO_2, 1.2% (?)	EcoFilm™ (HP high amylose starch)	TEOS (precursor), ethanol, NH_4, stearic acid	REX; 50% RH	–	–	σ_u^*, 27→41; σ_y^*: 33→45; ε_b^*: 14.0→4.5	–
Zheng et al. [275] and Chang et al.	Sb_2O_3 (D = 30–50 nm), stabilised by	Pea starch	Glycerol, 30% (s)	SC (sonicated); 50% RH,	–	T_d: decreased (seen from the trend)	σ_u, 4.1→9.4; ε_b: 58→31	P: 4.9×10^{-10}→2.7×10^{-10}

[276] CMC, 5% (s) — | 48 h

Reference	Filler	Matrix	Plasticizer	Processing	—	Thermal	Mechanical	Permeability
Ma et al. [108]	ZnO (D = 10 nm), stabilised by soluble starch, 4% (s)	Pea starch	Glycerol, 30% (s)	SC (sonicated); dried	–	T_g: 34.7→39.1	$\sigma_y{}^*$: 3.9→10.8; E: 50→137 $\varepsilon_b{}^*$: 42.2→20.4	P: 4.8×10^{-10}→2.2×10^{-10}
Yu et al. [273]	ZnO (D = 30–40 nm), stabilised by CMC, 4% (s)	Pea starch	Glycerol, 30% (s)	SC (sonicated); 50% RH, 48 h	–	T_g: 34.7→39.8	$\sigma_y{}^*$: 3.9→9.8; $\varepsilon_b{}^*$: 42.2→25.8	P^*: 4.8×10^{-10}→1.7×10^{-10}
Liu et al. [283]	ZrO$_2$·H$_2$O (D = 20–50 nm), 8% (s)	*T. Kirilowii* starch	Glycerol, 40% (s)	SC (sonicated); 50% RH, 48 h	–	T_d: 317→291	$\sigma_u{}^*$: 2.1→4.2; $\varepsilon_b{}^*$: 58.5→37.0	P^*: 5.7×10^{-9}→4.7×10^{-9}
Radhakrishnan et al. [278]	CdS (D = 3.6 nm), 3.2% (?)	Sago starch	–	SC; 58% RH, 7 d	decreased	T_m: 71.0→66.7 ΔH_m: 6.4→29.5 $T_d{}^*$: 320→290	–	M^*: 16→31 (99% RH, 300 h)

Abbreviations: LDH: layered double hydroxide; HSMP: sodium hexametaphosphate [$(NaPO_3)_6$]; REX: reactive extrusion; HTM: hexamethylene tetramine [$(CH_2)_6N_4$]; CMC, carboxylmethyl cellulose sodium; TEOS: tetraethyl orthosilicate; L: length; T: thickness; WA (WS): water absorption (solubility) by soaking in water.

[a] m: matrix

[c] The proposed chemical formulae of LDH prepared in unmodified maize starch and acid-modified maize starch were [$Mg_{0.66} \cdot Al_{0.36}(OH)_2$]($NO_3^-)_{0.34} \cdot nH_2O$ and [$Mg_{0.65} \cdot Al_{0.35}(OH)_2$]($NO_3^-)_{0.35} \cdot nH_2O$, respectively.

[d] The proposed chemical formula was [$Zn_{0.64} \cdot Al_{0.36}(OH)_2$]$Cl_{0.36} \cdot nH_2O$

Refer to Nomenclature and the foodnotes of Appendix 1 for other abbreviations and notes applicable here.